This is to certify that the

dissertation entitled

DIGITAL TERRAIN ANALYSIS AND SIMULATION MODELING TO ASSESS SPATIAL VARIABILITY OF SOIL WATER BALANCE AND CROP PRODUCTION

presented by

Bruno Basso

has been accepted towards fulfillment of the requirements for

Ph.D degree in Crop and Soil Sciences

Joe T. Ritchie
Major professor

Date 5 May 2000

DIGITAL TERRAIN
SPATIAL VARIABILIT

DIGITAL TERRAIN ANALYSIS AND SIMULATION MODELING TO ASSESS SPATIAL VARIABILITY OF SOIL WATER BALANCE AND CROP PRODUCTION

By

Bruno Basso

A DISSERTATION

Submitted to
Michigan State University
in partial fulfillment of the requirements
for the degree of

DOCTOR OF PHILOSOPHY

Department of Crop and Soil Sciences

2000

DIGITAL TERRAIN
SPATIAL VARIABILIT

Terrain characteri

They often modify enviro

sedimentation, as well as

soils becoming saturated i

convergence of both s

minimize a conventional,

model to evaluate the hy

surfaces. A new digital te

model how the terrain aff

and surface and in the s

TERRAE-SALUS ap

terrain was measured. T

interconnected series of

evaluated using three di

including the runoff-run

water contents compare

peak flow was highes

ABSTRACT

DIGITAL TERRAIN ANALYSIS AND SIMULATION MODELING TO ASSESS SPATIAL VARIABILITY OF SOIL WATER BALANCE AND CROP PRODUCTION

By

Bruno Basso

Terrain characteristics and landscape position control soil physical properties. They often modify environmentally sensitive processes such as leaching, erosion and sedimentation, as well as dynamic factors affecting crop production. The likelihood of soils becoming saturated increases at the base of slopes and in the depression where there is a convergence of both surface and subsurface flow. The objective of this study was to combine a conventional, one-dimensional soil water balance model with a terrain analysis model to evaluate the hydrological and agricultural processes occurring on sloping land surfaces. A new digital terrain model, TERRAE-SALUS was developed to study and model how the terrain affects the vertical and lateral movement of water occurring on the land surface and in the shallow, subsurface regimes. This study evaluated the capability of TERRAE-SALUS applied at a field scale with rolling terrain where the soil water content was measured. The model was able to partition the landscape into an interconnected series of element network from a grid DEM. TERRAE-SALUS was evaluated using three different scenarios to gain a better understanding of the factors affecting the runoff-runon processes. The high elevation point consistently showed lower water contents compared to the upper and lower saddles and depressions. The subsurface lateral flow was highest on the saddles between two peaks, indicating the

correct performance of th

elements located on the p

content varied from 0.22

the crop simulation mode

evaluate the ability of the

spatially variable landsca

simulation modeling and

yield variability, which a

correct performance of the model in predicting the contribution of water from the elements located on the peaks. The RMSE between measured and simulated soil water content varied from 0.22 cm to 0.68 cm. A second experiment was carried out applying the crop simulation model CROPGRO in combination with remote sensing data to evaluate the ability of the model to identify factors responsible for the yield variation in a spatially variable landscape. Results from this study showed that the combination of crop simulation modeling and remote sensing can identify management zones and causes for yield variability, which are prerequisites for zone-specific management prescription.

To my family, my friends, and my love Valentina!

I wish to express my sinc

have met Joe twelve ye

Since then, we became v

ne years I was in East La

here are no words able t

life for many years, trave

knowledge in various sc

He always let me make th

I want to thank Dr. Fran

is committee member an

I also want to extend a sp

Department of Agricultu

accepting to be on my gr

modeling.

Thanks to Dr. Jeff Andre

for their tutoring in the f

were excellent teachers a

A special thanks goes to

Australia for the develop

Canberra twice during

estimable.

ACKNOWLEDGMENTS

I wish to express my sincere gratitude and appreciation to my advisor Dr. Joe T. Ritchie. I have met Joe twelve years ago when I came to MSU for the first time to learn English. Since then, we became very good friends and a special relationship developed throughout the years I was in East Lansing. Joe and Ann basically became my family and I think there are no words able to express my gratitude to them. I had the fortune to be next to Joe for many years, travel around the world with him, and learned not only the knowledge in various scientific fields but also their applications to real world problems. He always let me make the decisions and face the consequences, trusting in my skills.

I want to thank Dr. Fran J. Pierce for his guidance, suggestions for my research, serving as committee member and for his friendship that developed throughout the years.

I also want to extend a special word of appreciation and gratitude to Dr. Jim Jones of the Department of Agricultural and Biological Engineering at University of Florida, for accepting to be on my graduate committee, and for his valuable advises on crop modeling.

Thanks to Dr. Jeff Andresen and Dr. Dave P. Lusch, members of my graduate committee for their tutoring in the field of Agricultural Climatology and Remote Sensing. They were excellent teachers and I will benefit from their lectures throughout my future career.

A special thanks goes to Dr. John C. Gallant of CSIRO-Land and Water in Canberra, Australia for the development of the digital terrain model TERRAE. I have visited John in Canberra twice during my Ph.D. project and his time, help and hospitality were inestimable.

I made many friends dur
ing forever. Brian Bear
and help. Thanks Brian!
friendship, help and sup
enjoying cappuccino tog
I also wish to extent my
CIMMYT and ICRISAT
Grace of CIMMYT and
Thanks to all my Now In
colleagues of such profe
Maria Vinocur and Aym
A number of people we
specially like to thank
field study. Thanks to B
for letting me making h
Last but not least, my d
My brothers, Giovanni a
Valentina for her love a

I made many friends during my stay at MSU, and the friendship with some of them will last forever. Brian Bear is one of them; I cannot ever thank him enough for his friendship and help. Thanks Brian! A very special friend that I would like to thank for his friendship, help and support is EdMartin. . Ed and I had many memorable conversations enjoying cappuccino together. Grazie fratello!

I also wish to extent my gratitude for their support to the International Research Center of CIMMYT and ICRISAT. A special thanks goes to my dear friends Tim Reeves and Peter Grace of CIMMYT and to Prabhakar Patak, Piara Singh and Dr.S. Virmani of ICRISAT. Thanks to all my Nowlin Chair colleagues for their friendship. Sharing the office with colleagues of such professional and human dimensions as Carlos Paglis, Scott Piggott, Marta Vinocur and Ayman Suleiman was a privilege.

A number of people were involved in the research project at the Durand site. I would especially like to thank Ricardo Braga for the memorable and fun days we had during the field study. Thanks to Brian Long and Cal Bricker for the field harvest and John Anibal for letting me making his field look like a Swiss cheese with my neutron probe access tubes.

Last, but not least, my deepest gratitude goes to my parents, Francesco and Angela, and my brothers, Giovanni and Claudio, for their love and support. I gratefully thank Valentina for her love and my friends in Napoli for their inestimable friendship.

TABLE OF CONTENTS

LIST OF TABLES

LIST OF FIGURES

Figure 4.25b. Soil water
types, high rainfall, with

Figure 4.26. Subsurface
high rainfall, with restri

Figure 4.27. Drainage o
with restricting soil laye

Figure 4.28a. Soil water
types, high rainfall, with

Figure 4.28b. Soil water
types, high rainfall, with

Figure 4.29a. Subsurfac
high rainfall, with restri

Figure 4.29b. Sum of su
types, high rainfall, with

Figure 4.30a. Simulated
3 different soil types, l

Figure 4.30b. Simulated
3 different soil types

Figure 4.31. Subsurface
types, low rainfall, with

Figure 4.32. Drainage o
rainfall, with restricting

Figure 4.33a. Simulated
3 different soil types, l

Figure 4.33b. Simulated
3 different soil types.

Figure 4.34. Subsurface
type, low rainfall, with r

Figure 4.35. Drainage o
rainfall, with restricting

Figure 5.5. Correlation

km

GIS

km

MI

MN

USDA

USGS

LIST OF ABBREVATIONS

cm	Centimeters
GIS	Geographic Information System
km	Kilometers
MI	Michigan
MX	Mexico
USDA	United States Department of Agriculture
USGS	United States Geological Survey

1.1. Background a

Most demographers
are chronically malr
challenges; it occurs
increases, the demar
population pressure
people whose existe
estimates that there
survive on less than
deteriorating condit
production systems.
world population; n
minute. Moreover, g
since we began keep

CHAPTER I

INTRODUCTION

1.1. Background and Rationale

Most demographers agree that almost 800 million people of the world's population today are chronically malnourished. In the developing nations, poverty presents increasing challenges; it occurs in more advanced countries as well. As the global population increases, the demand for food expands, with a growing diversity in diets. As a result of population pressure, the world's finite resources are taxed to the limits by those same people whose existence depends on them. The World Resources Institute (1992) estimates that there are about a billion people, roughly one in every five, who must survive on less than the equivalent of one US dollar per day. Equally alarming is the deteriorating condition of the natural resources that underpin our current agricultural production systems. We are now witnessing a never-before-seen rate of increase in the world population; nearly 200 new residents are added to this crowded planet every minute. Moreover, global food stocks, as a percent of utilization, are at their lowest level since we began keeping such records.

A report by the W
world is heading
degradation, and
years alone, an eq
billion hectares) h
impaired through
from soil loss by e
overgrazing, defor
activities that have
freshwater resourc
resources is in jeop
hectares of land glo
Solving the poverty
countries requires r
According to the Ur
and the key to allev
must have the incor
and then reversed.
demands of a growi
practices that susta
must be implemente
sustainable land ma
the factors that dete

A report by the World Resources Institute (1992) presents data that clearly show the world is heading for an uncertain future if present trends in population growth, land degradation, and water and atmospheric pollution continues unabated. In the past 50 years alone, an equivalent to almost 11 percent of the Earth's vegetated surface (1.2 billion hectares) has had its capacity to support productive forest and agricultural systems impaired through human-induced soil degradation. This degradation has resulted mainly from soil loss by erosion and from chemical and physical deterioration caused by overgrazing, deforestation, and inappropriate agricultural practices. Many of the same activities that have degraded soil resources have diminished the quality and availability of freshwater resources as well. Clearly, the long-term productivity of soil and water resources is in jeopardy. According to Rosensweigh and Hillel (1998) almost five billion hectares of land globally have been degraded in the past half century.

Solving the poverty problem and, thus the food insecurity problem in developing countries requires rapid increases in food production, income, and employment. According to the United Nations, agricultural production-the engine of the development and the key to alleviating poverty-must be tripled within the next 50 years, and the people must have the income to buy it. The erosion of the natural resource base must be halted and then reversed. If the environmental degradation is to be curtailed, and if the food demands of a growing human population are to be met, agricultural land management practices that sustain and enhance the long-term productivity of the natural resource base must be implemented. Successful implementation of these practices, referred to as sustainable land management (IBSRAM, 1991), will require quantitative evaluation of the factors that determine whether an agricultural system is sustainable or unsustainable.

Only by identifyin

long-term perform

task. The issue of

transcends concern

cultural, and politi

found to be sustain

The goal of agricu

by increasing crop

machinery) more e

from scientific rese

dependent, and the

years. We are inund

that affect them. Cl

and soil nutrient pr

disciplines to trans

models offer predi

cultivar, and mana

support field resea

time-consuming f

models can quant

al., 1989; Ritchie

easily available to

Only by identifying and measuring these factors will it become possible to evaluate the long-term performance of a given management practice. This, however, is not an easy task. The issue of what constitutes sustainable land management is complex and transcends concerns of a physical-chemical-biological nature to include socio-economic, cultural, and political concerns. Because of this complexity, a land management practice found to be sustainable at one site might not be equally sustainable at another site.

The goal of agricultural research is to improve agricultural productivity and sustainability by increasing crop yields and by using inputs (water, fertilizer, labor, and farm machinery) more efficiently and at less cost to the farmer and the environment. Results from scientific research based on a single discipline are site specific and time and weather dependent, and they often require many experiments at different locations over several years. We are inundated with information regarding site-specific crop yield and factors that affect them. Climatically driven crop growth simulation models which quantify water and soil nutrient processes, integrate experimental results and knowledge from various disciplines to transfer the scientific knowledge to other sites and other years. These models offer predictions and recommendations independent of location, season, crop, cultivar, and management. Crop growth simulation models are increasingly used to support field research, extension, and teaching. The number of costly, multi-treatment, time-consuming field trails can be substantially reduced by crop simulation as crop models can quantify the magnitude and variability in response to treatments (Ritchie *et al.*, 1989; Ritchie 1991; Jones and Ritchie, 1991). From 1970, when computers became easily available to help us deal with the complexity of crops, crop simulation modeling

developed rapidly.

and combined simp

The other was seen

physiological proce

1996). These two a

functional and mec

Mechanistic model

involved as current

Darcy's Law, and s

Because of the large

assumptions, mecha

developers. For this

except for academic

Functional models,

ways to model them

accurately as mecha

calculation. Becaus

without much diffi

tional empiricism

family of crop mod

mechanistic, as a n

1993). This minim

developed rapidly. Two distinct types of models emerged: one was essentially practical, and combined simple relationships and rules of thumb to predict the behavior of crops. The other was seemingly scientific in spirit, and sought to represent the biological and physiological processes thought to occur in plants and their environments (Passioura, 1996). These two approaches correspond to what Addiscott and Wagenet (1985) termed functional and mechanistic in their analysis of leaching models.

Mechanistic models incorporate most fundamental mechanisms of the processes that are involved as currently understood. For example, soil water flow would be modeled using Darcy's Law, and solute transport would involve mass flow and diffusion-dispersion. Because of the large amount of input information and the uncertainty of some assumptions, mechanistic models are usually not used by those other than their developers. For this reason, mechanistic models are seldom used for problem solving except for academic purposes.

Functional models, on the other hand, represent the same processes but use simplified ways to model them. These types of models may be able to express a process as accurately as mechanistic models, although they use less input data and require much less calculation. Because of that, they can usually be used by those others than the developers without much difficulty. The best functional models might be thought of as containing rational empiricism to express rather complex relationships. The well-established CERES family of crop models (Ritchie *et al.*, 1985) is predominantly functional rather than mechanistic, as a matter of fact they are built with the minimum data set concept (Nix, 1983). This minimum data set consists of information on weather, soil, crop genetic and

management. Th

model for several

strategic planning

analysis, and defin

particular cultivar

and development

plant growth and t

of the total produc

deficits on growth

growth and long-te

consequences of g

The soil water bala

soil and plant wate

leaching to the gro

establishing how m

gravity, and how m

soil layer can decre

The limits to which

each soil layer as th

capillary forces are

field saturation (S.A

the field, and accur

management. The CERES models were developed to provide users with an operational model for several purposes: assistance with farm decision making, risk analysis for strategic planning, within-year management decisions, large area yield forecasting, policy analysis, and definition of research needs. Models can predict the performance of a particular cultivar sown at any time, on any soil, in any climate. They estimate the growth and development of the crop, including the duration of each stage of growth, the rate of plant growth and they calculate the part of growth that becomes the economic component of the total production (Ritchie and NeSmith, 1991), the impact of soil water and nitrogen deficits on growth and development. Simulation models that accurately describe crop growth and long-term soil processes are also increasingly valuable tools for studying the consequences of global climate change (Adams *et al.*, 1990).

The soil water balance is calculated to evaluate the possible yield reduction caused by soil and plant water deficits, and the environmental impact of nutrients and pesticides leaching to the groundwater. The soil water balance model requires inputs for establishing how much water the soil will hold by capillarity, how much will drain out by gravity, and how much is available for root uptake (Ritchie, 1985). Water content in any soil layer can decrease by soil evaporation, root absorption, or flow to adjacent layers. The limits to which water can increase or decrease are input (volumetric fraction) for each soil layer as the lower limit (LL) of plant water availability, the limit where capillary forces are greater than gravity forces, the drained upper limit (DUL), and for field saturation (SAT). The values used for these limits must be appropriate to the soil in the field, and accurate values are quite important in situations where the water input

supply is marginal

have been describe

(1999).

The CERES famil

soils when the dra

such models is on

and time. To use s

terrain, the spatial

must be addressed

There are three ma

that occurs when a

Hortonian overlan

rate of the soil; an

conductive soil pr

a continuum of pr

(Freeze, 1972). In

precipitation fallin

runoff or overland

and may vary in si

conductivity, orga

content, and topog

supply is marginal (Ritchie, 1981). Determinations of these soil water extraction limits have been described in Ritchie *et al.*, (1986), Ritchie and Crum (1989), Ritchie *et al.*, (1999).

The CERES family models have proven to be effective in simulating the water balance of soils when the drainage is vertical, often an unrealistic assumption. Runoff produced by such models is only from a point in space and there is no account for the water over space and time. To use such models for erosion estimates and for poorly drained, sloping terrain, the spatial and temporal relationship between various hydrological processes must be addressed.

There are three main mechanisms that produce storm runoff: saturation overland flow that occurs when a rising water table intersects the soil surface, generating exfiltration; Hortonian overland flow that occurs when the rainfall intensity exceeds the infiltration rate of the soil; and subsurface flow in which water flows laterally through a highly conductive soil profile (Horton, 1933; Dunne, 1970, 1983). These mechanisms are part of a continuum of processes and may operate singularly, but more often in combination (Freeze, 1972). In the case of saturation overland flow and Hortonian overland flow, precipitation falling directly on the saturated zone at the soil surface produces surface runoff or overland flow. These saturated areas may occupy only a portion of a catchment and may vary in size depending upon soil properties such as saturated hydraulic conductivity, organic content, depth to restricting soil layers, antecedent soil water content, and topography. The Hortonian mechanism of runoff generation is most

important in ser

occurs.

Many hydrologi

nature of natural

hydrologic proce

hydrologic and e

power of these m

at the catchment

variation of inflo

topographic conv

a major impact on

The terrain often r

and sedimentation

accounting for the

possible. Terrain

geomorphological

between processes

Digital Elevation

topographic attrib

the spatial distribu

format, consisting

important in semiarid and desert areas, and on agricultural land when surface sealing occurs.

Many hydrologic and water quality models crudely represent the three-dimensional nature of natural landscapes and therefore crudely represent spatially distributed hydrologic processes. As transport modeling becomes increasingly important in hydrologic and environmental assessment, this becomes a limiting factor in the predictive power of these models. Not only do we need to know the temporal variation in discharge at the catchment outlet, we also need to be able to accurately predict the temporal variation of inflow depths and flow velocities throughout the catchment. The effect of topographic convergence and divergence on flow characteristics in natural landscapes has a major impact on the values of hydrologic variables (Moore and Grayson, 1991).

The terrain often modifies environmental sensitive processes such as leaching, erosion and sedimentation as well as dynamics factors affecting crop production. Without accounting for the terrain characteristics, accurate prediction of water quality is not possible. Terrain analysis is becoming increasingly important in the hydrological, geomorphological and ecological sciences for examining the spatial relationships between processes occurring on the land surface and the shallow subsurface regime. Digital Elevation Models (DEMs) provide the basic data for characterizing the topographic attributes of landscapes. A Digital Terrain Model (DTM), instead, includes the spatial distribution of terrain attributes. A DTM is a topographic map in digital format, consisting not only of a DEM, but also the type of land use, settlements, types of

drainage lines a

processing. DT

Algorithms hav

curvature, aspec

proximity variab

For closer corres

a need of partitio

the soil and topog

characterized by

1.2. Hypothesis

The overall hypot

control soil physi

soil horizon and s

position also dete

regulates how lon

it infiltrates or run

lateral subsurface

water to soils in to

characteristics du

drainage lines and so on. They are a major constituents of geographical information processing. DTMs help to model, analyze and display phenomena related to topography. Algorithms have been developed to estimate slope gradient, plan curvature, profile curvature, aspect direction, specific catchment area, and a variety of surface drainage proximity variables from the DTMs (Moore *et al.*, 1993; Bell *et al.*, 1994).

For closer correspondence in scale between model predictions and measurements, there is a need of partitioning landscapes into small areas where the hydrological processes, and the soil and topographic characteristics can be considered uniform or at least can be characterized by simple relationships.

1.2. Hypothesis

The overall hypothesis of this study is that terrain characteristics and landscape position control soil physical properties through organic matter accumulation and formation of soil horizon and soil structure, which highly influence the soil water balance. Landscape position also determines how much precipitation infiltrates into the soil profile because it regulates how long water can pond on the surface, as well as how much can pond before it infiltrates or runs off to other areas in the landscape. Hortonian overland flow and lateral subsurface flow of water are most likely to be significant on the backslope, adding water to soils in toeslope position. Thus, soil water is influenced by the terrain characteristics due to the effect of runoff-runon processes.

In this study. I
movement at a
and consequen
water from soi
balance. Accur
optimum mana
not like a bucke
influence of gra
the plants as rap
forces in soil.

Water infiltratin
lateral movemen
present. This rest
intensity exceeds
consequently cau
the soil properties
characteristic wil
Factors affecting
and time. Topogr
natural landscape

In this study, it is also hypothesized that the partitioning between vertical and lateral movement at a catchment level will help us to better predict the complete water balance and consequently the available water for the plants over space and time. Plants derive water from soil through their roots in an attempt to maintain a favorable hydraulic balance. Accurate evaluation of available soil water reservoir is vital to developing optimum management for rainfed crop production. However, the soil water reservoir is not like a bucket. Some water may percolate down out of the root zone under the influence of gravity. All water remaining in the root zone reservoir cannot be taken up by the plants as rapidly as needed because it is held too tightly by cohesive and adsoprtive forces in soil.

Water infiltrating into the soil profile moves vertically and laterally. The subsurface lateral movement occurs when a low conductivity soil profile or shallow water table are present. This restriction in the soil forces the water to move laterally and if the rainfall intensity exceeds the infiltration rate an overland flow occurs, increasing runoff and consequently causing erosion problems. The horizontal movement of water varies with the soil properties and with the terrain attributes. Accurate prediction of the terrain characteristic will lead us to a better prediction of the water balance and water quality. Factors affecting both crop production and environmental sensitivity vary in both space and time. Topographic convergence and divergence of water flow characteristics in natural landscapes have a major impact on the values of hydraulic variables.

The combina

movement o

understandin

affecting crop

1.3. Objective

The objective o

balance model

agricultural pro

A new digital te

the terrain affect

surface and in th

conductivity soil

The thesis is cons

Chapter 2 compre

development of d

elevation models

Chapter 3 present

and for modeling

The combination of crop growth models and DTM will enable us to predict the movement of water over space and time at a catchment level and will provide a greater understanding of the environmental sensitive processes as well as dynamic factors affecting crop production.

1.3. Objective

The objective of this study is to combine a conventional one-dimensional soil water balance model with more realistic terrain analysis to evaluate the hydrological and agricultural processes occurring on a sloping land surface.

A new digital terrain model, TERRAE-SALUS, was developed to study and model how the terrain affects the vertical and lateral movement of water occurring on the land surface and in the shallow, subsurface regime, where a shallow water table or a low conductivity soil layer may exist.

The thesis is constructed as follows:

Chapter 2 comprehensively reviews studies pertaining to soil water balance modeling, the development of digital terrain analysis, topographic attributes derived from digital elevation models and terrain-based hydrological modeling;

Chapter 3 presents TERRAE-SALUS: the new element network for deriving flow lines and for modeling the spatial variability of the soil spatial water balance;

Chapter 4 descri

Durand, Michig

Chapter 5 descri

identify the facto

agriculture conte

Chapter 6 gives

Agricultural ecos

simplify the comp

relationships occu

other sites where

advances in resea

in jeopardy.

Chapter 4 describes the application of TERRAE-SALUS at agricultural field scale in Durand, Michigan, USA to test the hypothesis of this research;

Chapter 5 describes and evaluate the application of crop models and remote sensing to identify the factors responsible for the spatial variability of crop production in a precision agriculture context;

Chapter 6 gives conclusions and implications of results from this dissertation.

Agricultural ecosystems are very complex entities. The scope of this thesis is not to simplify the complexity of nature but to be able to explore and explain how complex relationships occurring on the dynamic environment can be described and transferred to other sites where the need for such understanding is highly beneficial. Technology and advances in research should be applied to properly manage the natural resources that are in jeopardy.

This chapte

soil water ba

assessing app

The literature

for soil water

its application

Digital Elevati

related applicat

2.1. Soil Water I

More than 99% o

distributed. Humi

to dispose of exce

with a chronic sho

limited that life is

CHAPTER II

LITERATURE REVIEW

This chapter reviews the finding of other scientists that have studied problems related to soil water balance, hydrological modeling and the use of digital terrain analysis for assessing appropriate management strategies of natural resources in agricultural sciences. The literature review is divided in four sections. Section 2.1 discusses previous attempts for soil water balance modeling. Section 2.2. describes Digital Terrain Analysis (DTA), its applications in environmental modeling and the topographic attributes derived from Digital Elevation Models (DEMs). Studies pertaining to hydrological modeling and GIS-related application are presented in section 2.3.

2.1. Soil Water Balance Modeling

More than 99% of the water on earth is salty and the remaining fresh water is unevenly distributed. Humid regions have an abundance of it, so that frequently the problem is how to dispose of excess water. Arid and semiarid regions, on the other hand, are afflicted with a chronic shortage of it; and in some areas of arid regions, fresh is water is so limited that life is unbearable. Indeed, of all the major physico-chemical resources needed

by plants, water

water from prec

reservoir affect

Because of the c

models of the so

to interpret long

Factors affectin

Ritchie (1972) c

in his model for

incomplete cov

evaporation and

grain sorghum p

model at a wate

soil water conte

the equation wit

In 1985, Ritchie

change in the sto

(SWBM), comm

(Crop Estimation

atmosphere mode

Transfer (IBSNA

by plants, water is the most limiting factor. The temporal variation in the supply of soil water from precipitation, and the spatial variability in the soil factors affecting soil water reservoir affect crop productivity and create a risky environment for growing crops. Because of the difficulty in obtaining long-term variability in yield, computer simulation models of the soil water balance and crop growth are necessary for agricultural scientists to interpret long-term productivity.

Factors affecting the soil water balance have been exploited by several researchers. Ritchie (1972) developed a program to separate soil evaporation from plant evaporation in his model for calculating the daily evaporation rate from a crop surface with incomplete cover. The model provided close agreements between the simulated evaporation and the evaporation measured in the field using a weighing lysimeter in a grain sorghum plot. Richardson and Ritchie (1973) evaluated the soil water balance model at a watershed scale to study the effect of soil water content on runoff. The total soil water content was predicted accurately by substituting the simulated runoff needed in the equation with the runoff measurements available in the study.

In 1985, Ritchie presented a model of the soil water balance that estimates the daily change in the storage capacity (ΔS) of the profile. This soil water balance model (SWBM), commonly called the Ritchie model, is a major component of the CERES (Crop Estimation through Resource and Environmental Synthesis) family of crop-soil-atmosphere models which are used in the Decision Support System for Agrotechnology Transfer (IBSNAT, 1986, Hoogenboom, 1998). Ritchie (1987) and Kovac's et al. (1995)

used the Ritc

applicable fo

(1998) used t

able to closel

cm).

Yates (1996) p

(1972) equatio

the potential i

calibration usi

study area. Ph

based modelin

and regions.

Shanhoultz and

tillage practices

based on field m

only for the yea

limited.

Soil water balan

larger models an

fact there is exte

used the Ritchie soil water balance to simulate nitrate leaching. The model proved to be applicable for simulating the downward flow to the groundwater. Gerakis and Ritchie (1998) used the SWBM in the simulation of atrazine leaching and concluded that it was able to closely simulate the soil water content at three depths (13 cm., 26 cm., and 67 cm).

Yates (1996) presented a water balance model (WatBal) that used the Priestly-Taylor (1972) equation to estimate potential evaporation. The WatBal model was used to assess the potential impact of climate change on a river basin runoff. The model required intense calibration using test data sets, a major limitation for interpreting the results outside the study area. Physically based models, like Ritchie (1972) are more adaptable to a GIS-based modeling environment because there is little needed calibration for individual sites and regions.

Shanhoultz and Younos (1994) used a water balance approach to study the influence of tillage practices on soil water. In this study, evaporation was estimated with a model based on field measurements of pan evaporation. Results of this model were reported only for the years when the measurements were available, making the model's usefulness limited.

Soil water balance models can be stand-alone models as well as components of other larger models and their validation is often done through their evaluation. As matter of fact, there is extensive literature on the application and validation at different scales of

the water ba

models. Dier

Feddes et al.

content and c

used Ritchie (

soil water and

water balance

various pedoc

and a more acc

achieved. This

from bare or m

soils and compa

this study conclu

soil, while the a

the experimental

(1998) tested the

empirical for soil

components for l

independently. A

purpose. Soil hyc

from the literatur

reasonably well t

bicolor (L.) Merr.

the water balance components of the DSSAT models as well as other crop growth models. Diercks et al. (1988) used a soil water balance model (SWATRE) developed by Feddes et al. (1978) in conjunction with SUCROS crop model to estimate soil water content and crop yields under different irrigation strategies. This water balance approach used Ritchie (1972) model parameters. The model provided satisfactory results for both soil water and yield data. Gabrielle et al. (1995) evaluated the components of Ritchie's water balance at a field scale. The model was tested against field data collected from various pedoclimatic regimes in France. The authors modified the drainage coefficient and a more accurate prediction of the soil water storage and surface water content was achieved. This was confirmed by comparing the model output against independent data from bare or maize (*Zea mays* L.) cropped conditions and for silt loam or sandy loam soils and compared the modified version of the model with the original one. Results from this study concluded that the original water balance model preformed accurately in sandy soil, while the accuracy of the simulations performed with the modified model fell within the experimental error in the measurements for silty-loam soils. Maraux and Lafolie (1998) tested the ability of a model, mechanistic with respect to soil-water flow and empirical for soil-plant and plant-atmosphere interactions, to predict soil-water balance components for long periods of time when input parameters are measured or estimated independently. A data set gathered in Nicaragua during several months was used for this purpose. Soil hydraulic properties were measured independently and parameters taken from the literature were used for plant processes modeling. The model predicted reasonably well the soil-water balance for maize (*Zea mays* L.) sorghum [*Sorghum bicolor* (L.) Merr.] sequence and for a grass sod. Singh et al., (1999) used Ritchie's

model for lon

Vertic Inceptı

observed patt

The soil water

water balance

use such mode

necessary to ad

hydrological pr

increasingly im

examining the s

the shallow sub

2.2. Digital Terr

Terrain analysis

digital terrain sys

may be approach

Most attempts at

either looked at

and Olson, 1991

and can be a pow

model for long-term simulation of the water balance in a soybean-chickpea rotation on a Vertic Inceptisols. The authors observed that the simulated results were fairly close to the observed patterns.

The soil water balance models discussed have proven to be effective in simulating the water balance of soils when the drainage is vertical, often an unrealistic assumption. To use such models for erosion estimates, for a poorly drained soil in a sloping terrain, it is necessary to address the spatial and temporal relationships between the various hydrological processes occurring on the landscape. Terrain analysis is becoming increasingly important in the hydrological, geomorphological and ecological sciences for examining the spatial relationship between processes occurring on the land surface and the shallow subsurface regime.

2.2. Digital Terrain Analysis

Terrain analysis is the quantitative analysis of topographic surfaces. The purpose of a digital terrain system is the digital representation of terrain so that "real world" problems may be approached accurately and efficiently through automated means.

Most attempts at modeling landscapes have been unsuccessful because the landscape was either looked at in little detail or the landscape was considered in two dimensions (Hall and Olson, 1991). Three-dimensional data patterns have a very high information content and can be a powerful vehicle for conveying essential landscape surface information.

Topographic at

curvature can b

erosion (Bever

al., 1993d; Mo

al., 1993; Wils

properties of th

vegetation (Mo

Basically, digit

environmental r

management de

2.2.1. Digital E

There is a long

technology to m

Models are the

information along

layers in a GIS (

analysis (Frankli

elevation of any

spatially continuo

The sample is a

Topographic attributes, including specific catchment area, slope, aspect, and plan curvature can be calculated and used to predict spatial patterns of soil water content and erosion (Beven and Kirkby, 1979; Moore et al., 1991; Moore and Wilson, 1992; Moore et al., 1993d; Moore 1995; Wilson and Gallant, 1996); solar radiation estimation (Moore et al., 1993; Wilson and Gallant, 1998); spatial distribution of physical and chemical properties of the soil (Moore et al., 1993; Gessler, et al., 1995); spatial distribution of vegetation (Moore et al., 1993) and prediction of vegetation types (Brown, 1994). Basically, digital terrain analysis provides the basis for a wide range of landscape-scale environmental models, which are used for solving research-related problems as well as management decisions.

2.2.1. Digital Elevation Model

There is a long history of studying landscape surfaces and an abundant knowledge and technology to measure topographic attributes have been developed. Digital Elevation Models are the source of the primary data used as a source of topographic surfaces information alone (Pike, 1988), for landscape modeling (Moore et al., 1991, 1993) as data layers in a GIS (Wiebel and Heller, 1991) and as ancillary data in remote sensing image analysis (Franklin, 1991). In principle, a digital elevation model (DEM) describes the elevation of any point in a given area in digital format. A discrete representation of a spatially continuous surface is merely a sample of values from the continuous surface. The sample is a finite set of spatial points with definite value (x, y, z) in a given

coordinate sys

sampled to pr

surface is imp

representative

surface. A disc

is generated f

(1993b) stated

- accurately re
- minimize da
- maximize da

The type of sp

surface. No ma

surface, and ca

surface is a ve

be used to des

(faulting, erosi

ridges and vall

exposure to ero

There are thre

arrays of equ

coordinate system. A continuous surface has an infinite number of points that could be sampled to precisely represent the surface. Sampling the infinite points of the continuous surface is impractical and unnecessary; indeed a sampling method is used to extract representative points to build a surface model that approximate the actual continuous surface. A discrete sampling set of a continuous surface can still retain the continuity if it is generated from the original surface by following certain sampling procedure. ESRI (1993b) stated that a discrete surface model should:

- accurately represent the surface;
- minimize data storage requirements;
- maximize data handling efficiency;

The type of spatial surface dictates the representation and sampling method of the surface. No matter how smooth the landscape surface appears, it is not a mathematical surface, and cannot be represented using a single mathematical function. A landscape surface is a very particular continuous surface but no single mathematical function can be used to describe it. It is a product of the composition of many geological processes (faulting, erosion, and sedimentation). Geological young terrains typically have sharp ridges and valleys, in contrast to older terrains which have been smoothed by prolonged exposure to erosional forces (ERSI, 1993b).

There are three principal ways used to represent a surface in digital form: contour lines, arrays of equally spaced sample points, and irregularly spaced sample points (ESRI,

1993b). The
(stored as D
specified ele
storage, the
photographs
manipulation
is recorded o

The most pop
The surface i
elevation mod
single point a
Carter (1988)
surfaces. Topo
terrain is not p
has to be adju
terrain. It is a
and efficiently
problem the T
coordinate ran
would be dicta
that they woul
common form,

1993b). The Vector or Contour line model describes the elevation of terrain by contours (stored as Digital Line Graphs, DGLs), the x,y coordinate pairs along each contour of specified elevation. Vector DEMs are based on the most common form of elevation data storage, the topographic map. Topographic maps are prepared directly from aerial photographs or field surveys so the information has undergone the minimum of manipulation, therefore minimizing errors. In the digital contour structure the elevation is recorded only once per contour string.

The most popular way to represent a surface is an array of equally spaced sample points. The surface is represented by a "*regular grid*", or matrix, of elevation values. Gridded elevation models can be distributed as simple matrices of elevation, with the location of a single point and the grid spacing, implying the horizontal locations of all other points. Carter (1988) describes the methodologies for the digital representation of topographic surfaces. Topographic surfaces are non-stationary, more specifically, the roughness of the terrain is not periodic but changes from one land type to another. A regular grid therefore has to be adjusted to the roughest terrain in the model and be highly redundant in smooth terrain. It is apparent that, if one has to model these non-stationary surfaces accurately and efficiently, one must use a method that adapts to this variation. In response to this problem the Triangulated Irregular Network (TINs) was created. TINs are based on "coordinate random" but "surface specific" sample points. The location of these models would be dictated solely by the surface being modeled. By "surface specific" it is meant that they would be clustered in those regions of maximum roughness. In its most common form, the TIN is a set of irregularly spaced points connected into a network of

edges that for

according to

Thiessen poly

planar. The

primary adva

surface is rug

where the sur

include impor

along ridges

storage). The

Unlike a regu

of the matrix

et al., 1975).

z dimension

triangles).

applications

topographic

geomorpho

al., (1991)

edges that form space-filling, non-overlapping triangles. The points are usually connected according to a Delaunay triangulation, a procedure that joins the centers neighboring Thiessen polygons (Delaunay, 1934; Thiesse 1911). The facets are usually assumed to be planar. The irregular nature of the TIN has many advantages and disadvantages. The primary advantage is variable resolution: a TIN can include many points where the surface is rugged and changing rapidly, but at the same time, only a few points in areas where the surface is relatively uniform. Another significant advantage is the ability to include important surface points (peaks, pits, passes, road and stream intersections, points along ridges and drains) at their exact locations (due to the precision of the coordinate storage). These advantages are countered by complexities in storage and manipulation. Unlike a regular grid, which provides an implicit neighborhood through the mechanism of the matrix, a TIN system would have to include this neighborhood explicitly (Peucker et al., 1975). Indeed, the location of every point in a TIN must be specified in the x,y, and z dimensions, as well as the topology of the points (the edges and adjacencies of the triangles). An intensive comparison between these three structures, together with applications of terrain analysis methods based on these structures for calculating topographic attributes and terrain-based indices of a variety of hydrological, geomorphological and biological processes is discussed by Kumler (1990) and Moore et al., (1991).

2.2.2. *Data S*

In principle, a
a DEM data
elevation mo
frame points
stream chann
or stereo S
complementa
data in the fo
readily availa
published top
United States
DEM data:

- 7.5-minute
- 30-minute
  point spac
- 1-degree D
  meter spa

2.2.2. Data Source of Digital Elevation Models

In principle, any data that contains the elevation information with location context can be a DEM data source. Practically, the main source of data for producing the digital elevation model are topographic contour lines, randomly distributed elevation points, the frame points of land surface such as peak, sinks, passes, points of change in slope, ridges, stream channels and shorelines, as well as stereoplotter data (e.g. stereo aerial-photo pair or stereo SPOT image pair) etc. Stereocorrelated DEMs are created from two complementary images, aerial photographs, or satellite images (Schenk, A.F., 1989). Raw data in the form of stereo photographs or field survey (the accurate data source) are not readily available to potential end users of a DEM. Therefore, most users must rely on published topographic maps or DEMs produced by government agencies such as the United States Geological Survey (USGS). USGS produces several standard types of DEM data:

- 7.5-minute DEMs have a 30-by-30 meter point spacing in x and y;
- 30-minute DEMs have 2-by-2 arc second point spacing, approximately 60-by-60 meter point spacing in x and y;
- 1-degree DEMs have 3-by-3 arc second point spacing, approximately 100-by-100 meter spacing in x and y.

2.2.3. Spatial

The distance
and y horizon
spatial resolu
another is. Sp
increased. G
DEM. The n
increasing th
upon the pr
processing t

The optimu
landscape p
broad geog
resolution i
fine spatial
DEMs are
computed.
study of sc
an elevatio
in losing f
which the

2.2.3. Spatial resolution and accuracy of digital elevation model

The distance between two adjacent cells, or the geometric size of a cell or pixel in the x and y horizontal directions is called the spatial resolution of the DEM (or "grain"). The spatial resolution of a DEM is higher than another if its cell size is smaller than the another is. Spatial resolution is refined if cell size is decreased, or coarsened if cell size is increased. Generally, the finer the spatial resolution is the higher the accuracy of the DEM. The number of cells of a DEM covering a certain area will be increased when increasing the spatial resolution, and vice versa. The spatial resolution is very dependent upon the primary data used to produce the DEM, and the cost of computer storage and processing time.

The optimum spatial resolution of a DEM is closely related to the spatial scale of the landscape pattern analysis and geo-modeling. For example, when soil properties with broad geographic extent are required, then a DEM with relatively coarse spatial resolution is indicated. To model detailed spatial distribution of soil properties, instead, a fine spatial resolution DEM will be needed. The topographic attributes computed from DEMs are dependent on the resolution of the elevation data from which they are computed. A regular grid is not an ideal representation of topographic surfaces for the study of scale effects. Gallant and Hutchison (1997) pointed out that when we subsample an elevation grid to obtain another grid at coarser resolution, beside the intended change in losing fine scale features of the surface, we also change the number of square cells into which the surface is divided. This is of particular importance when studying a "specific

catchment ar

is important

properties of

appropriately

shape of featu

The accurac

source data s

have been c

the contour

high. Howe

could be lo

sampling p

Generally,

and anoma

resolution,

the more a

more deta

recover pe

given sou

of the la

resolution

surfaces

catchment area" that is computed by accumulating cell areas from adjacent cells. Thus, it is important not to confuse scale effects with grid effect if the objective is to study scale properties of a topographic surface. Gallant and Hutchinson (1997) suggested that to appropriately represent a topographic surface for the analysis of scale effects, the size and shape of features should be assessed at different scales.

The accuracy of DEMs in representing the land surface is mainly dependent upon its source data spatial resolution (USGS, 1987). If we build the DEM from contour data that have been captured directly from aerial photographs as primary data using a stereoplotter, the contours are highly accurate (ESRI, 1993b) and the accuracy of the DEM could be high. However, when the contours have been generated from point data, the accuracy could be lower because contours must be interpolated. A DEM usually uses discrete sampling points with raster structure to represent the relief of the landscape surface. Generally, it is difficult using discrete sampling points to represent every detailed feature and anomaly such as streams, ridges, peaks, and pits. Consequently, the higher the spatial resolution, the more detailed information content the DEM could represent and therefore the more accurate the DEM is. Conversely, a DEM with lower spatial resolution will miss more detailed information of the land surface. This generalization reduces the ability to recover position of specific features less than the interval spacing. Theoretically, for a given source data set, the only way to enhance the representation of detailed information of the landscape surface is to refine the spatial resolution of the DEM; as the spatial resolution is refined, there is an increasing likelihood that significant features of land surfaces will be represented. Nevertheless, it is not possible for a DEM to obtain more

detailed inf

how DEM r

the spatial r

surface vari

surface usu

resolution w

appropriate

points. Ther

on this stag

surface that

that are not

only becom

DEM. The a

the producti

2.2.4. Digit

Digital Ter

(Miller and

geographic

application

opportunity

DTMs incl

detailed information than that contained in the source data. Hutchinson (1996) shows how DEM resolution can be matched to information content of source data. Moreover, the spatial resolution of a DEM required to contain detailed information of a landscape surface varies with roughness characteristics of natural landscape surface. A rough surface usually needs a DEM with relatively fine resolution, while a coarse spatial resolution will be required by a smooth surface. After selecting the source data at the appropriate scale, the final stage is to interpolate the source data to a grid of elevation points. There are many choices here, and the quality of the DEM is critically dependent on this stage. General-purpose interpolation methods such as Kriging will produce a surface that is reasonably consistent with the data but may contain features such as sinks that are not really present in the real topography. They may also introduce biases that only become apparent when deriving terrain attributes such as slope and aspect for the DEM. The attention to shape and the drainage characteristics of the surface are critical to the production of a high quality DEM.

2.2.4. Digital Terrain Modeling

Digital Terrain Models (DTM) have been used in geoscience application since the 1950s (Miller and Laflamme 1958). Since then, they have become a major constituent of geographical information processing. They provide a basis for a great number of applications in the earth and the engineering sciences. In GIS, DTMs provide an opportunity to model, analyze and display phenomena related to topography. Indeed, DTMs include the spatial distribution of terrain attributes. The spatial distribution of

topographi

variability

2.2.5. *Lands*

Landscape

represent th

technology

Speight (19

et al., (199

primary an

from elevat

Secondary

indices that

on the land

The mather

can be foun

Topographi

topographic

surrounding

topographic attributes can thus be used as a direct or indirect measure of spatial variability of these processes.

2.2.5. Landscape topographic attributes

Landscape topographic attributes are spatial variables that are used to describe and represent the shape and pattern of the landscape surface. Digital terrain analysis and GIS technology provide tools to quantitatively define landscape attributes.

Speight (1974) described over 20 attributes that can be used to depict landforms. Moore et al., (1991, 1993) also described terrain attributes and divided them into categories: primary and secondary or compound attributes. Primary attributes are directly calculated from elevation data and include variables such as elevation, slope, aspect, curvature etc. Secondary or compound attributes involve combinations of the primary attributes and are indices that describe or characterize the spatial variability of specific processes occurring on the landscape such as soil water content or the potential for sheet erosion.

The mathematical representation of most attributes and the methods for calculating them can be found in Moore (1991, 1993), ESRI (1993), Gallant and Wilson (1996, 2000). Topographic attributes can also be divided in local, regional and catchment. Local topographic attributes are those that can be calculated from a small neighboring area surrounding the DEM cell using certain algorithm. The neighboring area is usually 3x3

cells. Table

attributes is

Regional to

larger geom

topographic

topographic

Catchment o

to the who

characteristic

certain comb

topographic a

Table 2.1. Lo

Attribu
Altitude
Slope
Aspect
Surface curva
Profile curvat
Plan curvatu
Tangent curva

cells. Table 2.1 gives most of these attributes. The accuracy of the local topographic attributes is closely related to the spatial resolution of the DEM.

Regional topographic attributes are those attributes that are calculated using considerably larger geometric area than the local topographic attributes (Table 2.2). The regional topographic attributes are less sensitive to the spatial resolution of the DEM than local topographic.

Catchment oriented topographic attributes (Table 2.3.) are those attributes that are related to the whole catchment area, and are the measurement of certain catchment characteristics. The output value of the attribute at each DEM cell is calculated from certain combinations of all of DEM cells in the catchment. The catchment oriented topographic attributes have very little sensitivity to the spatial resolution of the DEM.

Table 2.1. Local topographic attributes

Attribute	Definition
Altitude	Elevation above sea level
Slope	Maximum rate of change in elevation from each DEM cell
Aspect	Direction of the maximum rate of change in elevation from each cell DEM
Surface curvature	Measure of the surface convexity or concavity
Profile curvature	Curvature of a surface in the direction of steepest slope
Plan curvature	Curvature of a surface perpendicular to the direction of steepest slope
Tangent curvature	Plan curvature multiplied by the slope

Table 2.2 Regional topographic attributes

Attribute	Definition
Upslope area	Catchment area above a short length of contour
Upslope slope	Mean slope of upslope area
Upslope height	Mean height of upslope area
Upslope length	Mean length of flow paths to a point in the catchment
Dispersal area	Area downslope from a short length of contour
Dispersal slope	Mean slope of dispersal area
Dispersal length	Distance from a point in the catchment to the outlet
Flow path length	Maximum distance of water flow to a point in the catchment
Specific catchment area	Upslope area per unit width of contour
Elevation percentile	Ranking of the central point elevation compared to all the points in the surrounding region with a given area radius
Elevation difference	Difference between the central point elevation compared to all the points in the surrounding region with a given area radius
Elevation deviation	Elevation difference scaled by the standard deviation of elevation of the surrounding region with a given area radius
Elevation standard deviation	Standard deviation of the surrounding region with a given area radius
Elevation semi-variance	Two-dimensional semi-variogram of the surrounding region with a given area radius. It is an appropriate measure of the two-dimensional fractal dimension of the region

Table 2.3 C

	A
Ca	
Ca	
Ca	

Several rese

have found

soil drainag

sand, silt a

2.3. Terra

In recent

based ma

various so

water qua

movemen

largely d

availabili

(Moore e

Table 2.3 Catchment oriented topographic attributes

Attribute	Definition
Catchment area	Area draining to catchment outlet
Catchment slope	Average slope over the catchment
Catchment length	Distance from highest point to catchment outlet

Several researchers (Bell et al., 1992; Moore et al., 1993; Gessler et al.; 1995; Xu, 1999) have found high correlation between changes in these terrain variables and changes in soil drainage characteristics, A horizon depth, organic matter content, extractable-P, pH, sand, silt and soil taxonomic classes.

2.3. Terrain-based hydrological modeling

In recent years, considerable progress has been made in the development of computer-based mathematical and computational techniques to model hydrological processes for various scales of analysis. GIS technology has become widely used in hydrological and water quality modeling. Hillslope hydrologists have long assumed that the downslope movement of water can be described by surface topography since gravitational potential largely dominates hydraulic gradients in steep terrains. Hence with the increased availability of DTMs, surface topography is driving many popular hydrological models (Moore et al., 1993; Vertessy et al., 1993; Gallant and Wilson, 1996;). Since the first

computer-

hydrologis

(catchment

equations c

for the ph

computatio

concept wa

proposed a

(lines of ste

by this netw

contour line

an element c

contour line

elements for

their catchm

Environmen

beginning at

successively

has been use

dimensional

hydrologic m

the first is

depressionle

computer-based model hydrologic models were developed in the early 1960's, hydrologists have been attempting to use micro-scale process descriptions in meso-scale (catchment scale) hydrology. The massive computational effort required to solve equations describing processes in three dimensions and the intensive inputs requirement for the physically based model has limited the success of such models. However, computations may be reduced if the dimensions can be reduced from three to two. This concept was first applied by Onstad and Brakensiek (1968) and Onstad (1973). The proposed a flow net of gravitational potential between contours and their orthogonals (lines of steepest slope). Water was routed laterally down strips of land elements defined by this network and they termed this approach "stream path" or "stream tube". Adjacent contour lines and streamlines define irregularly shaped elements. Surface runoff enters an element orthogonal to the upslope contour line and exists orthogonal to the downslope contour line. Flow from one element can then be successively routed to downslope elements formed by the same stream tube. Moore et al., 1993 adopted this approach in their catchment partition model: TAPES-C (Topographic Analysis Programs for the Environmental Sciences-Contour. TAPES-C performs the partitioning of the catchment beginning at the contour line of lowest elevation and ending at the highest contour line, successively determining the elements for each adjacent pair of contour lines. TAPES-C has been used for distributed hydrological modeling that accounts for the effect of three-dimensional terrain on storm runoff generation. THALES (Grayson et al., 1992) is the hydrologic model that is coupled with TAPES-C. This DTM has two major limitations: the first is that it cannot handle depression for the flow network, thus requires a depressionless DEM, which is not a reality in many agricultural fields. The second

limitation

available.

variables a

The TAPE

TAPES-G

static mode

generation

environmen

available in

and only on

called D8 pr

for flow dir

random distu

produces a d

FD8 and FR

depends on t

terrain wetne

based on the

because the

found a stron

content. Gess

good predicto

limitation is that the model is mechanistic, it requires several inputs that are often not available. Also, there is inconsistency in scale between the measurements of field variables and the way they are applied in the models.

The TAPES model has also a grid version, TAPES-G (Gallant and Wilson, 1996). TAPES-G generates primary and secondary attributes from a DEM. It is considered a static model since it does not contains a dynamic water balance model. Through the generation of topographic attributes, TAPES-G has been applied in a variety of environmental modeling applications. For hydrological modeling, flow routing is available in TAPES-G with four different algorithms. Flow is routed from one cell to one and only one of its eight neighbor cells is based on the deepest descent. This algorithm called D8 produces parallel lines of flow along preferred directions. A second algorithm for flow directions (Rho8) aims to break up the parallel flow lines by introducing a random disturbance to the flow direction. The Rho8 algorithm is stochastic, indeed it produces a different flow network each time it is run. Flow dispersion is introduced in FD8 and FRho8, where the fractional amount of flow dispersed to each of the neighbors depends on the slope from the center cells to the neighbor. TAPES-G also computes the terrain wetness index (TWI), helpful in identifying areas of divergence and convergence based on the slope gradient. Where the slope gradient are low, the soil becomes wetter because the water is not removed to other downslope elements. Moore et al., (1988) found a strong correlation between this index and the distribution of surface soil water content. Gessler et al. (1995) found that the index, along with plan curvature, is a fairly good predictor of soil properties (A horizon depth, solum depth).

With a s

developed

and salt

framework

uses Richa

lateral sat

evapotransp

through a d

with the un

costly, time

guessed (Re

predict wat

compared w

runoff by le

Beven and

general thi

modeling b

on topograp

Several oth

have been

With a similar approach of TAPES-C, TOPOG, an ecohydrological model, was developed by CSIRO in Australia to predict plant growth and the three-dimensional water and salt balance of heterogeneous catchment. Vertessy et al., 1993 describe the framework of this physically based, distributed parameter catchment model. The model uses Richard's equations for vertical moisture flow, in multilayered soils, Darcy's Law for lateral saturated flow, the convection-dispersion equation for solute transport, and evapotranspiration based on the Penman-Monteith model. Soil water extraction is through a distributed root system from the multilayered soil, and there is water exchange with the underlying aquifer system. The model demands significant input data that are costly, time consuming and difficult to measure, so most of the model inputs have to be guessed (Refsgaard et al., 1992). Vertessy et al., (1993, 1996) have used TOPOG to predict water yield from a mountain ash forest. Modeled and observed daily runoff compared well. Over the full period of simulation (12 years) the model overpredicted runoff by less 5%.

Beven and Kirky, (1979) developed an hydrological model called TOPMODEL with the general thinking that variable source areas could be identified and the process of modeling basin hydrology be simplified, by summarizing the saturation potential, based on topographic position.

Several other terrain-based overland flow, runoff and non-point source pollution model have been reported in the literature, including the TIN-based models of Jones et al.

(1990); g

(1996). W

(1998).

The hydro

approach h

Nathan, 19

the concern

of them are

soil evapora

present (Rit

described in

(1990); grid-based models such as SHE (Abbott el al., 1986), MEDRUSH, Kirky et al., (1996), WEPP, Laflen et al., 1997, Cochrane and Flanagan, (1999), Wang and Hjelmfelt (1998).

The hydrological models examined in this review were all physically based and such approach has come under scrutiny in recent years (Grayson et al., 1992 a, b, Grayson and Nathan, 1993). There is a considerable skepticism about their use in hydrology, because the concerns related to the scarcity of appropriate input and validation datasets. Also most of them are based on Richards equations for water flow, that can produce good results for soil evaporation, but it cannot predict plant evaporation as well when the root system is present (Ritchie and Johnson, 1990). An alternative to the models described above is described in Chapter III.

This chapte

new metho

elements (G

TERRAE-S

3.1. TERR

TERRAE (C

contours fro

descent dow

at any elevat

created by T

and flow lin

of one eleme

A regular gr

Currently T

GRIDFLOA

CHAPTER III

TERRAE-SALUS

This chapter contains two sections. Section 3.1. presents the principles of TERRAE: the new methods for deriving flow lines and constructing a network of interconnected elements (Gallant, 1999). Section 3.2. discusses the spatial soil water balance of TERRAE-SALUS.

3.1. TERRAE: A new method for element network

TERRAE (Gallant, 1999) constructs a network of elements by creating flow lines and contours from a grid DEM, that is the only required input. A flow line is a line of steepest descent down the surface that represents the flow of water. TERRAE can create contours at any elevation in the grid and does not rely on pre-defined contours. Each element created by TERRAE is an irregular polygon with contours as the upper and lower edges and flow lines as the left and right edges. The elements are connected so that the flow out of one element flows into the adjacent downslope element.

A regular grid digital elevation model (DEM) provides the elevation data for TERRAE. Currently TERRAE reads floating point binary data exported from ARC/INFO using the GRIDFLOAT command. ANUDEM (Hutchinson, 1989), also available as TOPOGRID

within AE

or contou

TERRAE

channel he

which of T

To constru

This is an e

saddles are

maximum.

on each ass

peak. Two r

meet at this

the saddle. S

TERRAE ap

saddles and c

The resulting

form the fina

within ARC/INFO, is the recommended method for creating the DEMs from spot height or contour data.

TERRAE is controlled by a parameter file that specifies the names of the DEM file, channel head file and boundary file. This parameter file also contains settings that control which of TERRAE's functions are active and thresholds for sink clearance.

To construct the element network, TERRAE first identifies all flat points in the surface. This is an essential feature for modeling water routing across the landscape. Peaks and saddles are recognized as critical points for computing flow network. A peak is a local maximum. A saddle is mixed extreme with a minimum along a ridgeline and a maximum on each associated drainage line. Topography is more complex near a saddle than near a peak. Two regions of convergent topography and two regions of divergent topography meet at this point. Topography is divergent in the upper part and convergent after turning the saddle. Slope lines turn sharply if they pass close to the saddle.

TERRAE applies a user-specified boundary polygon, creates streamlines down from saddles and channel heads then adds ridge lines up from stream junctions and saddles. The resulting network of lines defines polygons that are then subdivided into elements to form the final element network.

Surface

TERRAE

contours.

results in

elevation

All flat po

are critical

identified b

steepest des

may be defi

UNGENER

Sinks and d

From each s

saddle until

connecting

determined

saddle is co

drained by

sinks are als

Surface

TERRAE uses a continuous surface derived from the DEM to construct its flow lines and contours. This surface is a quadratic B-spline with continuous first derivatives, which results in smoothly curved flow lines and contours. The surface exactly matches the elevation at every grid point in the DEM.

All flat points in the spline surface are identified before creating any flow lines, as these are critical points defining the topology of the surface. Peaks, sinks and saddles are identified by locating exactly all points in the surface where the slope is zero. The lines of steepest descent and ascent from saddles are also determined. A boundary for the analysis may be defined using the supplied boundary file. This file is in ARC/INFO UNGENERATE format. TERRAE builds a polygon from the supplied lines.

Sinks and depressions

From each saddle, TERRAE follows a flow line down the surface either side of the saddle until it terminates at the edge of the DEM or at a sink point. Once all the lines connecting saddles to sinks are known the lowest draining saddle for each sink is determined by working upwards from the lowest connected saddle to the highest. A saddle is considered connected when it drains to the edge of the DEM. The sinks that are drained by connected saddles are then marked and the other saddles flowing into these sinks are also marked as connected. This process is repeated until every sink has a lowest

draining

real. Whe

the flow is

side of the

constructed

determine

the param

Streams

Stream li

file, and

previously

line creat

junctions

For catch

combine

are treated

outlet poi

draining saddle. Depressions around sink points are considered to be either spurious or real. When constructing further flow lines, spurious depressions are cleared by following the flow line from the sink up to its draining saddle and continuing down from the other side of the saddle. Real depressions remain as features in the surface, and elements can be constructed within them. The depth and distance from the sink to the draining saddle determines whether a depression is classified as real or spurious using values specified in the parameter file.

Streams

Stream lines are constructed down from the channel heads defined in the channel head file, and from real depressions out over their draining saddles. When a line approaches a previously created line (including the user-specified boundary line) it can connect to that line creating a stream junction. Streamlines can also connect at sink points. These stream junctions become part of the set of critical points defining the surface topology.

For catchment modeling, the polygons defined from channel heads and stream junctions combine to form the modeling area. Catchment outlet points may also be provided; these are treated like stream junctions, so divide lines are constructed upwards either side of the outlet point.

In agricu

are small

the outlin

Ridge line

Ridgelines

a peak or th

boundary, it

upwards fro

cross, so the

streamlines.

follows the

Catchment c

unchanneled

Elements

The network c

TERRAE buil

head and real c

In agricultural applications channel heads will frequently not be used because the areas are smaller than natural first order catchment. In this case the boundary polygon provides the outline for the modeling area.

Ridge lines

Ridgelines are created from either side of each saddle and followed until they reach either a peak or the edge of the DEM. When a line approaches an existing ridgeline or the boundary, it can connect to it, creating a ridge junction. Ridgelines are also constructed upwards from stream junctions to form catchment divides. It is important that lines do not cross, so these catchment divide lines are started by interpolating between the incoming streamlines. When the interpolated line is sufficiently far from the streamlines, TERRAE follows the surface upslope as for other ridgelines.

Catchment divide lines may also be created for channel heads to delineate the unchanneled contributing area for the channel head.

Elements

The network of lines created at this point forms a series of polygons covering the surface. TERRAE builds the polygons by tracing these lines from each stream junction, channel head and real depression. At each critical point (sink, saddle, peak, stream junction or

nd

an

po

co

Th

an

bo

Th

co

Th

au

thr

pol

sub

A: e

elem

to th

con:

Comm

Contc

ridge junction) there may be several connected lines. TERRAE finds the next line in an anti-clockwise direction and follows each successive line until it returns to the starting point, forming a closed polygon. If a line terminates at the DEM edge, the polygon is considered to be open and is ignored.

The polygons created by this procedure are converted to elements by locating the lowest and highest point along each polygon boundary, which then form the lower and upper boundary of the element. These points are considered to be contours with zero length. These elements can then be subdivided into smaller elements for hydrologic modeling by constructing contour lines and flow lines within the initial elements. (Figure).

The subdivision of large elements into smaller elements can be done manually or automatically. The automatic method subdivides elements until they are smaller than a threshold area specified in the parameter file. The manual method displays the initial polygons and allows the user to interactively place contour lines and flow lines that subdivide elements.

At each subdivision, the connections to adjacent elements must be determined. When an element is split by a contour line, the entire contribution of the upper element is directed to the lower element. When an element is split by a flow line, both the inwards contribution from the element above and the flow out to the elements below must be connected correctly. The proportion of flow is determined by the relative lengths of contour between the two elements.

At

are

ea

ge

ele

of

Tha

dow

the

Dep

file

betw

dran

3.2. S

Refer

were

contai

At the end of the processing, a number of files are written. The most important of these are the files that describe the geometry, attributes and connectivity of each element. In each of these files, the elements are identified by a unique element number. The element geometry file (.elemgeom) contains the coordinates of the element boundaries. The element attribute file (.elemattr) specifies the slope, aspect, area, coordinates (x, y and z) of the centroid, upper and lower boundary lengths and other properties of each element. The element connectivity file (.elemconnect) contains the element numbers of the downslope neighbors of every element with the corresponding proportions of flow, and the sink number for elements that drain into real depressions.

Depressions also need to be described to permit modeling of ponding. The sink properties file (.sinks) contains the location and elevation of the sink, along with the relationship between depth and ponded volume and the number of the element it flows into when it drains over its draining saddle.

3.2. SALUS and Spatial Soil Water Balance Model

Reference pertaining to the development and validation of the soil water balance model were cited in chapter II (Ritchie, 1972; Ritchie, 1985 and Ritchie, 1998). This section contains two main parts, the first part describes the principle of soil water balance as

de

wa

sub

3.1

Th

and

das

wh

The

described by Ritchie 1998 and some of the revisions made recently in the SALUS soil water balance; the second parts discusses the spatial components for the surface and subsurface lateral movement of water: the main core of this research.

3.2.1. Soil water balance model

The one-dimensional (vertical) soil water balance model is calculated to account for soil and plant water stress at each point. The model calculates the profile water balance on a daily basis using the equation:

$$dS/dt = P + I - R - Es - Ep - D$$

where

dS/dt	=	the change in water storage (S) in time period t
P	=	precipitation
I	=	irrigation
R	=	runoff
Es	=	evaporation from bare soil surface
Ep	=	transpiration by plants
D	=	drainage from the profile

The soil water is distributed in several layers with fixed depths of :

0-1

cm

by

Th

de

sat

the

The

pon

The

cha

sur

(Da

The

of th

disc

rain

inter

1990

Pond

rain

0-2 cm, 2-7 cm, 7-15 cm, 15-26 cm, 26-40 cm, 40-57 cm, 57-77 cm, 77-100 cm, 100-125 cm, 125-150 cm, 150-175 cm, 175-200 cm. Water content in any soil layer can decrease by root absorption, flow to an adjacent layer, or by soil evaporation in the case of layer 1.

The input required by the model are the soil water limits to which water can increase or decrease (saturation, SAT; the drained upper limit, DUL, and lower limit, LL) and the saturated hydraulic conductivity (KSAT) for each layer. Definition and determination of these soil water extraction limits are described in Ritchie, 1998 and Ritchie et al., 1999.

The use of KSAT has recently been introduced to calculate runoff based on the time-to-ponding approach instead of the Soil Conservation Service Curve Number (CN) method. The CN method was proven to be inadequate in representing variation in infiltration characteristics associated with differences in tillage and residue management. The soil surface KSAT varies as function of tillage, soil compaction, surface residue amounts (Dadoun, 1993) and it is the main parameter controlling the time-to-ponding curve. The time-to-ponding approach was first described by White et al., 1989. The application of the semi-empirical version of White equation used in the soil water balance model is discussed in chapter 4 of this dissertation. The time-to-ponding (TP) curves relate rainfall intensity to infiltration rate and define the point at which cumulative rainfall intensity exceeds the infiltration capacity of the soil (White et al., 1989, 1990; Chou, 1990), at which time water ponding in micro-depressions in the soil surface occurs. After ponding begins, infiltration is equal to the amount predicted by the TP curve as long as rainfall rate exceeds the infiltration capacity. When the rainfall rate becomes less than the

in

po

Ru

co

wi

ob

on

cal

wh

The

mo

Fina

infiltration capacity, rainfall plus the surface ponded water are infiltrated until the amount ponded is depleted.

Runoff is predicted using a new methodology (Ritchie and Gerakis, personal communication). In this methodology a new parameter ("*a*") is introduced that varies with the time of the year. The *a* coefficient can vary for each month of the year and is obtained by calculating the slope for every month of the curve of cumulative rainfall (cm) on the Y axis, and the cumulative rain hours on the X axis. The *a* coefficient is then calculated using the following equation:

$$a = \mathrm{EXP}\,(-1.3 * \ln(S) - 5.9$$

where

S = slope of the curve of the cumulative rain (cm) vs cumulative rain time (hours)

The slope of the curve of the daily runoff (cm hr^{-1}) vs daily rain is described with the model:

$$RS = \mathrm{EXP}\,(a * KSAT)$$

Finally the runoff (cm) can be estimated by the following equation:

$$R = RS * (P - PM)$$

where

R = Runoff (cm)

P = Daily Precipitation (cm)

PM = Ponding capacity (cm)

Water is moved downward from the top soil layer to lower layers using a cascading approach. Water entering a layer in excess of the holding capacity of that layer (SATi-DUL i) is passed directly to the layer below by saturated flow.

The drainage coefficient (K) is also been recently modified. The calculation for the Es and Ep are taken primarily from the work of Ritchie (1972) and by using Priestly-Taylor type equation (1972) instead of the Penman equation to calculate the potential evaporation (Eo). Eo is calculated as function of the air temperature and solar radiation levels. Potential soil evaporation is a function of the potential evaporation Eo and the current leaf area index (LAI). LAI is the ratio of leaf area to ground area. As LAI increases, potential soil evaporation is decreased because of the protection from the wind and the shading from the leaf cover.

The root water uptake routine has also been modified, but it is not described here. Ritchie, 2000 (unpublished data), discusses details of those modifications.

3.2.2. Spatial Soil Water Balance Model

The element network created by executing TERRAE allows for the lateral movement of water across the landscape. Surface runoff and subsurface lateral movement is routed from one element to the next starting from the top element and moving downward. The spatial soil water balance model allows the presence of different soil types for each of the elements created if needed.

The spatial routines initialized by reading information from the file "filename.elements" produced by TERRAE containing the element attributes. The element attributes are: the element number, the area of the element, the slope of the element, the X,Y, and Z coordinate of the center of the element and the topology (the connections of the elements).

Surface Runoff

The daily time loop is initiated by reading the weather file and by calculating the soil water balance for the downward flow for each of the element. The surface runoff produced by each element will move laterally to the next downslope element. The amount of surface runoff is calculated by multiplying the surface runoff of the upslope element by the area of the element. This amount of water will be added onto the next downslope elements as additional precipitation. If there is no downslope element, the surface water runs off to field outlet.

Subsurface lateral flow

The downward flow is calculated by introducing a correction factor to account for the slower flow that occurs at the deeper layers. The correction factor consists in separating the KSAT variable into a KSAT for the effective vertical flow (KSAT-Vert) and a KSAT for the saturated flow (KSAT-Macro). The correction factors is calculated as follow for the various depth:

KSAT-Vert at 0 cm	= KSAT-Macro * 1 + 0*SIN (slope)
KSAT-Vert at 50 cm	= KSAT-Macro * 0.75 + 0.25*SIN (slope)
KSAT-Vert at 100 cm	= KSAT-Macro * 0.50 + 0.50*SIN (slope)
KSAT-Vert at 150 cm	= KSAT-Macro * 0.25 + 0.75*SIN (slope)
KSAT-Vert at 200 cm	= KSAT-Macro * 0 + 1*SIN (slope)

At the soil surface there is no difference between KSAT-Vert and KSAT-Macro, thus there is not need for a correction factor. At 200 cm the correction factor will be the SIN of slope, creating a lower conductivity.

The subsurface lateral flow is computed using the following equation:

$$SLF = Kef\ (dH/dx) * (Aup/Adw)$$

Where

SFL = Subsurface lateral flow (cm day^{-1})

Kef = Saturated hydraulic conductivity calculated as harmonic mean between Ksat of the upslope element and the downslope element (cm day^{-1})

*d*H = distance between the saturated layer and the soil surface

dx = distance between the center of the upslope element and the downslope element

Aup = area of the upslope element (m^2)

Adw = area of the downslope element (m^2)

The hydraulic head (*d*H) is calculated by the soil water balance model, while dx is calculated by TERRAE.

The Kef is calculated as harmonic mean as follows:

$$Kef = 2/ (1/KSATup + 1/KSATdw)$$

where

KSATup = KSAT of the upslope element

KSATdw = KSAT of the downslope element

The subsurface lateral flow occurs only when the SIN of the slope is greater than 0. The subsurface lateral flow is added to the next downslope elements into the layer that has the capacity to take it in, starting from the bottom layer and moving upwards.

If the SIN of the slope is zero and the amount of water is greater than the KSAT-Macro, then the water backs up within the same element. Subsurface lateral flow will occur again if a hydraulic head is created; dH/dx is then equal to the distance between the saturated layer of the upslope element and the saturated layer of the downslope element. Applications of the spatial soil water balance described above are presented in Chapter 4.

The routines and the codes for the spatial soil water balance simulation are given in Appendix B.

CHAPTER IV

ASSESSING AND MODELING SOIL WATER BALANCE IN A SPATIALLY VARIABLE TERRAIN USING TERRAE-SALUS

4.1. Introduction

Water has been long known to be essential for plants' life and at the same is one of the most limiting factors for their growth. In many agricultural regions of the world, the supply of water is highly variable due to variations that occur spatially and from year to year. One of the most important properties of the soil is that it is a reservoir for water. Without access to such a reservoir, most plants would not survive periods between rains. The factors that affect the soil water content include (1) soil characteristics: soil water limits (saturation-SAT, drained upper limit-DUL, lower limit-LL), saturated hydraulic conductivity (KSAT), thickness of the hydrologically active zone; (2) topography: local slope (a measure of the hydraulic gradient), specific catchment area (a measure of the potential maximum water flux), plan curvature (a measure of the rate of flow convergence and divergence), profile curvature (a surrogate for the rate of change of hydraulic gradient), and aspect and topographic shading (together with slope these influence the amount of solar radiation and in turn, evapotranspiration); (3) vegetation: variation in surface cover and water use characteristics; and (4) weather: net rainfall, net radiation, wind, and temperature (Moore, et al., 1991; Barling et al., 1994).

The
imp
hav
(Ri
effe
unr
and
esta
bet
sor
con
forc
an c
The
attr

Ther
that
Hort
rate c
conclu
a cong

The ability to characterize the spatial variability of soil water content is of major importance. Models that consider the dynamics of soil water balance and crop growth have been extensively used to quantify the risk related to the uncertainty in water supply (Ritchie 1994, Jones and Ritchie, 1996). The CERES family models have proven to be effective in simulating the water balance of soils when the drainage is vertical, often an unrealistic assumption. Runoff produced by such models is only from a point in space and there is no account for the water over space and time. To use such models for erosion estimates and for poorly drained, sloping terrains, the spatial and temporal relationship between various hydrological processes must be addressed. The water infiltrating into the soil profile moves vertically and laterally. The lateral movement occurs when a low conductivity soil profile or shallow water table are present. This restriction in the soil, forces the water to move laterally and if the rainfall intensity exceeds the infiltration rate an overland flow occurs, increasing runoff and consequently causing erosion problems. The horizontal movement of water varies with the soil properties and with the terrain's attributes.

There are three main mechanisms that produce storm runoff: saturation overland flow that occurs when rising water tables intersect the soil surface, generating exfiltration; Hortonian overland flow that occurs when the rainfall intensity exceeds the infiltration rate of the soil; and subsurface flow in which water flows laterally through a highly conductive soil profile (Horton, 1933; Dunne, 1970, 1983). These mechanisms are part of a continuum of processes and may operate singularly, but more often in combination

(Fra
pre
run
and
con
con
imp
occ
sign
infl

Sub
the
and
sub
sa
ex

(Freeze, 1972). In the case of saturation overland flow and Hortonian overland flow, precipitation falling directly on the saturated zone at the soil surface produces surface runoff or overland flow. These saturated areas may occupy only a portion of a catchment and may vary in size depending upon soil properties such as saturated hydraulic conductivity, organic content, depth to restricting soil layers, antecedent soil water content, and topography. The Hortonian mechanism of runoff generation is most important in semiarid and desert areas, and on agricultural land when surface sealing occurs. Hortonian overland flow and lateral subsurface flow of water is most likely to be significant on the backslope adding water to soils in toeslope position. Thus, soil water is influenced by the terrain characteristics due to the effect of runoff-runon processes.

Subsurface storm flow is generally considered to occur as lateral movement of water in the upper soil layers. Van de Griend and Engman (1985) reviewed the reasons for this and reported the influence of hard pans (plow pans) and impeding layers. When subsurface flow converges, the capacity of the soil to transmit the flow is exceeded and saturated areas are formed. These saturated areas are impermeable so in addition to exfiltration, all rainfall on them becomes runoff.

Many hydrologic and water quality models crudely represent the three-dimensional nature of natural landscapes and therefore crudely represent spatially distributed hydrologic processes. As transport modeling becomes increasingly important in hydrologic and environmental assessment, this becomes a limiting factor in the predictive power of these models. Not only do we need to know the temporal variation in discharge

at the catchment outlet, we also need to be able to accurately predict the temporal variation of in flow depths and flow velocities throughout the catchment. The effect of topographic convergence and divergence and divergence on flow characteristics in natural landscapes has a major impact on the values of these hydrologic variables (Moore and Grayson, 1991). Topography can also affect the location of zones of surface saturation and the distribution of soil water content (i.e., the soil water content overlying an impermeable or semi permeable soil horizon at shallow depth). The likelihood of soils becoming saturated increases at the base of slopes and in depressions where there is a convergence of both surface and subsurface flow (Kirkby and Chorley, 1967; Moore et al., 1988a). Hall and Olson (1991) determined the effects of landscape morphology on soil physical and chemical properties and soil water movement across the landscape. Without accounting for the terrain characteristics, accurate prediction of the soil water balance was not possible.

The automation of terrain analysis and the use of Digital Elevation Models (DEMs) has made it possible to easily quantify the topographic attributes of the landscape and to use topography as one of the major driving variables for many hydrological models. These topographic models, commonly called Digital Terrain Models (DTMs), partition the landscape into a series of interconnected elements based on the topographic characteristics of the landscape and they are usually coupled to mechanistic soil water balance models (Moore et al., 1993 Grayson, etc al., 1993, Kirkby et al, 1979; Vertessy et al.,1996). These DTMs have two major limitations: the first is that they cannot handle depression for the flow network, thus requiring a depressionless DEM, which is not a

reality in many agricultural fields. These DTMs were designed for large-scale applications and for quantifying water quality running into streams, thus the sinks and depressions are filled to have a continuos flow of water down to the streams. The second limitation is that the mechanistic soil water balance models require several inputs that often are either not available, costly, time consuming and difficult to measure, so in most of the cases they have to be estimated (Refsgaard et al., 1992). Also, there is inconsistency in scale between the measurements of field variables and the way they are applied in the models.

There is a considerable skepticism about their use in hydrology, because the concerns related to the scarcity of appropriate input and validation datasets. Also, most of them are based on Richards equations for water flow, that can produce good results for soil evaporation, but it cannot predict plant evaporation as well as water extraction from the root system (Ritchie and Johnson, 1990).

The idea of creating a DTM that would include the topographic effect on the soil water balance and would be coupled with a functional soil water balance to spatially simulate the soil water balance became clear from the reasons mentioned above. This lead to the development of TERRAE-SALUS, a DTM for predicting the spatial and temporal variability of soil water balance (Chapter 3). The model requires a DEM for the creation of the element network for landscape partitioning, weather and soil information for the soil water balance simulation.

Soil information required by the model include (SAT, DUL, LL, KSAT). These parameters can be obtained through measurements or estimated using empirical equations (Ritchie et al., 1999). For an accurate soil water balance simulation, the depth of the lowest KSAT should also be included. Indeed, significant contributions of water from subsurface lateral flow occur in saturated conditions. This information is difficult to obtain, but it can be estimated based on topography, or using historical information on the site (knowing the dry and wet areas across the field). Soil surveys could also be helpful providing information on the drainage characteristics of the soil (i.e. soil poorly drained indicates the presence of shallow water table or low conductivity layer). If no information is available on the soil, crop data could be used as indicators of stresses through remote sensing, where imagery interpretation can help identify areas to be sampled and determine soil information necessary for the model.

The overall hypothesis of this study is that the terrain characteristics and landscape positions control soil physical properties through organic matter accumulation, formation of soil horizons and soil structure that highly influence the soil water balance. Landscape position also determines how much precipitation infiltrates into the soil profile and for how long water can pond on the surface, as well as how much water can pond before it infiltrates or runs off to other areas in the landscape.

In this study, it is also hypothesized that the partitioning between vertical and lateral movement at a field-scale level will help us to better predict the complete soil water balance and consequently the available water for the plants over space and time. Accurate

predictions of the terrain characteristics will lead to better predictions of the soil water balance.

The objective of this study is to combine a conventional one-dimensional soil water balance model with a more realistic terrain analysis to evaluate the hydrological and agricultural processes occurring on a sloping land surface.

A new digital terrain model, TERRAE-SALUS, was developed to study and model how terrain affects the vertical and lateral movement of water occurring on the land surface and in the shallow, subsurface regimes, where a shallow water table or a low conductivity soil layer exist. This study evaluates the capability of TERRAE-SALUS applied at field scale with rolling terrain where the soil water content was extensively measured. The model was evaluated using three different scenarios (Scenario 1, Scenario 2, Scenario 3) to gain a better understanding of the factors affecting the runoff-runon processes occurring on the landscape.

4.2. Methodology

4.2.1. Models description

Digital Terrain Model: TERRAE

TERRAE is a new method for creating element networks where landscape depressions are included. TERRAE constructs a network of elements by creating flow lines and

contours from a grid DEM. A flow line is a line of steepest descent down the surface that represents the flow of water. TERRAE can create contours at any elevation in the grid and does not rely on pre-defined contours. Each element created by TERRAE is an irregular polygon with contours as the upper and lower edges and flow lines as the left and right edges. The elements are connected so that the flow out of one element flows into the adjacent downslope element.

A regular grid digital elevation model (DEM) provides the elevation data for TERRAE. To construct the element network, TERRAE first identifies all flat points in the surface. This is an essential feature for modeling water routing across the landscape. Peaks and saddles are recognized as critical points for computing flow network. TERRAE then applies a user-specified boundary polygon, creates streamlines down from saddles and channel heads then adds ridge lines up from stream junctions and saddles. The resulting network of lines defines polygons that are then subdivided into elements to form the final element network. These elements can then be subdivided into smaller elements for hydrologic modeling by constructing contour lines and flow lines within the initial elements. The subdivision of large elements into smaller elements can be done manually or automatically. The automatic method subdivides elements until they are smaller than a threshold area specified in the parameter file. The manual method displays the initial polygons and allows the user to interactively place contour lines and flow lines that subdivide elements.

At the end of the processing, a number of files are written. The most important of these are the files that describe the geometry, attributes and connectivity of each element. In each of these files, a unique element number identifies the elements. The element geometry file (.elemgeom) contains the coordinates of the element boundaries. The element attribute file (.elemattr) specifies the slope, aspect, area, coordinates (x, y and z) of the centroid, upper and lower boundary lengths and other properties of each element. The element connectivity file (.elemconnect) contains the element numbers of the downslope neighbors of every element with the corresponding proportions of flow, and the sink number for elements that drain into real depressions.

Depressions also need to be described to permit modeling of ponding. The sink properties file (.sinks) contains the location and elevation of the sink, along with the relationship between depth and ponded volume and the number of the element it flows into when it drains over its draining saddle.

Spatial Soil Water Balance Model

The element network created by executing TERRAE allows for the lateral movement of water across the landscape. Surface runoff and subsurface lateral movement is routed from one element to the next starting from the top element and moving downward. The

spatial soil water balance model allows the presence of different soil types to a maximum equal to the number of the elements created. Basically, each element created could have different soil characteristics if necessary.

The spatial routine is initialized by reading information from the file "filename.elements" produced by TERRAE containing the element attributes. The element attributes are: the element number, the area of the element, the slope of the element and the x, y and z coordinates of the center of the element and the topology (the connections of the elements).

The daily loop is initiated by reading the weather file and by calculating the soil water balance for the downward flow for each of the element. The surface runoff produced by each element is moved laterally to the next downslope element. The amount of surface runoff is calculated by multiplying the surface runoff of the upslope element by the area of the element. This amount of water is added onto the next downslope elements as additional precipitation. If there is not a downslope element, the surface water runs off to the field outlet.

The downward flow is calculated by introducing a correction factor to account for the slower flow that occurs at the deeper layers. The correction factor consists in separating the KSAT variable into a KSAT for the effective vertical flow (KSAT-Vert) and a KSAT for the saturated flow (KSAT-Macro). The correction factors are discussed shown in Chapter 3.

The subsurface lateral flow is computed using the following equation:

$$SLF = Kef\ (dH/dx) * (Aup/Adw)$$

where

SFL = Subsurface lateral flow (cm day^{-1})

Kef = Effective saturated hydraulic conductivity calculated as harmonic mean between Ksat of the upslope element and the downslope element (cm day^{-1})

*d*H = distance between the saturated layer and the soil surface

dx = distance between the center of the upslope element and the downslope element

Aup = area of the upslope element (m^2)

Adw = area of the downslope element (m^2)

The hydraulic head (*d*H) is calculated by the soil water balance model, while dx, the distance, is calculated by TERRAE. The effective saturated hydraulic conductivity (Kef) is calculated as a harmonic mean as follows:

$$Kef = 2/\ (1/KSATup + 1/KSATdw)$$

where

KSATup = KSAT of the upslope element (cm day^{-1})

KSATdw = KSAT of the downslope element (cm day^{-1})

The subsurface lateral flow occurs only when the sine of the slope is greater than zero. The subsurface lateral flow is added to the next downslope elements into the layer that has the capacity to take it in, starting from the bottom layer and moving upwards. If the sine of the slope is zero and the amount of water is greater than the KSAT-Macro, then the water backs up within the same element. Subsurface lateral flow will occur again if an hydraulic head is created; dH/dx is then equal to the distance between the saturated layer of the upslope element and the saturated layer of the downslope element.

4.2.2. Model simulation

The first simulation run of TERRAE-SALUS was done using a single, uniform soil type with no restricting soil layer for the entire area with a high rainfall (76 mm) occuring on the first day. This simulation done was chosen to demonstrate the ability of the model to partition the vertical and horizontal subsurface flow.

The second simulation run of TERRAE-SALUS used three different soil types with a low conductivity layer (KSAT=0.01 cm hr-1) at 120 cm. The soil types were a shallow sandy soil for the high elevation zones and peaks; a medium sandy-loam for the medium elevation zones and saddles areas; and a loamy soil for the low elevation areas and depressions. The rainfall was the same as scenario 1 (76 mm). This scenario was selected to have a direct comparison with scenario 1 but with a restricting layer at 120 cm that altered the vertical flow.

The final simulation run of TERRAE-SALUS was done to perform a model validation at field scale. Similar to scenario 2, the model was set up using three different soil types with low conductivity layer (KSAT=0.01 cm hr-1) at 120 cm. The soil types were a shallow sandy soil for the high elevation zones and peaks; a medium sandy-loam for the medium elevation zones and saddles areas; and a loamy soil for the low elevation areas and depressions.

Field measurements of profile soil water content were taken on a three ha portion of a field located 10 km south of Durand, MI, to compare with model values. The field was planted with soybeans on May 5, 1997. A digital elevation model (DEM) was created for the site using a high accuracy differential global positioning system (DGPS) at 1 m grid resolution (F.J Pierce and T.G.Mueller, personal communication, 1997). Using the DEM, the following topographic attributes were determined for the site: elevation, slope, plan curvature and profile curvature. A regular grid consisting of 28 grid locations spaced 30.5 m apart was imposed on the experimental area. Latitude, longitude and elevation of each grid points were determined with DGPS.

Neutron probe access tubes were installed at each of the 28 grid locations. A neutron moisture gauge was used to measure the spatial variability of soil water content at 15-cm increments to the depth of the C horizon or a maximum of 150 cm depth, which ever occurred first. Neutron probe calibration was obtained by filling four large metal cylinders with soil collected from two different location in field. The locations were

selected based on the soil type. Two cylinders were filled with the predominant soil type present in the field (sandy loam), and the other two were filled with the sandy soils that characterized the high elevations points and the peak. Each cylinder was carefully filled reproducing the field bulk density. For each soil type, one cylinder was filled with air-dry soil and the other was brought to saturation. This methodology is the most appropriate for neutron probe calibration. It allows the correct determination of the slope of the lines that joins the the driest and wettest point for that soil. It also decreases the errors obtained by fitting a curve through a clouds of points as observed from the traditional field methods measurements.

Measurements on soil water were taken on a weekly basis throughout the season. During the installation of the neutron probe access tubes, soil samples were taken at the intersection of each of the 28 grid points in 25-cm increments and stored for analysis. Soil samples were air-dried and passed through a 2 mm sieve. Particle size was determined for each segment of each soil profile using the hydrometer method (Gee and Bauder, 1986). The upper and lower limit of soil water availability was determined using soil water measurements taken in the field, and from empirical equations based on soil texture (Ritchie et al., 1999).

A datalogger (Licor 1000) was installed to collect weather data on solar radiation, minimum and maximum temperature, and precipitation, which are required as model inputs. Precipitation was measured with an electronic tipping bucket rain gauge every five minutes to record rainfall intensities as well as daily total amounts.

The spatial structure for each parameter was assessed using a semivariance analysis. Soil water measurements taken on each grid point were interpolated using punctual kriging technique available in GS+ Version 3.1a (Gamma Design Software, 1999).

The first day selected for the model validation was July 3, 1997, day of the year (DOY) 184. The rainfall that occurred on this day was 7.5 mm. This day was chosen to test the performance of the model under a low rainfall amount. The simulations started with the soil profile at DUL for the first 100 cm of the soil profile and at saturation for 100 cm to 200 cm for all scenarios. The performance of the model was evaluated by using the RMSE between the predicted and observed values.

4.3. Results and Discussions

4.3.1. Topographic attributes

The topographic attributes are shown in Figure 4.1 through 4.6. "Images and figures of this dissertation are presented in color". The elevation map (Figure 4.1) shows that the field had an elevation relief of 3.6 m. The north part of the field is the highest point but two other small areas (peaks) also have high relief. These two peaks can be observed in the slope map (Figure 4.2). The slope of the field varies from zero in the flat areas to 3.4

% on the backslopes of the peaks. Surface curvatures are shown in Figure 4.3 (profile curvature) and Figure 4.4 (plan curvature). They can be thought of as the curvature of a line formed by the intersection of a plane and the topographic surface. This intersection is in the direction of the maximum slope for the profile curvature and transverse to the slope for the plan curvature. Profile curvature is negative for slope increasing downhill (convex flow profile, typically on upper slopes) and positive for slope decreasing downhill (concave flow profile, typically on lower slopes). Plan curvature or contour curvature measures the topographic convergence and divergence and hence, the concentration of water in the landscape. The plan curvature is negative for diverging flow (on ridges) and positive for converging flow (in valleys).

The maximum ponding capacity is purely a function of slope. Indeed, this can be observed in the maximum ponding capacity map (Figure 4.5) that shows an opposite trend from the slope map. The maximum ponding capacity varied from zero observed on the backslope of the peaks to 3.0 on the flat areas.

Figure 4.6 depicts the location and the number of the elements created by executing TERRAE study area. The highest point in the landscape is represent by one element while the bottom of landscape is represented by several elements that describe the lowest elevation point of the field (depressions).

4.3.2. Model Simulations

Scenario 1-- Day 1. The model results for scenario 1 (uniform soil type across the landscape, no restricting layer, 76 mm rainfall on the first day) are shown in Figures 4.7 through 4.17. The units used in the outputs for all the variables are in cm (height of water). The soil water content for the 0-26 cm (Figure 4.7a) is quite uniform across the field, except for the low elevation areas, which are higher due to accumulation of surface flow onto the elements. These areas also showed higher water content for the profile at the 26-77 cm depth (Figure 4.7b). The cumulative surface leaving the element was high, as expected, due to the quantity of rainfall (Figure 4.8a). However, the surface water balances out as can be seen from the map of the cumulative surface flow out of the each element (Figure 4.8b). The model predicted that water not infiltrated on the element located on top of the landscape runs off to the next element downslope as runon. This explains the balance observed between flow out and flow in. Both maps clearly show the effect of the landscape in the surface water routing. The highest amount of water leaving and entering each element is 65 cm and it is observed in the depression areas due to the contributions from the upperslope elements. The net surface flow (Figure 4.9) is calculated by subtracting the amount of water coming into the element from the one leaving the element. The highest value (-5) is observed on top of the landscape since those elements do not have water running onto them. Figure 4.10 shows the surface ponding. The model was able to correctly determine that the depression areas have higher surface ponding capacities. The subsurface lateral flow is shown in figure 4.11. The highest amount of horizontal flow is observed in the depressions due to high soil water

content present at these locations. The vertical drainage is depicted in figure 4.12. The drainage amount predicted is quite small throughout the landscape. This may be due to the rapid occurrence of saturation in each soil layer due to the high rainfall amount. If the elements have a slope greater than zero, the model allows the water to flow horizontal through the KSAT corrections factors that decreases the vertical flow.

Day 2. The soil water content for the second day of simulation is shown in figures 4.13a and 4.13b. The 0-26 cm soil water content (Figure 4.13a) decreased from the previous day on the high elevation zones and peaks, but did not greatly change in the saddles and depressions due to the higher water flow coming onto the elements and ponding conditions occurring at these zones. Similar phenomenon was also observed for the 26-77 cm soil profile (figure 4.13b). Ponding conditions disappeared on this day, as well as the flow in and out of the elements. The subsurface lateral flow (figure 4.14) also decrease for the second day of simulation but the highest amount (0.3 cm) was still observed in the low elevation areas. The drainage (Figure 4.15) did not vary significantly from the previous day, both for the amounts and locations of occurrence.

Day 7. The soil water content at 0-26 cm (Figure 4.16a) indicates that soil surface dried out quite uniformly across the field. The 26-77 cm soil water content (Figure 4.16b) shows a high water content (14.10 cm) at the lowest point on the landscape as result of the higher water content, ponding, surface water flow onto the element and subsurface lateral flow affecting this area. Figure 4.17 shows the sum of the subsurface lateral flow for the seven days of simulation. The highest value (3.6 cm) was observed in the lower

u

d

an

sc

Fig

con

scen

the h

elevation areas and depressions as expected. The drainage for day 7 is shown in Figure 4.18. The drainage consistently decreased from the previous days but was still present. Subsurface flow, however, had terminated by day 4.

Scenario 2--Day 1. The simulated results for scenario 2 are shown in Figures 4.19 through 30. Figure 4.19a and 4.19b show the soil water content for the 0-26 cm and 26-77 cm. The model predicted a higher amount of soil water on depression areas and sinks as compared to scenario 1 for the 0-26 cm and 26-77 cm soil profiles. Since the rainfall amount used for scenario 2 was the same for scenario 1, the surface water flow in and out of the elements Figure 4.20a and 4.20b showed similar values and locations to the maps of flow in and out produced for scenario 1 on day 1. The surface ponding (Figure 4.21) is also similar to the previous scenario. The net surface flow is shown in figure 4.22 and showed the same values predicted for scenario 1, since the values of runoff and runon were also similar with the ones observed in scenario 1. The lowest negative value was observed on the high elevation areas since there was no water contribution from the upslope elements. The subsurface lateral flow, shown in figure 4.23, was higher on the depressions due to the higher water content consistently present on the low elevation areas. The value for the subsurface lateral flow was lower compared to the ones from scenario 1 since most of the water remained on the surface as ponding for scenario 2. Figures 4.24 depicted the drainage that occurred on first day. The values were lower compared to scenario 1 due to the restricting soil layer present at 120 cm depths. In scenario 2 the effects of the three different soil types were not visible. This may be due to the high rainfall amount that minimized the soil type influence.

Day 2. The 0-26 cm soil water content (Figure 4.25a) did not change from day 1. Similar results were also found for the 26-77 cm soil depth (Figure 4.25b). Runoff did not occur on day 2. The subsurface lateral flow was highest on the saddles between two peaks, indicating the contribution of water from the elements located on the peaks (Figure 4.26). Drainage values for day 2 (Figure 4.27) were low due to the low conductivity layer. Also on day 2, the effect of the different soil types was not present.

Day 7. The soil water content for the 0-26 cm depth (Figure 4.28a) decreased on the high elevation zones, but it remained the same for the low elevation zones and depressions. The soil water content for the 26-77 cm depth (Figure 4.28b) did not change significantly across the field. The vertical drainage terminated on day 4, while the subsurface later flow was still occurring (Figure 4.29a). The sum of the subsurface flow (Figure 4.29b) is higher (4.6 cm) compared to the one for scenario 1 (3.6), showing the influence from the low conductivity layer.

4.3.3. Validation study-- Scenario 3

Scenario 3 includes a validation with field measured data on soil water content. The simulated soil water content for the 0-26 cm depth is shown in Figure 4.30a. The model predicted higher water content for the saddles and depression areas. The simulated soil water content varied from 1.8 cm to 6.2 cm. Figure 4.30b shows the simulated soil water content for the 26-77 cm soil depth. The highest values of soil water were also observed at the saddle point and depressions and varied across the field from 3.2 to 13.4. The

subsurface lateral flow was higher in the saddles and depression area (Figure 31) due to the contribution from runon that increased the amount of potential infiltration on those areas. The values predicted by the model for the vertical drainage (Figure 32) were lower than those predicted for the lateral flow. The locations in the field that had the highest amount of water draining vertically were the areas located on the high and medium elevation. TERRAE-SALUS correctly simulated higher amount of vertical drainage in the areas occupied by the sandy soil. The soil water content slightly changed on DOY 188 (July 7) both for 0-26 cm and 26-77 cm (Figure 4.33a and b). The simulated subsurface lateral flow for day 188 is shown in Figure 4.34. The saddles and depressions showed the highest amount of lateral flow (0.0045 cm). The lowest value of flow was a result of the low rainfall occurring on day 184. Figure 4.35 shows the drainage that occurred on day 188. Its values are also small, almost identical and at the opposite locations where the subsurface lateral flow took place, indicating correct partitioning being employed by the model. Figure 4.36 depicts the error maps from the measured and observed soil water content for day 184 and for the 0-26 cm depth.

Figure 4.37 shows the predicted versus the observed measurement compared to a 1:1 line for the soil water content at 26-77 cm depth and for the entire season on the highest elevation point. The model provides accurate results for the entire season but it slightly underestimates the soil water content measured. Figures 4.38 through 4.41 show the measured and simulated results for the soil water content for 0-26 and 26-77 cm soil depth for the entire season using four points along a streamline (from the top-peak, to the bottom of landscape-depression). The model performance was compared using the root mean square error (RMSE). Figures 4.38a shows the comparison between the measured

and simulated results for the 0-26 cm and 26-77 cm for the point located on the highest elevation point of the field (264 m). The RMSE observed was 0.51 cm, for the 0-26 cm depth and 0.62 cm for the 26-77 depth. The simulated soil water content for the point located in the upper saddle (263 m) are compared with soil water measurements in Figure 4.38 b. The RMSE observed for this comparison were 0.39 cm for the 0-26 cm depth and 0.52 cm for the 26-77 cm depth. Figure 4.39 shows the comparison between simulated and simulated soil water content for the lower saddle point (262 m). A RMSE of 0.46 cm and 0.49 was observed for this comparison for the 0-26 cm and 26-77 cm depth. An evaluation of the model performance was also done for the depression area of the streamline selected (260 m) The RMSE observed for this evaluation were 0.47 cm for the 0–26 cm and 0.59 cm for the 26-77 cm depth.

The soil water content simulations and field observations were also compared as function of elevation. The RMSE for this evaluations are shown in Figure 40 a and b. The high elevation point consistently showed a lower water content compared to the upper and lower saddles and for the depressions. The days used in this final evaluation of the model, the soil water content did not change significantly for the saddle points and for the depressions. This is due to the contributions of water running downhill from the peaks.

4.4. Conclusions

This chapter discussed the application of TERRAE-SALUS, a digital terrain model with a functional spatial soil water balance model, at a field scale to simulate the spatial soil water balance and how the terrain affects the water routing across the landscape.

The first part of the chapter described the principles for the two models. The second parts discussed the capability of the model tested under three different scenarios. The scenarios were selected to evaluate the model sensitivity with a soil having no vertical drainage restrictions and for one that had basically almost no vertical flow. The model was able to partition the subsurface lateral flow and the vertical drainage differently for the two scenarios, but the high amount of rainfall seemed to have an higher effect through the amount of runoff and ponding that occurred on the first day, making the rest of the days quite similar between the scenarios.

The model provided excellent results when compared to the field measured soil water content. The RMSE between measured and simulated results varied from 0.22 cm to 0.68 cm. The performance of TERRAE-SALUS is very promising and its benefits can be quite substantial for the appropriate management of water resources as well as for identifying the areas across the landscape that are more susceptible for erosion. It is necessary to further validate the model at different sites with different soils and weather characteristics.

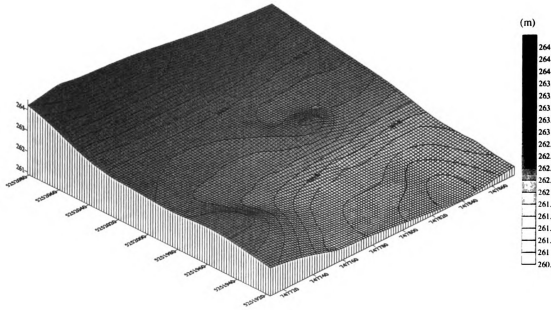

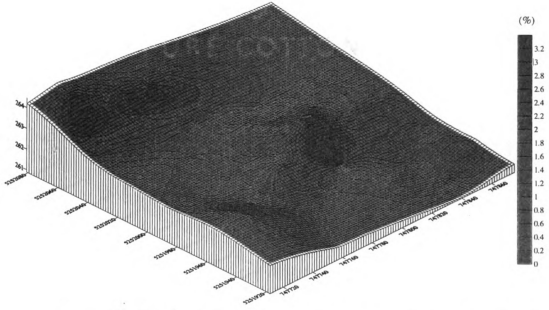

Figure 4.1. Elevation at 1 m grid resolution for the study area, Durand, MI.

Figure 4.2. Slope for the study area, Durand, MI.

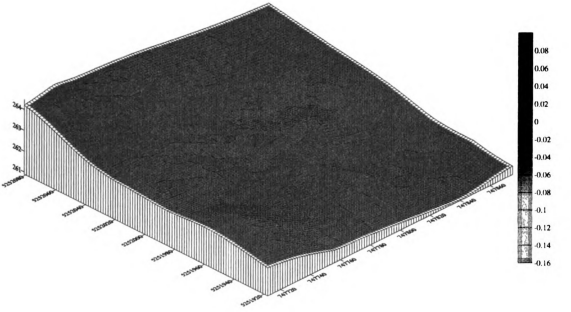

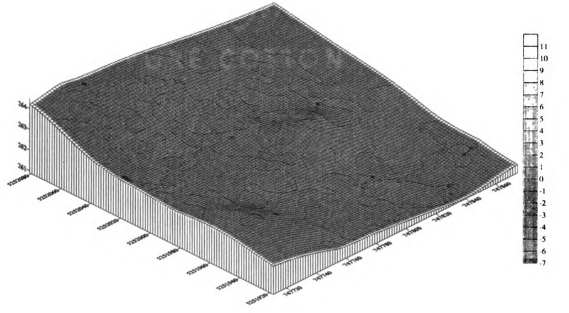

Figure 4.3. Profile curvature of the study area, Durand, MI.

Figure 4.4. Plan curvature of the study area, Durand, MI.

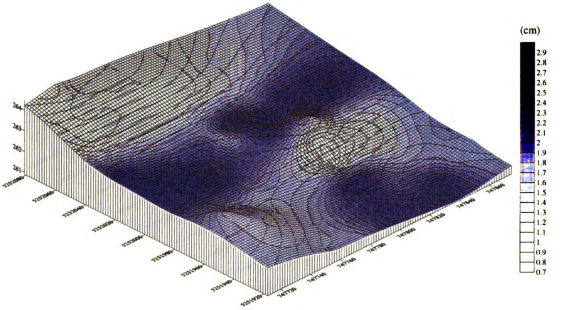

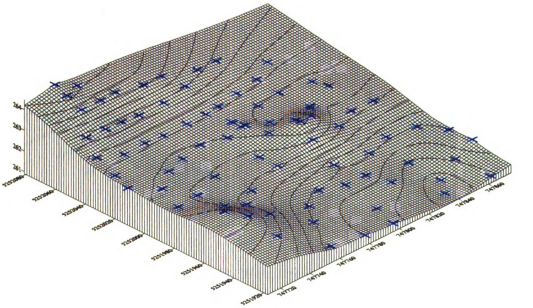

Figure 4.5. Maximum ponding capacity for the study area in Durand, MI.

.

Figure 4.6. Location in the landscape of the element network created by TERRAE (Gallant, 1999).

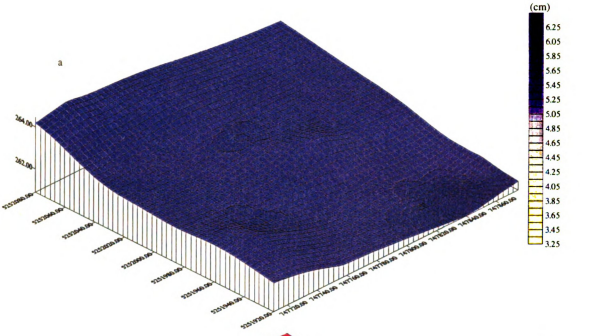

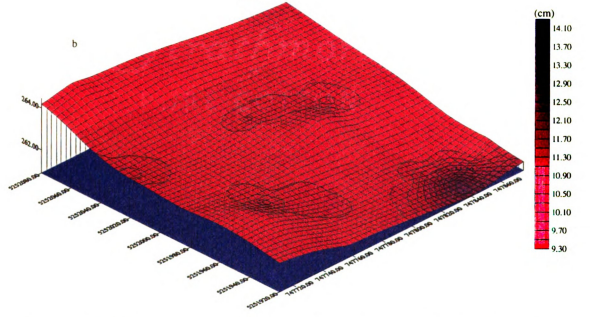

Figure 4.7.a. Soil water content (0-26 cm) on day-1 for *scenario 1* (1 uniform soil type, high rainfall, no restricting soil layer).

Figure 4.7.b. Soil water content (26-77 cm) on day-1 for *scenario 1* (1 uniform soil type, high rainfall, no restricting soil layer).

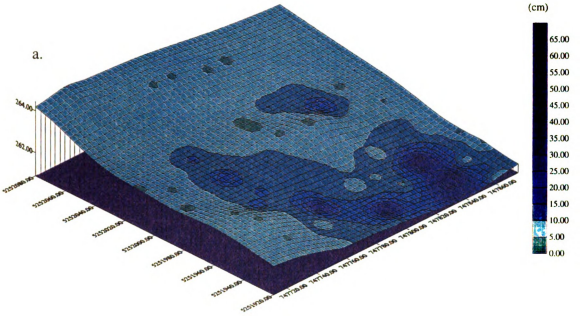

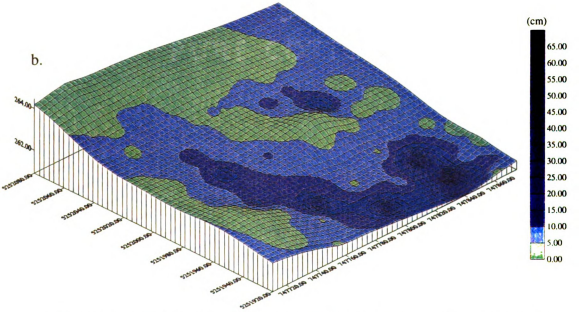

Figure 4.8.a. Cumulative surface water flow out of the elements on day-1 for *scenario 1* (1 uniform soil type, high rainfall, no restricting soil layer).

Figure 4.8b. Cumulative surface water flow onto the elements on day-1 for *scenario 1* (1 uniform soil type, high rainfall, no restricting soil layer).

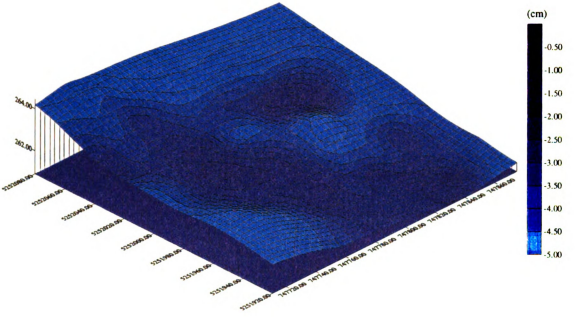

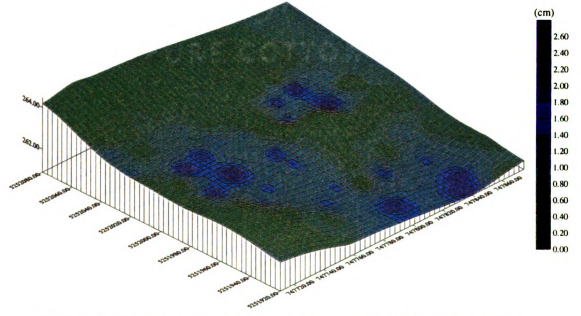

Figure 4.9. Net surface flow on day-1 for *scenario 1* (1 uniform soil type, high rainfall, no restricting soil layer).

Figure 4.10. Surface ponding for day-1 for *scenario 1* (1 uniform soil type, high rainfall, no restricting soil layer).

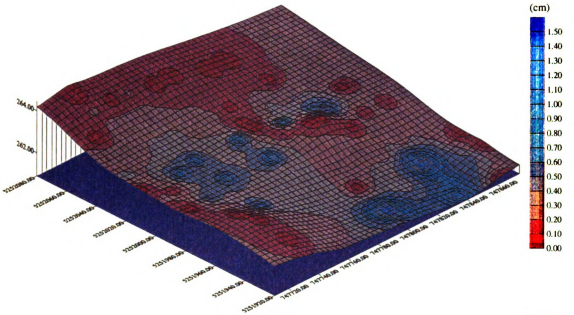

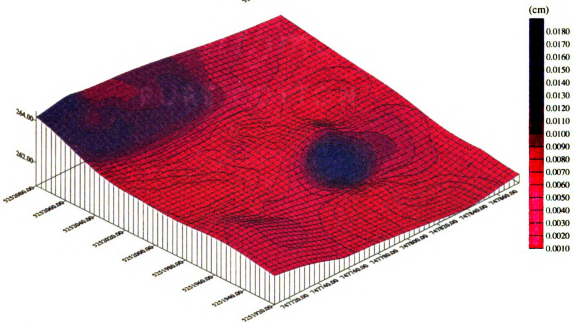

Figure 4.11. Subsurface lateral flow on day-1 for *scenario 1* (1 uniform soil type, high rainfall, no restricting soil layer).

Figure 4.12. Drainage on day-1 for *scenario 1*(1 uniform soil type, high rainfall, no restricting soil layer).

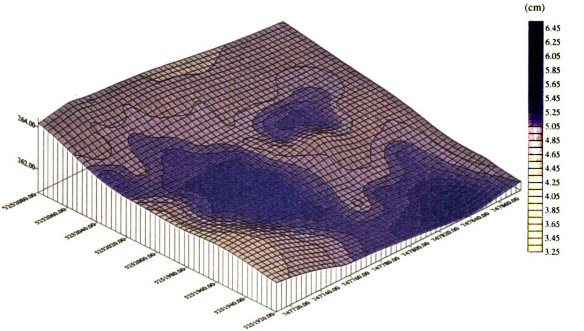

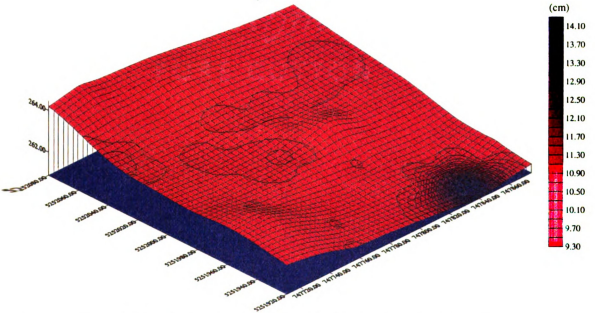

Figure 4.13.a. Soil water content (0-26) on day-2 for *scenario 1*(1 uniform soil type, high rainfall, no restricting soil layer).

Figure 4.13.b. Soil water content (26-77) on day-2 for *scenario 1*(1 uniform soil type, high rainfall, no restricting soil layer).

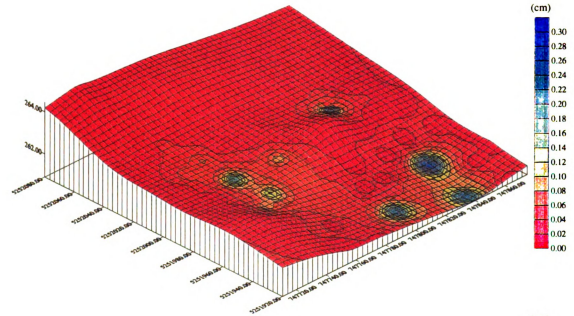

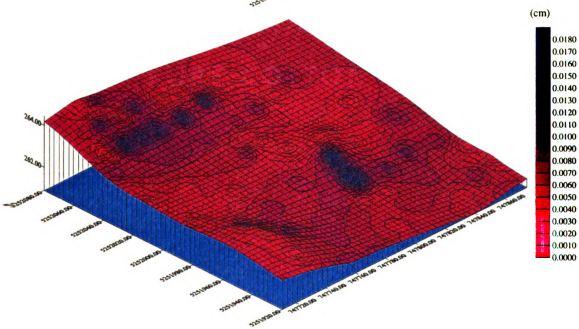

Figure 4.14. Subsurface lateral flow on day-2 for *scenario 1*(1 uniform soil type, high rainfall, no restricting soil layer).

Figure 4.15. Drainage on day-2 for *scenario 1*(1 uniform soil type, high rainfall, no restricting soil layer).

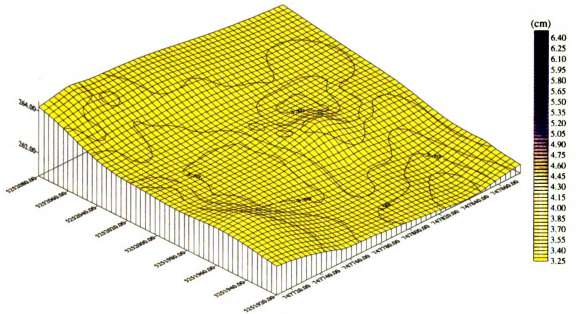

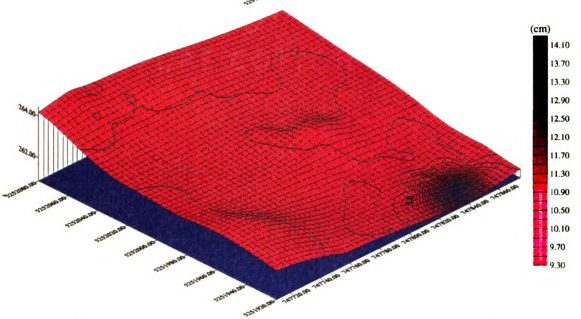

Figure 4.16 a. Soil water content (0-26) on day-7 for *scenario 1*(1 uniform soil type, high rainfall, no restricting soil layer).

Figure 4.16 b. Soil water content (26-77) on day-7 for *scenario 1*(1 uniform soil type, high rainfall, no restricting soil layer).

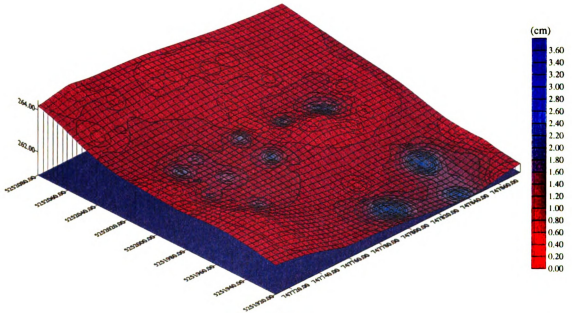

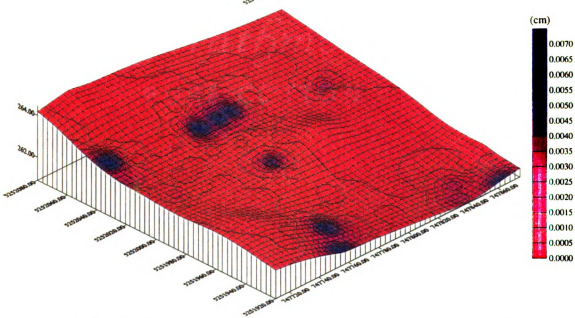

Figure 4.17. Sum of the subsurface lateral flow on day-7 for *scenario 1* (1 uniform soil type, high rainfall, no restricting soil layer).

Figure 4.18. Drainage on day-7 for *scenario 1* (1 uniform soil type, high rainfall, no restricting soil layer).

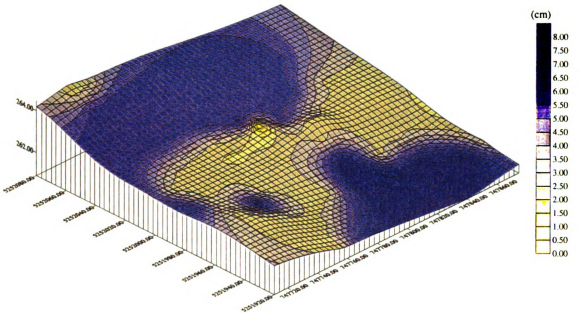

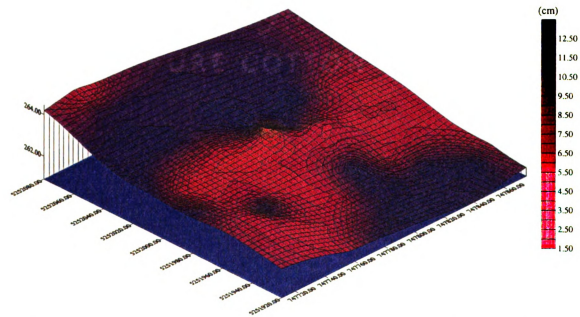

Figure 4.19.a. Soil water content (0-26 cm) on day-1 for *scenario 2* (3 different soil types, high rainfall, with restricting soil layer at 120 cm).

Figure 4.19.b. Soil water content (26-77 cm) on day-1 for *scenario 2* (3 different soil types, high rainfall, with restricting soil layer at 120 cm).

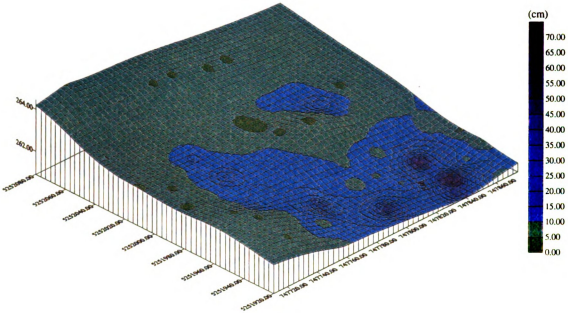

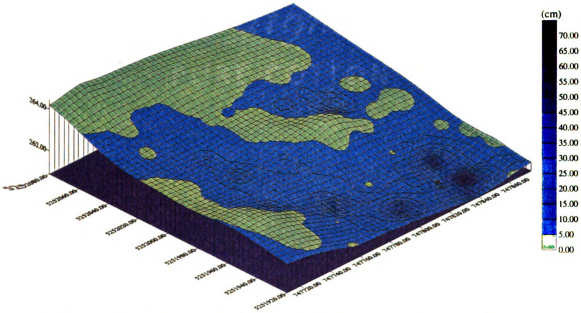

Figure 4.20.a. Cumulative surface water flow out of the elements on day-1 for *scenario 2* (3 different soil types, high rainfall, with restricting soil layer at 120 cm).

Figure 4.20. b. Cumulative surface water flow onto the elements on day-1 for *scenario 2* (3 different soil types, high rainfall,with restricting soil layer at 120 cm).

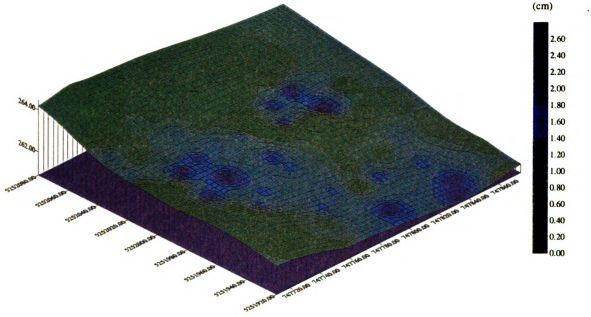

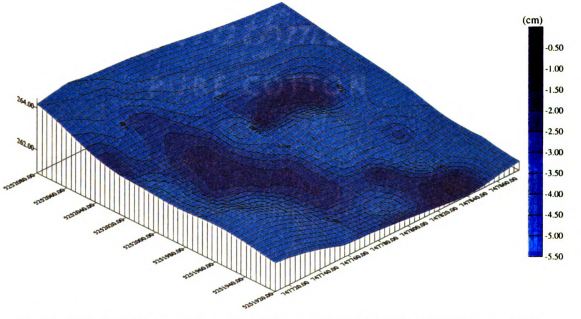

Figure 4.21. Surface ponding on day-1 for *scenario 2* (3 different soil types, high rainfall, with restricting soil layer at 120 cm).

Figure 4.22. Net surface flow (cm) on day-1 for *scenario 2* (3 different soil types, high rainfall, with restricting soil layer at 120 cm).

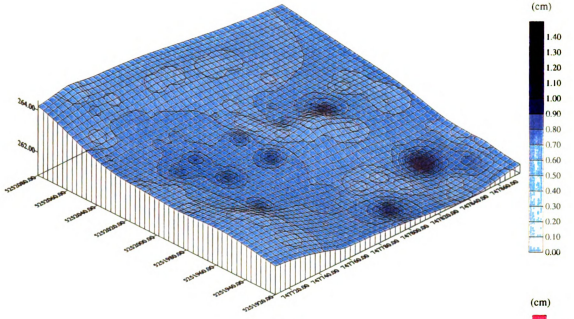

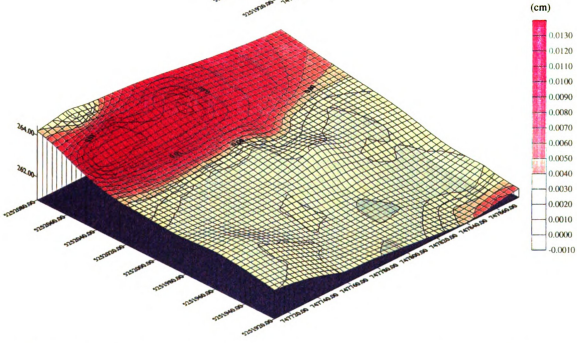

Figure 4.23. Subsurface lateral flow on day-1 for *scenario 2* (3 different soil types, high rainfall, with restricting soil layer at 120 cm).

Figure 4.24. Drainage on day-1 for *scenario 2* (3 different soil types, high rainfall, with restricting soil layer at 120 cm).

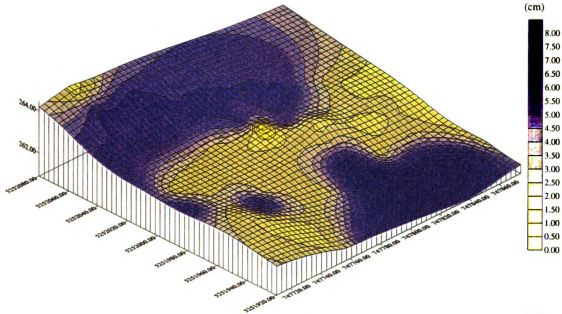

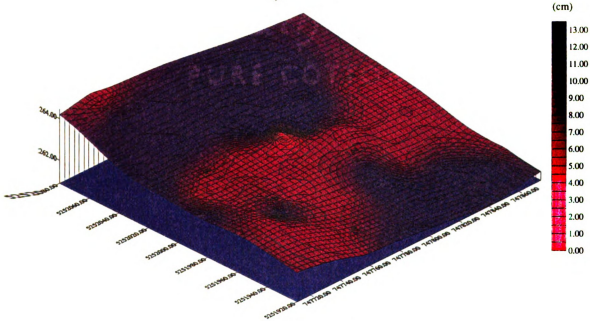

Figure 4.25.a. Soil water content (0-26 cm) on day-2 for *scenario 2* (3 different soil types,high rainfall, with restricting soil layer at 120 cm).

Figure 4.25.b. Soil water content (26-77 cm) on day-2 for *scenario 2* (3 different soil types,high rainfall, with restricting soil layer at 120 cm).

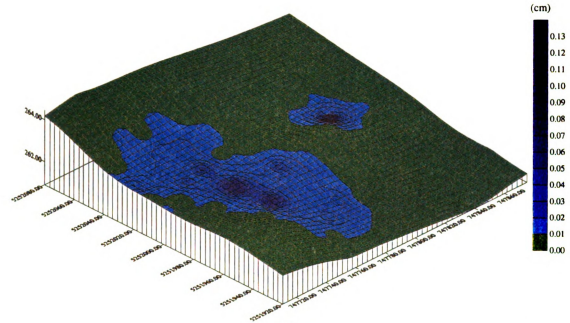

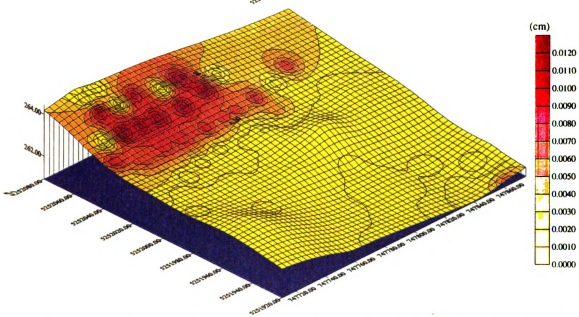

Figure 4.26. Subsurface lateral flow on day-2 for *scenario 2* (3 different soil types, high rainfall, with restricting soil layer at 120 cm).

Figure 4.27. Drainage on day-1 for *scenario 2* (3 different soil types, high rainfall, with restricting soil layer at 120 cm).

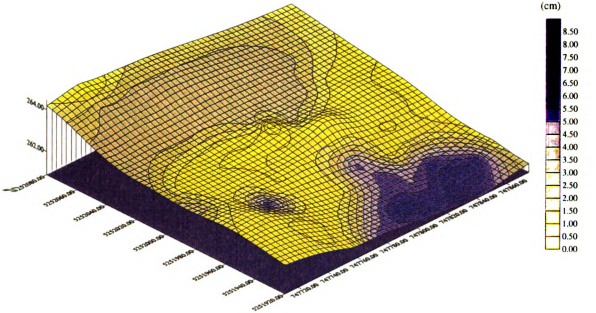

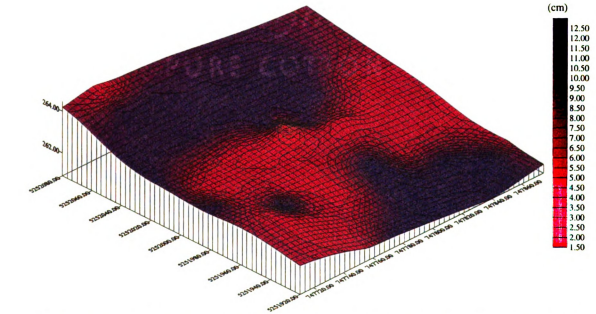

Figure 4.28. a. Soil water content (0-26 cm) on day-7 for *scenario 2* (3 different soil types, high rainfall, with restricting soil layer at 120 cm).

Figure 4.28. b. Soil water content (26-77 cm) on day-7 for *scenario 2* (3 different soil types, high rainfall, with restricting soil layer at 120 cm).

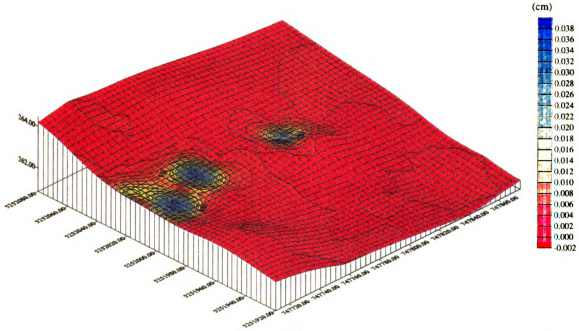

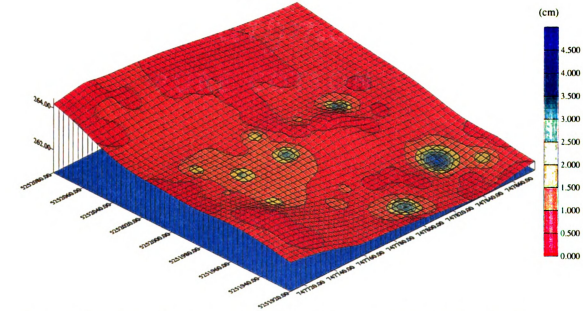

Figure 4.29. a. Subsurface lateral flow on day-7 for *scenario 2* (3 different soil types, high rainfall, with restricting soil layer at 120 cm).

Figure 4.29. b. Sum of subsurface lateral flow on day-7 for *scenario 2* (3 different soil types, high rainfall, with restricting soil layer at 120 cm).

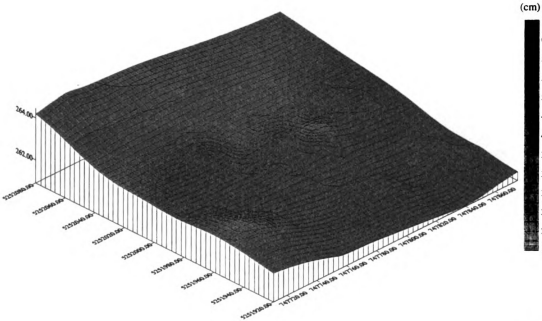

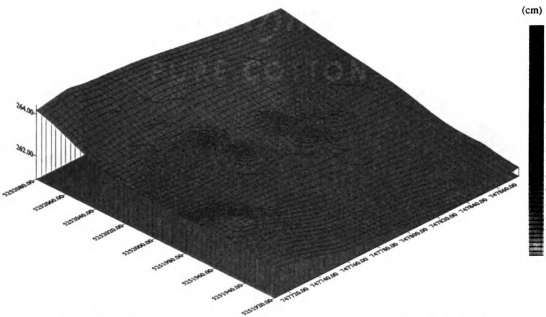

Figure 4.30.a. Simulated soil water content (0-26 cm) on day 184 (July 3) for *scenario 3* (3 different soil types, low rainfall, with restricting soil layer at 120 cm).

Figure 4.30.b. Simulated soil water content (26-77 cm) on day 184 (July 3) for *scenario 3* (3 different soil types, low rainfall, with restricting soil layer at 120 cm).

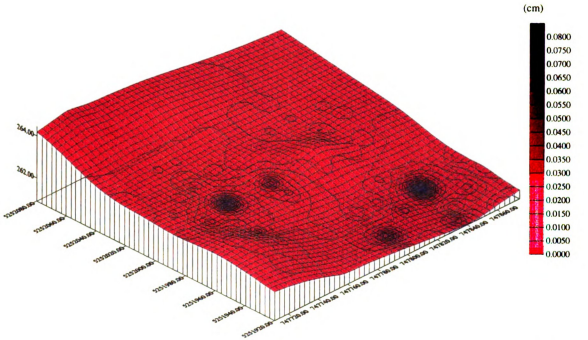

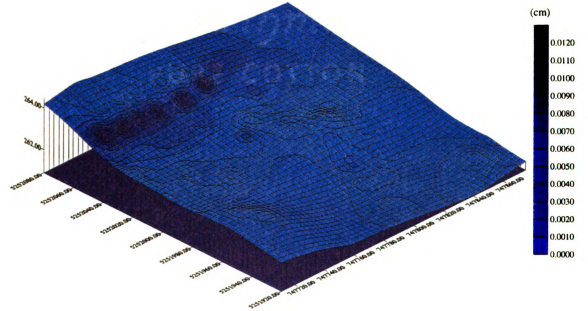

Figure 4.31. Subsurface lateral flow on day 184 (July 3) for *scenario 3* (3 different soil types, low rainfall, with restricting soil layer at 120 cm).

Figure 4.32. Drainage on day 184 (July 3) for *scenario 3*(3 different soil types, low rainfall, with restricting soil layer at 120 cm).

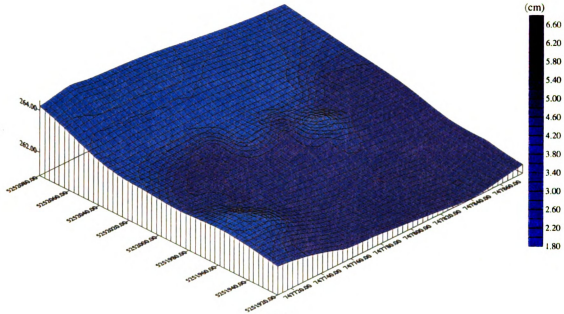

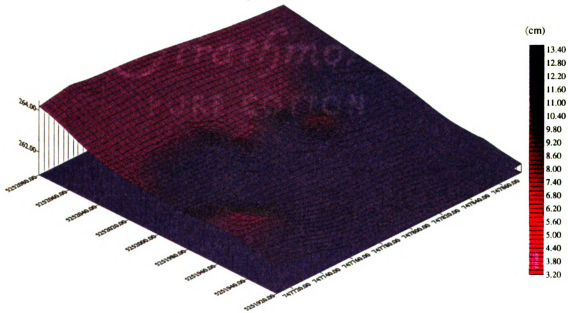

Figure 4.33 a. Simulated soil water content (0-26 cm) on day 188 (July 7) for *scenario 3* (3 different soil types, low rainfall, with restricting soil layer at 120 cm).

Figure 4.33 b. Simulated soil water content (26-77 cm) on day 188 (July 7) for *scenario 3* (3 different soil types, low rainfall, with restricting soil layer at 120 cm).

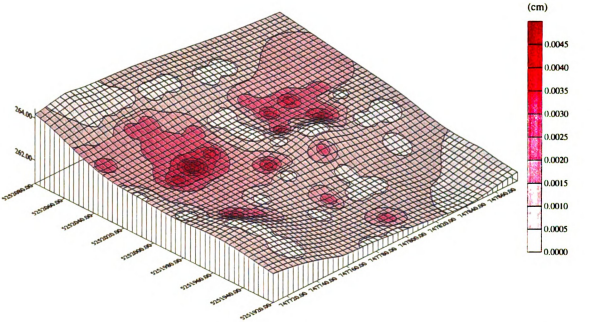

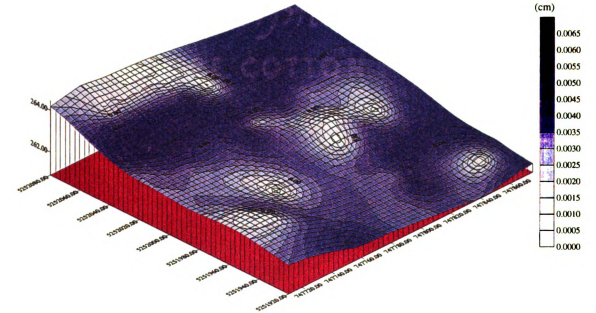

Figure 4.34. Subsurface lateral flow on day 188 (July 7) for *scenario 3* (3 different soil types, low rainfall, with restricting soil layer at 120 cm).

Figure 4.35. Drainage on day 188 (July 7) for *scenario 3* (3 different soil types, low rainfall, with restricting soil layer at 120 cm).

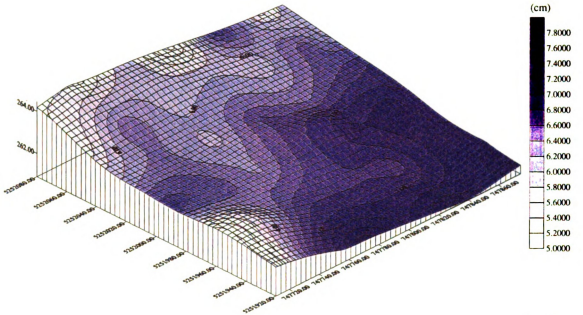

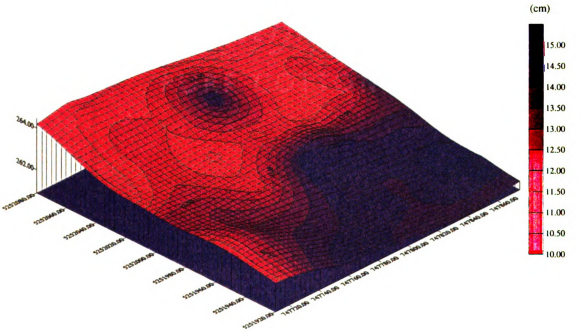

Figure 4.36. Measured soil water content (0-26 cm) on day 184 (July 3).

Figure 4.37. Measured soil water content (26-77 cm) on day 184 (July 3).

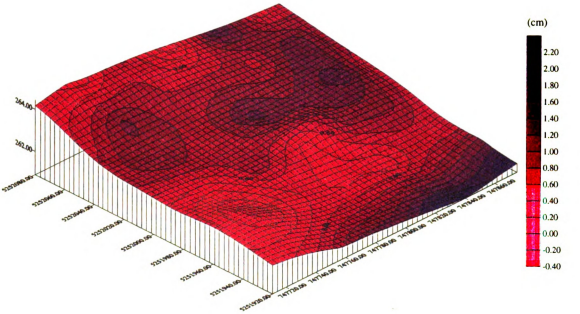

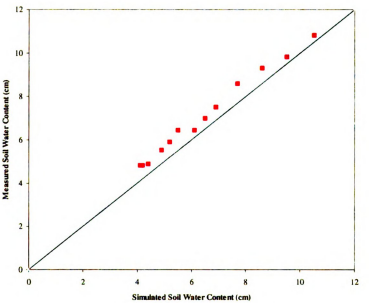

Figure 4.38.a. Error map of soil water content (0-26 cm) on day 184 (July 3) for *scenario 3* (3 different soil types, low rainfall, with restricting soil layer at 120 cm).

Figure 4.38.b. Measured and simulated soil water content (26-77 cm) for the entire season on the high elevation point (peak).

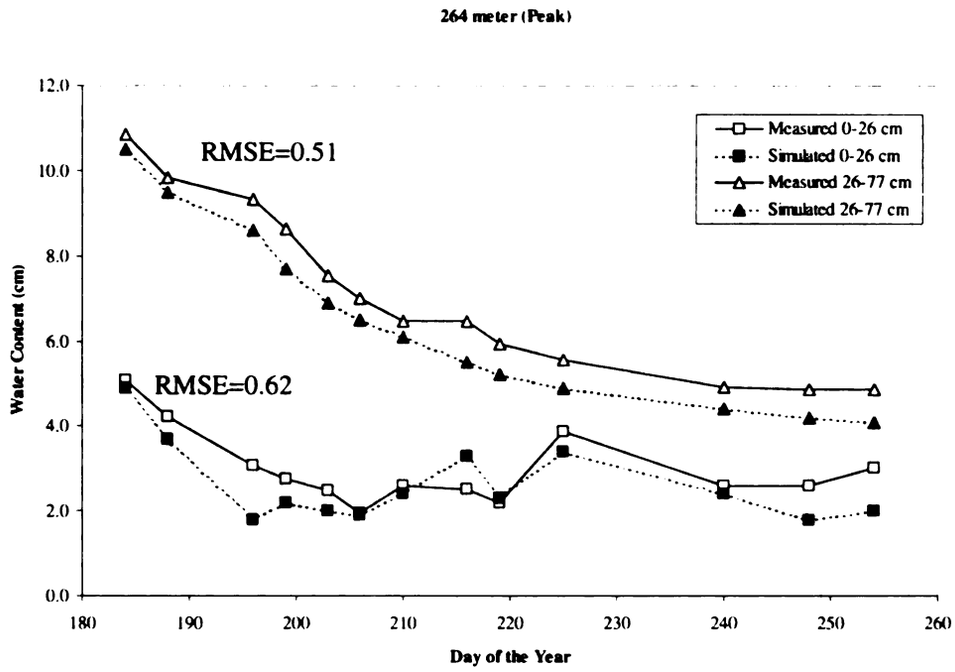

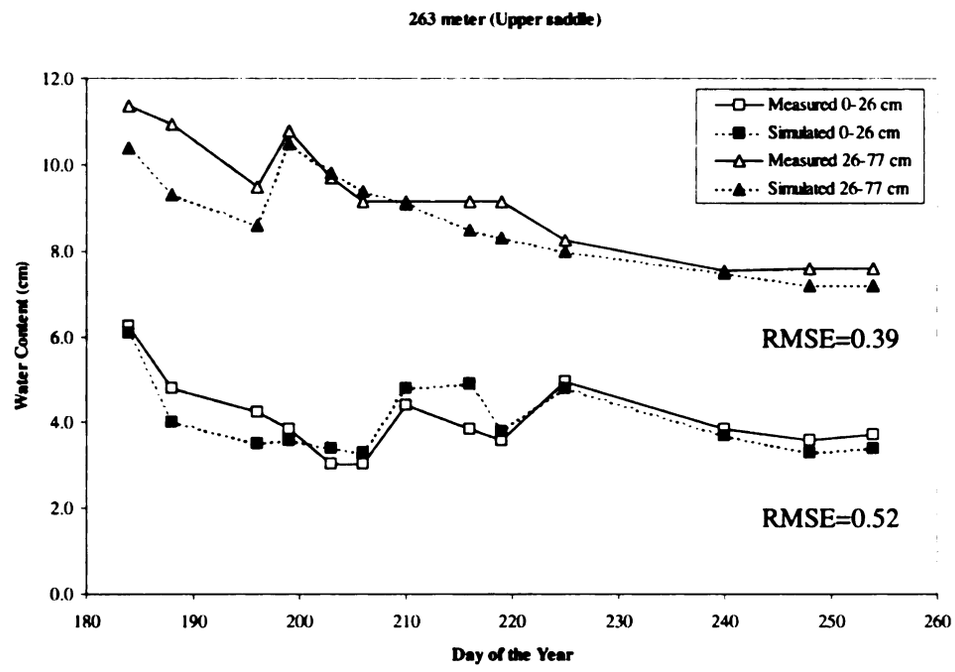

Figure 4.39 a. Measured and simulated water content for the soil profile (0-26 cm) and (26-77 cm) for the high elevation zone (peak) for the entire season.

Figure 4.39 b. Measured and simulated water content for the soil profile (0-26 cm) and (26-77 cm) for the medium elevation zone (upper saddle) for the entire season.

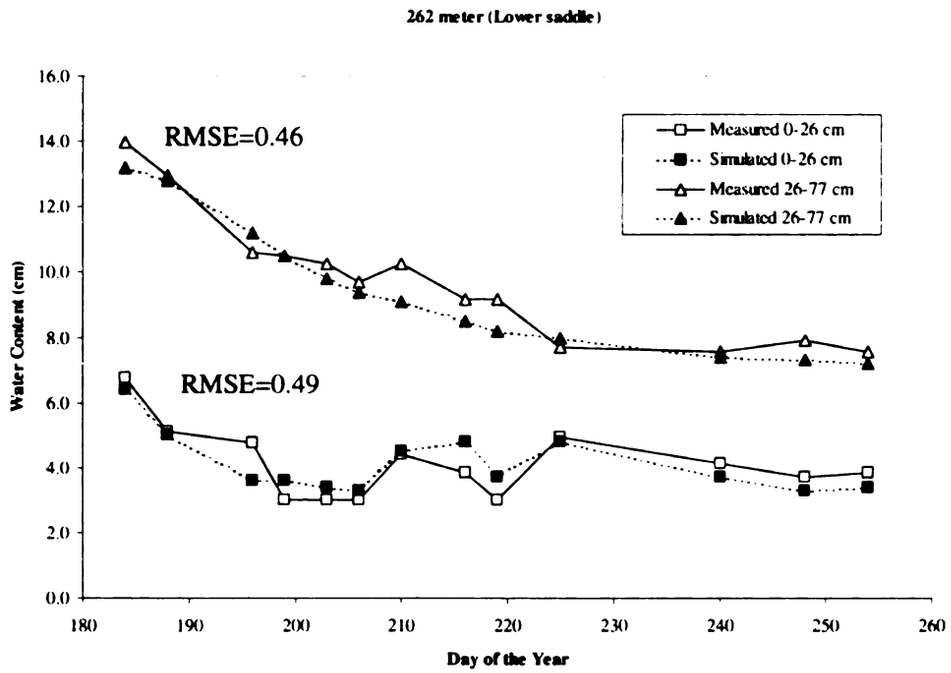

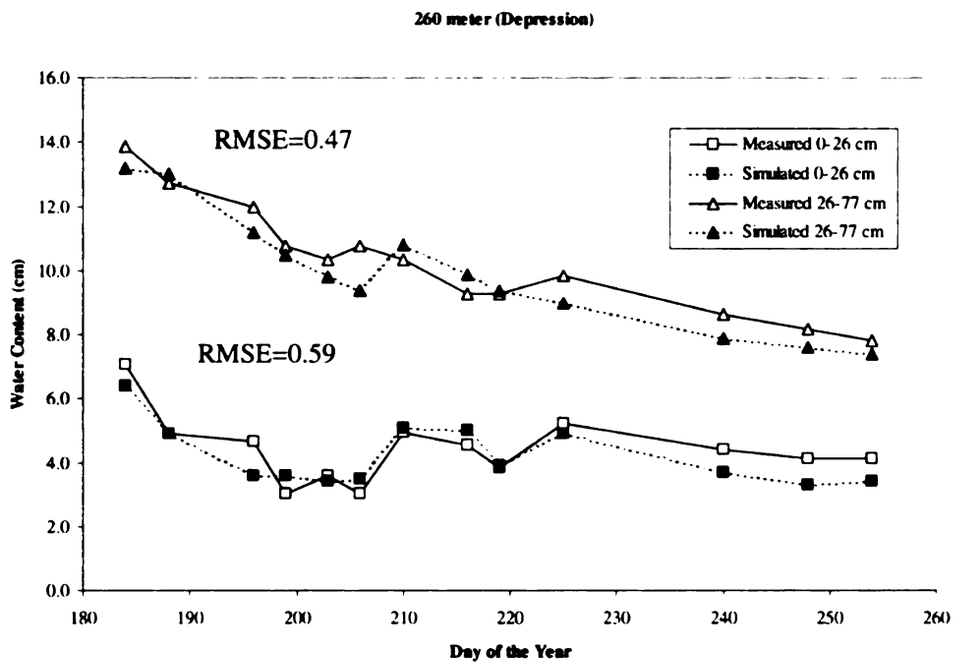

Figure 4.40 a. Measured and simulated water content for the soil profile (0-26 cm) and (26-77 cm) for the medium elevation zone (lower Saddle) for the entire season.

Figure 4.40 b. Measured and simulated water content for the soil profile (0-26 cm) and (26-77 cm) for the medium elevation zone (depression) for the entire season.

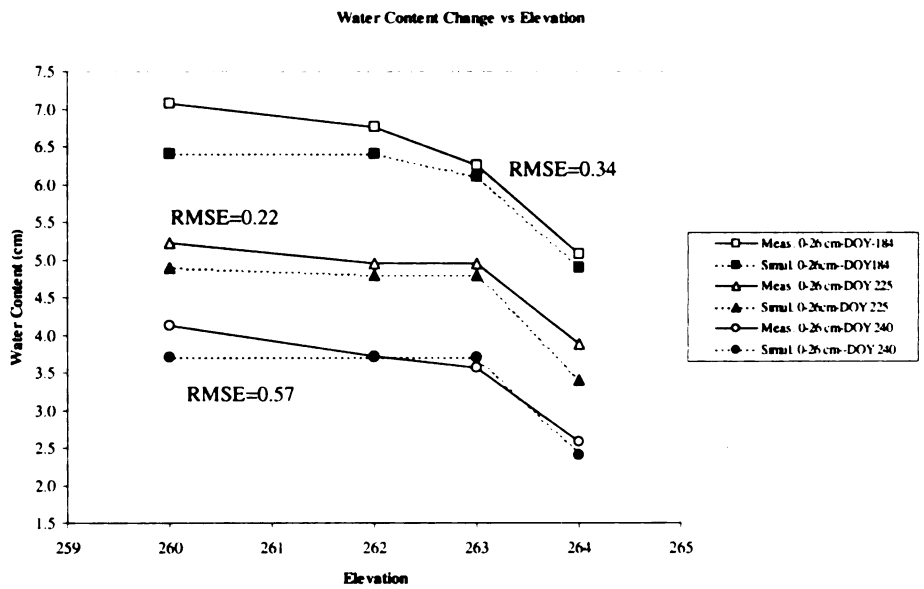

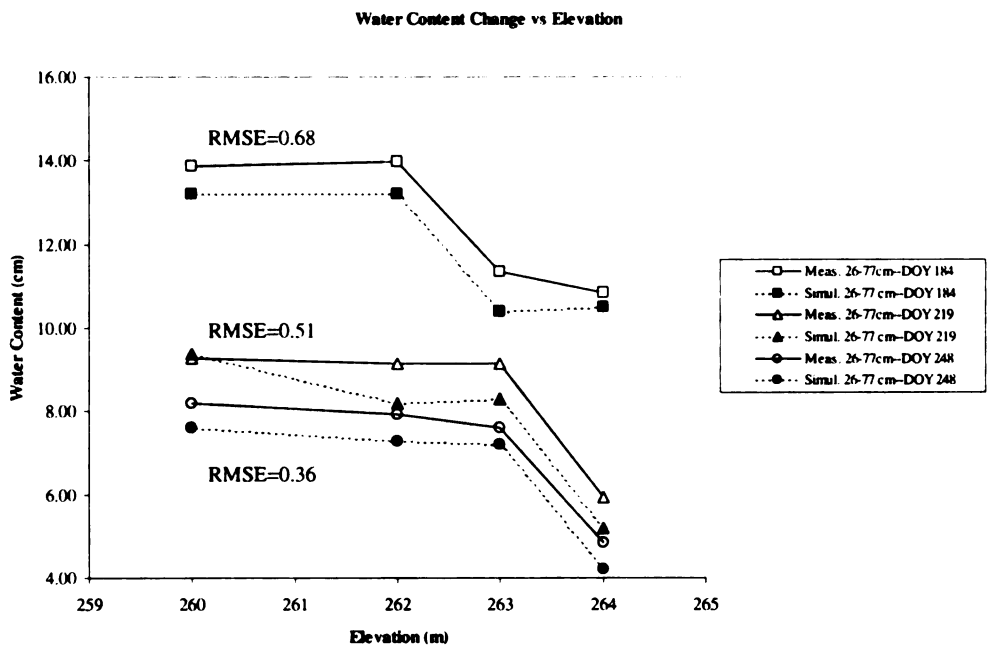

Figure 4.41 a. Water content change as function of elevation for 0-26 cm soil profile for day 184 (July 3), day 225 (August 13) , and day 240 (August 28).

Figure 4.41 b. Water content change as function of elevation for 26-77 cm soil profile for day 184, day 219 (August 7), and day 248 (September 5).

CHAPTER V

UNDERSTANDING SOYBEAN YIELD VARIABILITY USING CROP MODELS AND REMOTE SENSING

5.1. Introduction

Agricultural production systems are inherently variable due to spatial variation in soil properties, topography, and climate. To achieve the ultimate goal of sustainable cropping systems, variability must be considered both in space and time because the factors influencing crop yield have different spatial and temporal behavior (Pierce and Nowak, 1999). Advances in technologies such as Global Positioning Systems (GPS), Geographic Information Systems (GIS) and remote sensing have created the possibility to assess the spatial variability present in the field and manage it with appropriate site-specific practices (Verhagen et al., 1995). Site-specific management (SSM) strategies may be able to optimize production, but their potential benefits are highly dependent on the accuracy of the assessment of such variability (Pierce and Nowak, 1999).

Traditional analytical techniques, such as regression of static measurements against yield, have failed to explain the reasons for yield variability because the dynamic, thus temporal, interactions of stresses on the crop growth and development cannot be accounted for (Jones et al., 1989; Cambardella et al., 1996; Sudduth et al., 1996). Process

oriented crop simulation models, such as the CERES and CROPGRO models (Ritchie et.al, 1998; Boote et al., 1998), have the capability to integrate the effects of temporal and multiple stress interactions on crop growth processes under different environmental and management conditions. Even though crop models have shown high potential for optimizing production and minimizing environmental impact, their application for SSM has been limited thus far. Crop models can be used for understanding yield variability, leading to a more sustainable environment (Sadler and Russell, 1997, Cora et al., 1998). Batchelor et al. (1998) and Paz et al., (1999), used CERES-Maize and CROPGRO-Soybean simulation model to determine the effect of soil water variation throughout the season on yield spatial variability optimizing for soil water limit parameters. The differences between measured and simulated yield for 224 grid points over a 3 year period ranged from ± 10% for 70% of the grids and ± 20% for 96% of the grids in maize and for soybean from ± 10% for 84% of the grids and ± 20% for 92% of the grids.

Recent advances on the resolution and availability of remote sensing imagery, coupled with a decrease in its associated costs, have allowed the collection of timely information on soil and crop variability by examining spatial and temporal patterns of vegetation indices (Moran et al., 1997). Such information can be useful to derive inputs for crop models in a GIS environment (Moran et al., 1997; Barnes et al., 1998, Johannsen et al., 1999). Vegetation indices involve mathematical relationship between near infrared and red reflectances and they have been extensively used with the goal of estimating vegetation amount (Wiegand et al., 1990; Jackson and Huete, 1991; Price, 1992). Among vegetation indices, the normalized difference vegetative index (NDVI) is the one most

commonly used to quantify canopy vigor and density (Price, 1992; Carlson and Ripley, 1997). NDVI is defined as:

$$NDVI = \frac{NIR - RED}{NIR + RED}$$

where NIR and RED represent the surface reflectance averaged over ranges of wavelengths in the near infrared ($\lambda \sim 0.8$ μm) and the visible ($\lambda \sim 0.6$ μm) regions of the spectrum, respectively. NDVI increases almost linearly with increasing leaf area index (LAI, leaf area per unit land area) until LAI exceeds values of 3-4, above which NDVI rapidly approaches an asymptotic limit (Liu and Huete 1995; Jasinski 1996, Carlson and Ripley, 1997). NDVI analysis performed on images taken at critical times during a growing season can help characterize spatial variability in crop performance.

Clearly, the goal of crop simulation in precision agriculture is to explain the spatial variability of crop performance mapped with grain yield monitoring systems and to help guide in management decisions related to the site-specific management of crop inputs. It is also clear that crop simulations cannot be performed everywhere given that the cost and the availability of detailed inputs would be prohibitive. A more balanced approached to the application of crop simulation models to precision agriculture would be to delineate zones within the field of similar crop performance. One approach may be to obtain vegetation indexes derived from remotely sensed imagery during critical times during the growing season to select spatial patterns to sample and to use the results of the target sampling as inputs for the models. Model validation can be performed at selected sites within these delineated management zones.

The objective of this study was to examine a new procedure for spatial validation of crop models for use in precision agriculture that uses the CROPGRO-Soybean model to simulate soybean performance using a progressive increase of spatial inputs. The procedure also uses the crop model to validate management zones across the field delineated using a NDVI classification procedure.

5.2. Materials and Methods

5.2.1. Site Description and Field Measurements

The study area consisted of a seven ha portion of a field located 10 km south of Durand, MI. The field has been cropped to a corn-soybean rotation for more than 10 years. Soils are variable containing five soil map units and considerable spatial variability in soil fertility (Pierce et al., 1995; Pierce and Warncke, 2000) with the major soil type in the experimental area mapped as Capac loam (Udollic Ochraqualf fine, loamy, mixed, mesic). Soybean was grown in 1997. The field was planted on May 5 by direct drilling soybean (Variety Asgrow 1901, a Roundup Ready variety) in 37-cm rows at a seeding rate of 494,000 seeds ha^{-1}.

A regular grid consisting of 52 grid locations spaced 30.5 m apart was imposed on the 7 ha experimental area after planting. Latitude, longitude and elevation of each grid point were determined with a high-resolution differential GPS. Neutron probe access tubes

were installed at each of the 52 grid locations. A neutron moisture gauge was used to measure the spatial variability of soil water content at 15-cm increments to the depth of the C horizon or a maximum of 150 cm depth, which ever occurred first. Measurements were taken on a weekly basis throughout the season. During the installation of the neutron probe access tubes, soil samples were taken at the intersection of each of the 52 grid points in 25-cm increments and stored for analysis Soil samples were air-dried and passed through a 2 mm sieve. Particle size was determined for each segment of each soil profile using the hydrometer method. Soil organic matter was determined on the surface 25 cm of each soil profile by dry combustion using a CHN analyzer (Carlo Erba Instruments, Italy). The upper and lower limits of soil water availability were determined using soil water measurements taken in the field during the season, and also from using Ritchie's simple model to estimate soil water limits using soil texture data (Ritchie et al., 1999). Soil depth for each grid point was determined using the deepest depth observed during the installation of neutron probe access tubes. Potential extractable soil water (PESW) was determined by subtracting the lower limit of plant water availability from the upper limit for each soil layer and integrated for the entire profile.

A 5 m^2 area was delineated at each grid location for selected plant measurements. Plant population and the distance between plants were measured at emergence (May 20) and at the 3rd leaf stage of development (June 15). A non-destructive optical device with a fish-eye sensor (LAI- 2000; LI-COR) was used to quantify the LAI at the 52 grid points on July 15 and August 10. Soybean yield was obtained by harvesting four rows along a 20 m

length centered on each grid point using a plot combine. Grain moisture was obtained after harvest on a subsample from each harvested area.

A datalogger (Licor 1000) was installed to collect weather data on solar radiation, minimum and maximum temperature and precipitation, which are required as model input. Precipitation was measured with an electronic tipping-bucket rain gauge every five minutes to record rainfall intensities as well as daily total amounts.

Standard statistical analyses were done for the variables measured in the field. The spatial structure for each parameter was assessed thorough a semivariance analysis. Measurements taken on each grid point were interpolated using the punctual kriging technique available in GS+ Version 3.1a (Gamma Design Software, 1999). Correlation matrices were developed to determine the relationships among variables for each single class and for the 52 grid points.

5.2.2. Remote Sensing Data

The airborne false color composite images in the green, red and NIR portion of the spectrum were taken on June 1, June 28, July 18, July 29, August 13, August 29, September 15 at 1 meter pixel resolution. The images provided spatial information about the condition of the crop throughout the season. Each image was used to generate NDVI maps of the field and to identify spatial patterns across the field. The false color composite image taken on July 18 (figure 5.1a) was selected for quantifying areas with

similar reflectance by grouping areas into classes of similar NDVI values (Figure 5.2) using supervised classification technique available in Idrisi v32 software (Clark Labs, 1999). Pixels of similar reflectance were queried across the field after trying various ranges of values able to reproduce the spatial patterns visible in the original false-color composite image (Figure 5.3).

5.2.3. Crop Growth Model

CROPGRO-Soybean v.3.5 is a process oriented model that simulates plant responses to environmental conditions (soil and weather), genetics and management strategies. A detailed description of the inputs required for the model is described in Ritchie and Dent (1990). This model is part of the Decision Support System for Agrotechnolgy Transfer (DSSAT 3.5, Hoogenboom et al., 1998) that provides several tools for model application. The soil water limits used to run the simulation experiments varied spatially and according to the observed data of soil texture and soil water content at the 52 grid points. The model was evaluated using the Root Mean Square Error (RMSE):

$$RMSE = \left[\frac{1}{n} \sum_{i=1} \left(y_i - \hat{y}_i \right)^2 \right]^{1/2}$$

where y_i are the measurements, $\hat{y}_i$ the predictions, and n is the number of comparisons.

5.2.4. Simulation Experiments

The soybean model was used to simulate yields in the field using progressive increase of spatial inputs. Yields simulations were made using five different scenarios. These scenarios varied from one that assumed uniform soil and management conditions across the field to one that used field-measured, spatially variable inputs for the soil water balance parameters (LL, DUL, SAT and soil depth) and plant populations, to one that simulated three areas identified by the NDVI analysis. The five cases are described in table 5.1.

5.3. Results and Discussion

5.3.1. Field Measurements

The yield was spatially variable across the field (Figure 5.2a), ranging from 1900 to 3600 kg ha^{-1} with a mean value of 2953 kg ha^{-1} and a standard deviation of 433 kg ha^{-1}. The spatial distribution of yield was consistent with other field measurements (LAI and plant population) and by the remote sensing image that showed high reflectance in the high yielding areas (Figure 5.1 and 5.2).

Field measurements of LAI on August 8, (Figure 5.2b), reflected the different soil water regimes present across the field. The highest value of LAI was 4.6 and it was observed in

areas of high plant population, deeper soil and high PESW. The areas of the field with rocky soil and highest elevation had the lowest LAI value of 1.7. The mean and the standard deviation for LAI were 3.6 and 0.6 respectively. The areas showing high LAI corresponded with the remote sensing image areas with high reflectance as depicted in figures 5.1 and 5.2.

Record cool weather in May delayed soybean emergence and resulted in variable population densities across the field (Figure 5.2c). Plant populations varied from 22 to 60 plants m^{-2} with a mean value for the 52 grid-points of 47 plants m^{-2} and a standard deviation of 8 plants m^{-2}. Plant stand is highly influenced by the environmental condition (soil and weather) at planting time.

Soil textural analysis from the 52 grid-points showed high spatial variability for sand and clay particles. The clay content varied across the field from 8% in soil of the high relative elevation areas to 25% in soil in low relative elevation areas. Sand percentage varied from a minimum of 40% to a maximum of 82% and logically had an opposite spatial distribution from the clay content. Based on textural analysis results and their spatial distribution, three main soil types were detected across the field. A deep-dark sandy-loam soil located in lower elevation areas of the field, a sandy loam characterizing the flat areas and a sandy-rocky soil present in the higher elevation areas.

Soil depth measurements also showed the presence of high spatial structure across the field (Figure 5.3a). Spatial variations in soil depth had similar trends as clay (Figure

5.3b). Peaks had lower soil depth due to erosion phenomena. Soil depths ranged from 95 cm to 150 cm with a mean value for the 52 grid-points of 130 cm and a standard deviation of 14-cm.

Potential extractable soil water (PESW) values are shown in Figure 5.3c. PESW is a function of soil depth and soil texture, thus the spatial distribution of these variables were similar. A maximum PESW of 140 mm was observed in the low elevation areas, while the lowest value of 70 mm was found at high elevations. The mean PESW value for the field was 111 mm with a standard deviation of 19 mm.

The field is characterized by a rolling terrain that caused high spatial variability of soil properties. Landscape position and relative elevation highly influenced soil physical properties thorough erosion processes that occurred over the years (Mueller, 1998). The spatial dependence was determined for each soil and crop variable measured in the field. Geostatistical analysis revealed spatial structure for all the variables giving ranges of distance that varied from 60 m for the plant population to 150 m for the yield (Table 5.2a). The spherical model fitted the semivariance well. Table 5.2b reveals that the yield measured at the 52 grid points is highly correlated to LAI, PESW and NDVI as shown by the correlation coefficients of 0.86, 0.87 and 0.97.

5.3.2. Simulation Experiments

5.3.2.1. Scenarios 1-4

Error in yield prediction decreased as the level of input detail increased for the simulation scenarios tested (Table 5.1). The field average of 2995 kg ha^{-1} was underestimated under scenario 1 which predicted a soybean yield of 2530 kg ha^{-1}. The RMSE for scenario 1 was 465 kg ha^{-1}. Under scenario 2, adding site-specific plant population data as model input improved model performance by decreasing the RMSE to 296 kg ha^{-1}, a reduction of 36 % over scenario 1. Using site-specific soils data at constant plant populations in scenario 3 improved yield prediction 18 % more than scenario 2 as evidenced by an RMSE of 245 kg ha^{-1} and 47% over scenario 1. Using both site-specific soils and plant population input further reduced RMSE improving the prediction of soybean yield over scenario 1 by 58% (Figure 5.4a).

5.3.2.2. NDVI Classes

The 18 July composite image and the corresponding NDVI image clearly show spatial variability in soybean performance (Figure 5.1b). The correlation between NDVI and crop yield for the 52 grid points was very strong (Figure 5.5). Classification of the NDVI image indicated three classes of importance in this field. Note that the areas of different classes are not contiguous. Table 5.3 summarizes the areal distribution and properties of these classes as well as the data for soils and plant populations used as input in the crop

simulations under scenario 5. Yield predictions for the three NDVI classes were very good as evidenced by an RMSE values for the three classes (Table 5.4, Figure 5.1c). These RMSE were the lowest of all crop simulation scenarios evaluated showing that the NDVI reclassification procedure adopted in the study was appropriate and proven to be a useful way of creating zones in the field. Multi-year simulation with this approach would allow for the characterization of the field.

The progressive use of site specific model inputs combined with the NDVI-reclassification has a major advantage over an issue that thus far has limited the power and application of simulation model in precision agriculture: scale! The site-specific input approach is scale-independent because the scale is controlled by the observed variation in the field and that is the scale at which the model will be applied.

5.4. Conclusion

Analysis of remote sensing imagery processed into the NDVI identified the spatial patterns of crop growth variability. The variability in soybean populations within the field provided validation of the plant population and soil type effects on soybean yields predicted by the CROPGRO- Soybean model. The model gave accurate predictions of the yield across the field when the correct inputs were used showing great potential for use in yield map prediction and interpretation in the context of site-specific management. This

study showed that the soil types present in the field could be managed differently using different cultivars or plant density to achieve higher yield while minimizing the costs.

It is clear that zone-specific management to optimize production can be developed through a combination of remote sensing and simulation models. This is a more affordable alternative to the use of traditional soil sampling and micro-scale sensing. It also answers questions related to the scale issue by applying the model at the scale of variability observed through remote sensing and NDVI image reclassification.

Scenario No.	Model Input	Model Runs	RMSE Kg ha^{-1}
1	Average of grids (Average soil type and target plant population)	1	465
2	Average soil type and grid plant population	52	296
3	Grid soil type and target plant population	52	245
4	Grid soil type and grid plant population	52	198
5	Average soil and plant population for 3 NDVI Classes	3	101

Table 5.1. Model inputs, number of model runs and RMSE for each simulation scenarios.

Variables	**Model**	**Nugget**	**Sill**	**Range**
Yield	Spherical	0.295	1.294	150
LAI	Spherical	0.279	1.156	120
Plant Population	Spherical	0.110	1.094	60
Soil Depth	Spherical	0.202	1.149	100
Clay	Spherical	0.210	1.095	110
PESW	Spherical	0.281	1.107	100

Table 5.2a. Semivariograms parameters for the variables measured in the field.

Variables	**LAI**	**Plant Population**	**Yield**	**Elevation**	**Soil Depth**	**% Clay (0-75 cm)**	**% Sand (0-75cm)**	**PESW**	**NDVI**
LAI	1								
Plant Population	0.76	1							
Yield	0.86	0.68	1						
Elevation	-0.42	-0.44	-0.49	1					
Soil Depth	0.32	0.26	0.31	-0.18	1				
% Clay (0-75 cm)	0.05	0.07	0.03	-0.15	0.17	1			
% Sand (0-75cm)	-0.18	-0.18	-0.13	0.14	-0.23	-0.81	1		
PESW	0.82	0.64	0.87	-0.46	0.32	0.19	-0.34	1	
NDVI	0.87	0.65	0.97	-0.48	0.29	0.09	-0.18	0.88	1

Table 5.2b. Correlation matrix among variables measured in the field at the 52 grid-point.

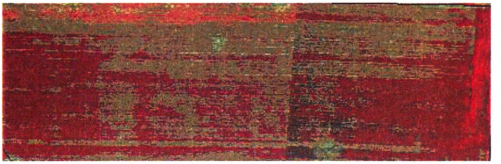

Figure 5.1 a. False-color composite image taken on July 18, 1997 (original image delivered by Emerge).

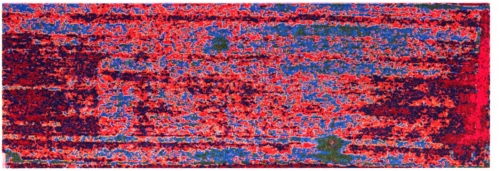

Figure 5.1 b. NDVI Image.

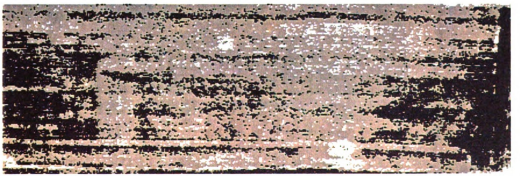

Figure 5.1 c. Reclassified NDVI Image. The areas in white are NDVI-Class 1, the areas in grey are NDVI-Class 2 and the areas in black are NDVI-Class 3.

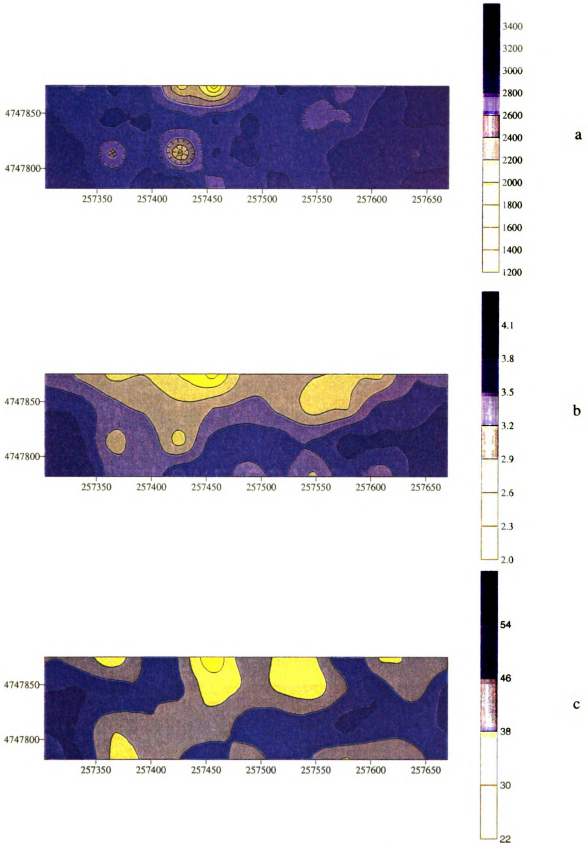

Figure 5.2. Krigged map of measured soybean yield (Kg ha^{-1})(a); LAI measured on August 8 (b); plant population measured on June 5 (plant m^{-2}) (c).

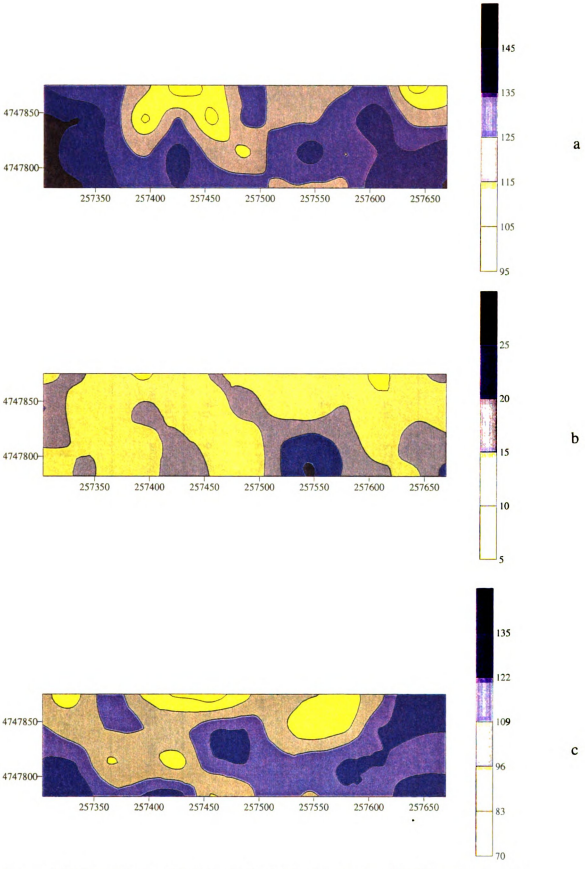

Figure 5.3. Krigged map of soil depth (cm) (a); clay content (%) (b); and potential extractable soil water (mm) (c).

Class ID	Cell Counts	NDVI Class Range	LAI		Plant Population		Yield		Elevation		Soil Depth		PESW		NDVI	
			Mean	St.Dev	Mean (pl m^{-2})	St. Dev. (pl m^{-2})	Mean (Kg ha^{-1})	St. Dev. (Kg ha^{-1})	Mean (m)	St. Dev. (m)	Mean (cm)	St. Dev. (cm)	Mean (mm)	St. Dev. (mm)	Mean	St. Dev.
1	3159	0-0.25	2.16	0.41	36	13	1635	339	263.6	0.8	110	22	73	6	0.10	0.03
2	42528	0.25-0.5	3.24	0.44	42	7	2729	217	262.7	0.4	128	7	94	9	0.43	0.05
3	23916	>0.5	3.95	0.38	50	7	3155	183	262.4	0.7	134	13	120	12	0.59	0.05
52 Grid Points	69603	_	3.6	0.6	47	8	2953	433	262.5	0.7	130	14	111	19	0.51	0.14

Table 5.3. Variables measured in each NDVI class and average for the 52 grid points.

Simulation Experiments	Number of Grid Point	Total Area (ha)	Measured Yield (Kg ha^{-1})	Simulated Yield (Kg ha^{-1})	RMSE (Kg ha^{-1})
Average Inputs within **NDVI-Class 1**	7	0.32	1199	1216	17
Average Inputs within **NDVI-Class 2**	15	4.25	2785	2802	17
Average Inputs within **NDVI-Class 3**	30	2.39	3087	3203	116
Weighted Average across **all NDVI Classes**	52	6.96	2849	2950	101

Table 5.4. Summary table for measured and simulated yield for each NDVI Class and area weighted average across the field.

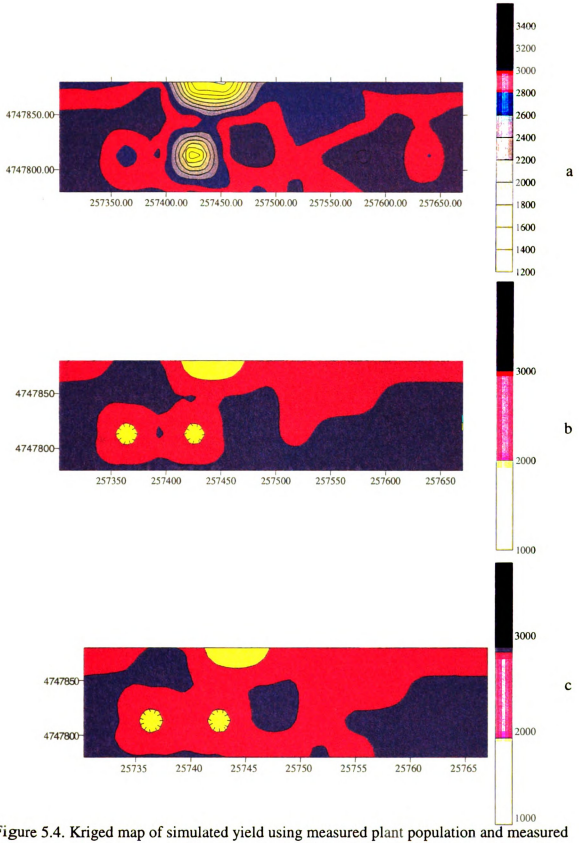

Figure 5.4. Kriged map of simulated yield using measured plant population and measured soil type for the 52 grid point (a); measured yield for the three NDVI classes (b); simulated yield for the three NDVI classes using average measured inputs.

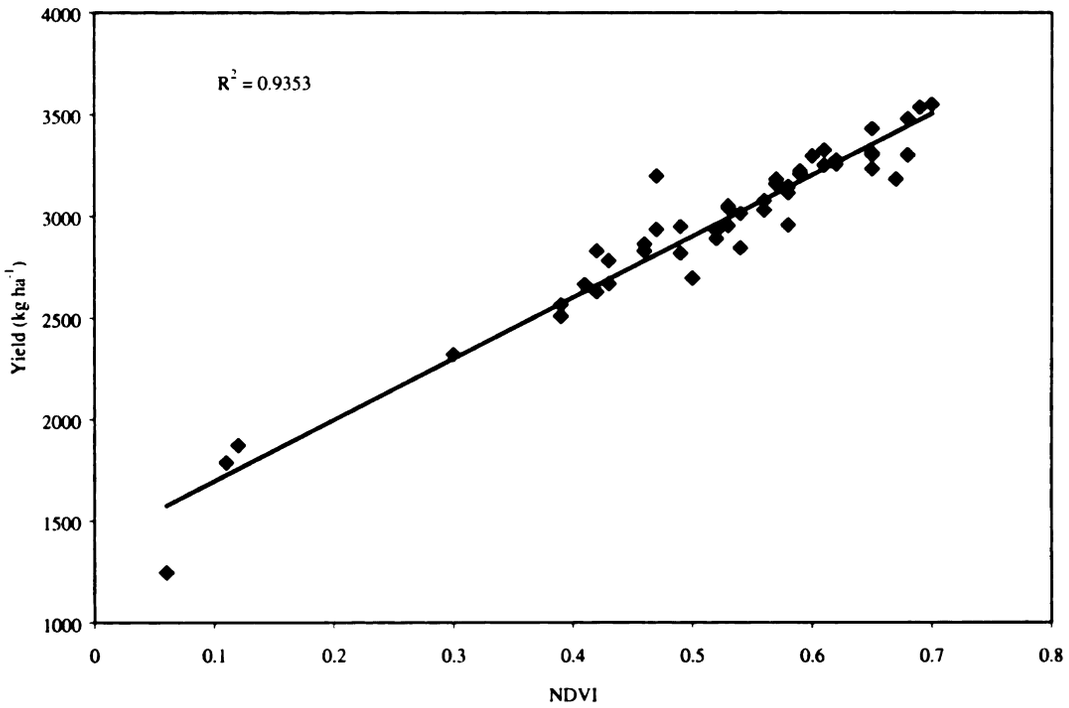

Figure 5.5. Correlation between NDVI (image taken on July 18) and yield.

CHAPTER VI

CONCLUSIONS AND RECOMMENDATIONS

This chapter summarizes the importance of using simulation modeling and digital terrain analysis to evaluate the effect of topography and soil physical properties on spatial soil water balance.

Chapter one presented the rationale and background of this dissertation. A detailed literature review (chapter two) was done for the terrain analysis, reviewing existing digital terrain models and soil water balance models. From this chapter, it was shown that a new hybrid model that combined a digital terrain model with a spatially sensitive soil water balance was needed in order to better simulate water movement over the terrain. The terrain model and the spatial component of the soil water balance models were discussed in chapter three. The model was able to partition the landscape into an interconnected series of element network from a grid DEM. The soil spatial water balance of SALUS was able to partition the downward water flow in the vertical and horizontal dimensions. The model was rapid in its simulations and output outcome.

Chapter four was the primary focus of this dissertation. In this chapter, data were presented on the newly developed TERRAE-SALUS model and its ability to simulate the spatial soil water balance as affected by landscape topography. The model was applied at a field scale in Durand, Michigan, were an extensive data set on soil water measurements was available. The RMSE between model and observed results varied from 0.22 cm to 0.68 cm of water. In addition, two scenarios were presented illustrating the model capabilities to partition the subsurface lateral flow and the vertical drainage as well as the surface water runoff-runon as affected by landscape positions and by rainfall amount. TERRAE-SALUS was able to simulate satisfactorily the soil water content. The biggest advantage of this model appears to be its simplicity and at the same time accuracy. Due to the functional approach of the soil water balance, the data inputs requirements are also minimum and easy to obtain.

Chapter five described the integration of the current technology available in agriculture to predict the spatial variability of soybean yield. The crop simulation model CROPGRO was applied in combination with remote sensing data to evaluate the capability of the model to identify factors responsible for the yield variation in a spatially variable landscape. Results from this study showed that a combination of crop simulation model and remote sensing can identify management zones and causes for yield variability, which are prerequisites for zone-specific management prescription.

The processes of modeling the soil water balance over space and time is of crucial importance for the appropriate management of the water resources, especially in areas

where they are in continuous jeopardy. Although, this is not an easy task due to the difficulties related to the complexity of the soil-water-atmosphere systems, uncertainty of weather, and lacking of good quality data to be used for the model evaluation. The scale issue is also a restriction on the power of the existing simulation models if applied at the inappropriate scale to simulate a process characterized by different scale characteristics. Moreover, it must not be forgotten that any model is a simplification of reality. If the biological processes modeled were not dynamic, the modeling of such system would have been much easier.

In the case of this study, TERRAE-SALUS has been shown to produce satisfactory results in its field application. The accuracy of the model results is highly dependent on the quality of inputs used, especially pertaining to soil characteristics, elevation data and weather information. Further investigations are recommended to evaluate approaches to the problems of up scaling model simulations. The up-scaling is not solely achieved by running the model patch scale models for larger areas consisting of many patches, but that different processes and connectivities emerge as dominant as we move from the plot scale to catchment scale. The promising results showed by TERRAE-SALUS demonstrated that its application can be beneficial in water resources management. My vision for the future is that digital terrain modeling will be become increasingly important in simulating the most sustainable soil and water resources management practice. The application of DTM can help in identifying areas across the landscape more susceptible to erosion and with the highest surface runoff. Moreover, the model does not need to be applied on the entire landscape, requiring large amount of inputs but it can be executed

on small areas and then extend the output to areas that are alike across the landscape, avoiding in this way repetitive data collection, not necessarily needed.

APPENDICES

APPENDIX A

USING TERRAE

TERRAE requires a grid DEM. TERRAE is run with a single argument specifying the parameter file:

```
Unix> TERRAE dem.params
```

The parameter file contains all the information required to run the program, including the names of the DEM, channel head and boundary files as well as numeric parameters such as the maximum sink depth and logical parameters specifying which components of TERRAE are active. The most commonly used parameters are:

- Grid file = dem.flt

  The name of the DEM file exported from ARC/INFO using GRIDFLOAT. TERRAE expects to find the header file (eg dem.hdr) in the same directory as the binary DEM file. A full path name may be used. This parameter must be set (there is no default).

- Channel head file = channels.txt

  The channel heads, as ASCII x y values one per line. This is an optional parameter; if it is not set or the file cannot be opened, channel heads will not be used.

- Diversion line file = boundary.ung

  The boundary polygon in ARC/INFO ungenerate format. This is an optional

parameter; if it is not set or the file cannot be opened, no boundary polygon will be used.

- Remove sinks = yes or no

  If yes, sinks will be cleared if they are within the depth and/or distance thresholds. Default is yes.

- Sink depth threshold = number

  The maximum depth of a depression that will be considered a spurious sink. There is no default value, so if "Remove sinks" is set, a value must be provided.

- Sink draining distance threshold = number

  The maximum distance from sink to saddle for a spurious sink. The default value is twice the grid spacing.

- Sink threshold combine logic = AND or OR

  Use AND if both thresholds must be satisfied to drain the sink; use OR if either can be satisfied. Default is OR.

- Construct polygons = yes or no
- Construct elements = yes or no

  These two settings must be yes for elements to be created. The default for both is yes.

- Subdivision size = number

  This sets the target area for automatically subdividing elements. The initial set of elements will be automatically subdivided until each element is smaller than the specified area.

- Create flow lines out from depressions = yes or no

  If this is set to yes, stream lines will be created from the depression over its draining saddle as if the depression was a channel head. Default is yes.

- Spaced flowline spacing = number

  Apart from creating element networks, TERRAE can operate in a simpler mode by creating a set of flowlines at fixed spacing across the landscape. In this mode, the lines do not connect to form ridge and stream junctions. Set this parameter to a number and set "Construct polygons" to no to use this mode.

After its processing, TERRAE writes the following files:

- Dem.sinks, dem.saddles, dem.peaks

  The locations and properties of each flat point.

- Dem.ridgelines, dem.valleylines

  The set of lines generated by TERRAE

- Dem.streamj, dem.ridgej

  The stream and ridge junction points

- Dem.polygons

  The outlines of each polygon

- Dem.elemgeom, dem.elemattr and dem.elemconnect

  The element description files (described above)

- Dem.topology

  Description of the line network topology – each peak, sink, saddle, stream junction

and ridge junction and the lines they connect to; sinks and saddles have additional information.

These files are all in simple x y z format (apart from the .topology file) that can be plotted directly using GNUPLOT or converted to ungenerate format to read into ARC/INFO.

APPENDIX B

Program Spatial Soil Water Balance

```
C (SALUS-TERRAE)
C DEFINITIONS OF VARIABLES ARE LISTED AT THE END OF THE PROGARM

    USE elemwatbal
    IMPLICIT NONE
    CHARACTER HEAD*32,FNAME*8,doystring*3
    type(soil_type)     :: Soils(MaxSoils)
    type(element_type)  :: Elements(MaxElems)
    REAL  LAT,LONG,ALT,Press
    REAL  CROPEC,VPDMIN,RGRATE,RTLMR
    REAL  MEANDEP, CUMDEP, Depth
    REAL  DTT,LAI,RLD(MaxLayer), RootDep, RootDepIncr
    REAL  SOLAR,TMAX,TMIN,RAIN
    REAL  OutFlow
    REAL  SWSTR
    REAL  SWTot,SW0_26,SW26_77,SW77_Bot

    INTEGER YR,DOY,L,I,EMDAY,ELEM,NUMELEMS,
   1      elemnum,elemdown,downnum,numsoils,soil

    REAL    FINDY,LAI_TAB(2,100),REAL_DOY
    integer  month                          !AG
    real a(12), b(12), runoff_slope(maxsoils) !AG
!
!*************************READING INPUT
DATA***************************
    WRITE(*,*)' ENTER WEATHER (___.WTH) FILE NAME WITHOUT
EXTENSION'
    READ(*,'(A8)')FNAME
    OPEN(UNIT=11,FILE=trim(FNAME)//'.WTH', STATUS='OLD')
    OPEN(UNIT=12,FILE='SOIL.DAT',STATUS='UNKNOWN')
    OPEN(UNIT=14,FILE='CROP.DAT',STATUS='UNKNOWN')
    OPEN(UNIT=13,FILE=trim(FNAME)//'.PRN', STATUS='UNKNOWN')
    OPEN(UNIT=15,FILE=trim(FNAME)//'.PRF', STATUS='UNKNOWN')
    OPEN(UNIT=17,FILE=trim(FNAME)//'.PRL', STATUS='UNKNOWN')
    OPEN(UNIT=18,FILE='RUNOFF.DAT', STATUS='UNKNOWN')

!SPATIAL: Need files to read elements information from
    OPEN(UNIT=19,FILE=trim(fname)//'.elemparams',STATUS='OLD')
    OPEN(UNIT=110,FILE=trim(fname)//'.elemsoils',STATUS='OLD')
```

```
! ***** Read values for LAI and root depth for given days of the year***
    OPEN(UNIT=120,FILE='LAI.DAT',STATUS='OLD')
    CALL READXY(120,LAI_TAB)
    CLOSE(120)
    READ(11,'(A32)')HEAD

!   Read till the line with Latitude, Longitude and elevation is found

700  READ(11,5,ERR=700,END=900)LAT,LONG,ALT
    IF(LAT .EQ. 0.0 .AND. LONG .EQ. 0.0 .AND. ALT .EQ. 0.0) GOTO 700
5    FORMAT(8X,2F9.3,F7.1)

!   Read the runoff parameters:                          !AG

    read (UNIT = 18, fmt = 300) (month, a(i), b(i), i = 1, 12)        !AG
300  format (/, 12(1x, i2, 2(1x, f7.4), /))                    !AG

    READ(14,*)
    READ(14,*)
    READ(14,*)CROPEC,VPDMIN,RGRATE,RTLMR
    READ(12,*)
    soil=1
    DO WHILE(.TRUE.)
      READ(12,*,END=790)
      IF(soil.GT.maxsoils) THEN
        WRITE(*,*) 'Too many soils: maximum is ', maxsoils
        STOP
      ENDIF
      READ(12,*) Soils(soil).NLAYR,Soils(soil).COEFW,
   1          Soils(soil).KSMICRO,Soils(soil).PONDMAX
      READ(12,*)
      CUMDEP=0.
!SPATIAL read element data
!*******************INITIALIZING AND READING SOILS
FILE***************
      WRITE(*,*) 'Soil number ', soil
      DO L=1,Soils(soil).NLAYR
        READ(12,*)Soils(soil).DLAYR(L),Soils(soil).SWLL(L),
   1       Soils(soil).SWDUL(L),Soils(soil).SWSAT(L),
   2       Soils(soil).KSMACRO(L),Soils(soil).RHF(L),
   3       Soils(soil).INITSW(L),Soils(soil).BD(L)
        CUMDEP=CUMDEP+Soils(soil).DLAYR(L)
        Soils(soil).ZLayr(L) = CumDep
        Soils(soil).SWAD(L)=0.44*Soils(soil).SWDUL(L)**2
        MEANDEP = (CUMDEP + (CUMDEP - Soils(soil).DLAYR(L)))/2
```

```
        Soils(soil).FLOWUCO(L)=0.63/MEANDEP**2*
  1        (0.495+EXP(2.804-10.76*Soils(soil).SWDUL(L)))
        IF(L.LT.5)THEN
          Soils(soil).RUCO(L)=Soils(soil).RHF(L)*0.15
        ELSE
          Soils(soil).RUCO(L)=Soils(soil).RHF(L)*0.10
        ENDIF
        RLD(L)=0.0
        WRITE(*,10)CUMDEP,Soils(soil).DLAYR(L),Soils(soil).SWLL(L),
  1       Soils(soil).SWDUL(L),Soils(soil).SWSAT(L),
  2       Soils(soil).KSMACRO(L),Soils(soil).RHF(L),
  3       Soils(soil).INITSW(L)
 10      FORMAT(2F6.0,3F6.3,F6.1,F6.3,F6.3)
      ENDDO
      Soils(soil).FLOWUCO(1)=Soils(soil).FLOWUCO(1)*
  1      (0.82-4.7*(0.45-Soils(soil).SWDUL(1))**2)
      WRITE(13,'(A32)')HEAD
      WRITE(15,'(A32)')HEAD
      WRITE(17,'(A32)')HEAD
      WRITE(13,18)LAT,LONG,ALT,CROPEC,VPDMIN,Soils(soil).PONDMAX,
  1      Soils(soil).KSMICRO
 18    FORMAT('LAT',F5.1,' LONG',F6.1,' ALT',F5.0,' CROPEC',F5.1,' VPD
  1MIN',F6.2,' PONDMAX',F5.1,' KSMICRO',F5.1)
      WRITE(13,30)
      WRITE(15,31)
      WRITE(17,32)
      WRITE(17,33)
      WRITE(13,15)(Soils(soil).INITSW(I),I=1,12)
 15    FORMAT(8X,'----------cm/day----------        cm',2X,12F5.3)
!      Soils(soil).PONDY=0.0

    soil=soil+1
    ENDDO

!SPATIAL - Read information from TERRAE about element attributes(area, slope, etc.)
!and connection (topology, which is the downslope elements, etc) from the
'filename.Elements'.

 790 CONTINUE
    numelems = 0

!    The Element array is sparse.  The USED variable will tell the program
!    which elements have valid data

    Elements.Used = .FALSE.
    DO WHILE(.TRUE.)
```

```
      READ(19,*,end=791) elemnum, Elements(elemnum).centreX,
     1     Elements(elemnum).centreY,Elements(elemnum).centrez,
     2     Elements(elemnum).Area,
     3     Elements(elemnum).ndownslope,Elements(elemnum).slope
          Elements(elemnum).Used = .TRUE.
          WRITE(*,*) 'Elem ',elemnum,' has ',
     1     Elements(elemnum).ndownslope,'connections'
      if(Elements(elemnum).ndownslope .gt. maxdown) then
        WRITE(*,*) 'Too many connections: maximum is ', maxdown
        STOP
      endif
      do downnum=1, Elements(elemnum).ndownslope
        READ(19,*) Elements(elemnum).downslope(downnum),
     1             Elements(elemnum).downfrac(downnum)
        WRITE(*,*) downnum, Elements(elemnum).downslope(downnum),
     1             Elements(elemnum).downfrac(downnum)
      enddo
      READ(110,*) elemnum,soil
      Elements(elemnum).Soil = soil
      do i=1,Soils(Soil).nlayr
        Elements(elemnum).sw(i) = Soils(Soil).initsw(i)
      enddo
      Elements(elemnum).pond = 0.0
      Elements(elemnum).pondMax = Soils(Soil).PondMax
      numelems = max(numelems, elemnum)
    enddo

! initialise depth to saturated layer in all elements
    do elem=1,numelems
      soil = Elements(elem).Soil
      Elements(elem).SatDepth = 9999
      Elements(elem).SatLayer = Soils(soil).nlayr + 1
      do L=Soils(soil).nlayr,1,-1
        if (Elements(elem).sw(L) .lt. Soils(soil).swdul(L)) then
          exit
        else
          Elements(elem).SatDepth = Soils(soil).Zlayr(L) -
     1                      Soils(soil).Dlayr(L)
          Elements(elem).SatLayer = L
        endif
      enddo

!     convert depth from cm from the top of the soil to meters above some
!     base level

      Elements(elem).SatDepth = Elements(elem).CentreZ -
```

```
     1                    (Elements(elem).SatDepth/100.0)
     enddo


791  CONTINUE
     PRESS=101.-0.0107*ALT
     ROOTDEP=0.0
     EMDAY=0
     YR=1

! write out Arc LUT for element parameters

     OPEN(UNIT=111,FILE=trim(FNAME)//'.area', STATUS='UNKNOWN')
     do elemnum = 1,numelems
       if (Elements(Elemnum).Area .gt. 0) then
         WRITE(111,*) elemnum, Elements(Elemnum).Area,
     1     Elements(Elemnum).centrex,Elements(Elemnum).centrey,
     2     Elements(Elemnum).centrez, Elements(Elemnum).Slope
       endif
     enddo
     close(UNIT=111)

!    Open a Sufer DAT file to store some non-volitle data

     Open(20,file=trim(fname)//'_fixed.dat',status='unknown')
     write(20,'(7A13)')"X","Y","Z","Slope","Area",
     1            "PondMax","ElemNum"

     do elemnum = 1,numelems
       if (Elements(elemnum).Used) then
         soil = Elements(elemnum).Soil

!        Initialize variable needed for the water balance

         CALL ElemCSWB(INIT, DOY, YR, SOLAR, TMAX, TMIN, RAIN,
     1       LAT, LONG, ALT, Press, dTT, LAI, RLD, SWSTR, Elemnum,
     2       Soil,Soils(soil),Elements(elemnum),CROPEC,RTLMR,RGRATE,
     3       Elements,Soils)
         write(20,'(6f13.3,I13)') Elements(Elemnum).centreX,
     1      Elements(Elemnum).centrey,Elements(Elemnum).centreZ,
     2      Elements(Elemnum).Slope,Elements(Elemnum).Area,
     3      Elements(Elemnum).PondMax,ElemNum
       endif
     enddo
     close (20)
```

```
! ***************DAILY LOOP (READ WEATHER AND CALCULATE WATER
BALANCE*******


    DO WHILE(YR.GT.0)
800     READ(11,20,ERR=800,END=900)YR,DOY,SOLAR,TMAX,TMIN,RAIN
      IF (DOY .EQ. 0) GOTO 800
20      FORMAT(I2,I3,4F6.1)
      REAL_DOY = REAL(DOY)
      dTT = amax1(0.,(Tmax + Tmin)/2 -10.)
      LAI = FINDY(REAL_DOY,LAI_TAB)
      do elem=1,numelems
        Elements(elem).surfinflow = 0
        Elements(elem).subsurfinflow = 0
        Elements(elem).inflowdepth = 9999
          enddo
          outflow = 0
          WRITE(doystring,'(I3.3)') doy
!       OPEN(UNIT=111,FILE=trim(FNAME)//'.wat'//trim(doystring),
!        1                    STATUS='UNKNOWN')

!    Open a Sufer DAT file to store some daily data

    Open(20,file=trim(fname)//trim(doystring)//'.dat',
   1    status='unknown')
    write(20,'(25A13)')"X","Y","ElemNum","Runoff","RunOn",
   1       "NetSurfFl","Ponding",
   2       "SW 0-26","SW 26-77","SW 77-Bot","Tot. SW",
   3       "SubFlow","SumSubFlow","Drainage"


      DO ELEM=1,NUMELEMS
        if (.not. Elements(ELEM).Used) then
!          no element specified, go on to next one
          cycle
        endif
        soil = Elements(ELEM).Soil
        WRITE(13,*) 'Water balance for element ',elem
!*************************************************************************
!       RATE calculations
!*************************************************************************
        CALL ElemCSWB(RATE, DOY, YR, SOLAR, TMAX, TMIN, RAIN,
   1        LAT, LONG, ALT, Press, dTT, LAI, RLD, SWSTR, Elem,
   2        Soil,Soils(soil),Elements(elem),CROPEC,RTLMR,RGRATE,
   3        Elements,Soils)
!*************************************************************************
```

```
!       INTEGERATION calculations
!*********************************************************************
        CALL ElemCSWB(INTEG, DOY, YR, SOLAR, TMAX, TMIN, RAIN,
   1       LAT, LONG, ALT, Press, dTT, LAI, RLD, SWSTR, Elem,
   2       Soil,Soils(soil),Elements(elem),CROPEC,RTLMR,RGRATE,
   3       Elements,Soils)

! SPATIAL if there is no downslope element, we let the surface
!       water run off and the subsurface water drain using the
!       slope of the element. Outflow is reported as a volume

        WRITE(13,*) 'Runoff = ', Elements(elem).runoff
        if(Elements(elem).ndownslope .eq. 0) then
          outflow = outflow + Elements(elem).runoff *
   1              Elements(elem).Area
        else
          do downnum=1, Elements(elem).ndownslope
            elemdown = Elements(elem).downslope(downnum)
            Elements(elemdown).surfinflow =
   1          Elements(elemdown).surfinflow +
   2          Elements(elem).runoff *
   3          Elements(elem).downfrac(downnum)*
   4          Elements(elem).Area/Elements(elemdown).Area
          enddo
        endif

        SWTot = sum(elements(Elem).SW(1:Soils(Soil).NLayr) *
   2            Soils(soil).DLayr(1:Soils(Soil).NLayr))
        SW0_26 = sum(elements(Elem).SW(1:4) *
   2            Soils(soil).DLayr(1:4))
        SW26_77 = sum(elements(Elem).SW(5:7) *
   2            Soils(soil).DLayr(5:7))
        SW77_Bot = sum(elements(Elem).SW(8:Soils(Soil).NLayr) *
   2            Soils(soil).DLayr(8:Soils(Soil).NLayr))


        if (swtot < 0.) then
          write(*,*) 'Something wrong'
        endif
        write(20,'(2f13.3,I13,20F13.3)') Elements(Elem).centrex,
   1       Elements(Elem).centrey,Elem,Elements(Elem).runoff,
   2       Elements(Elem).surfinflow,
   3       Elements(Elem).surfinflow - Elements(Elem).runoff,
   4       Elements(Elem).Pond,SW0_26,SW26_77,SW77_Bot,SWTot,
   5     Elements(elem).SumSubInFlow - Elements(elem).SumSubInFlowYest,
   6       Elements(elem).SumSubInFlow,
```

```
   7       Elements(elem).FlowD(Soils(soil).NLayr)

      ENDDO

      Close(20)

!      close(UNIT=111)

    ENDDO
900  CONTINUE
    STOP
 30  FORMAT(' YR DOY  RAIN ROFF DRAN   ES   EP  LAI RTDEP    SW1  SW2
   1 SW3  SW4  SW5  SW6  SW7  SW8  SW9 SW10 SW11 SW12')
 31  FORMAT(' YR DOY  RAIN RNOFS RNOFD  POND  FLOW1  FLOW2  FLOW3
F
   1LOW4  FLOW5  FLOW6  FLOW7  FLOW8  FLOW9 FLOW10 FLOW11
FLOW12')
 32  FORMAT('            ROOT LENGTH DENSITY FILE --units cm/cm^3')
 33  FORMAT(' YR DOY  DEP1  DEP2  DEP3  DEP4  DEP5  DEP6  DEP7  DEP8  D
   1EP9 DEP10 DEP11 DEP12')
    END


    SUBROUTINE READXY (INUNIT,POINTS)
C
C    Subroutine to read an arbitrary number of xy points and put them
C    into the array POINTS
C
    INTEGER     I,J,INUNIT,NUMPOINTS
    REAL        POINTS(2,*)
C
C    Read number of points for this equation from the file
C
    J = 0
    READ(INUNIT,*,ERR=100,END=100) NUMPOINTS
C
C    Repeat until error (ie. a line without two real numbers on it)
C
    DO J = 1,NUMPOINTS
      READ(INUNIT,*,ERR=100,END=100) (POINTS(I,J),I=1,2)
    END DO
100  CONTINUE
C
C    Place end of points marker
C
    IF (J .EQ. 0) THEN
```

```
      POINTS(1,1) = -9999.0
    ELSE
      POINTS(1,J) = -9999.0
    ENDIF
    IF (J .LE. 1) THEN
      WRITE(*,*) 'No points read!'
    ENDIF
    RETURN
    END


    REAL FUNCTION FINDY (X,POINTS)
C
C   From the arbitrary X,Y values in the POINTS array find a Y
C   value for a given X value.
C
    INTEGER  I
    REAL     POINTS(2,*),WEIGHT,X   !variable X added

C
C   If input X is less than minimum X set Y to value of first X
C
    IF (X .LE. POINTS(1,1)) THEN
      FINDY = POINTS (2,1)
    ELSE
      I = 2
      DO WHILE ((X .GT. POINTS(1,I)).AND.(POINTS(1,I) .GE. -9998.0))
        I = I + 1
      END DO
C
C     If input X is greater than maximum X set Y to value of last Y
C
      IF (POINTS(1,I) .LT. -9998.0) THEN
        FINDY = POINTS (2,I-1)
      ELSE
        WEIGHT = (X-POINTS(1,(I-1)))/(POINTS(1,I)-POINTS(1,(I-1)))
        FINDY = POINTS(2,I-1) + (POINTS(2,I) - POINTS(2,I-1))*WEIGHT
      ENDIF
    ENDIF
    RETURN
    END

C==================================================================
========
C NAILUJ, Subroutine
C
```

```
C Determines Julian date
C-----------------------------------------------------------------
C Revision history
C
C 1. Written
C 2 Modified by
C 3. Header revision and minor changes          P.W.W.    2-8-93
C-----------------------------------------------------------------
C INPUT : JULD,NYRCHK
C
C LOCAL : RNAME(),NSUM,JCOUNT,NDIF,MON()
C
C OUTPUT : NDAY RMON
C-----------------------------------------------------------------
C Called : SEHARV SENS SEPLT SETIME OPDAY
C
C Calls : None
C-----------------------------------------------------------------
C                    DEFINITIONS
C
C RMON  :
C RNAME():
C NSUM  :
C JCOUNT :
C NDIF  :
C JULD  :
C NYRCHK :
C NDAY  :
C MON() :
C=================================================================
=========

      SUBROUTINE NAILUJ (JULD,NYRCHK,month)

      IMPLICIT   NONE

      CHARACTER*3 RMON,RNAME(12)
      INTEGER    NSUM,JCOUNT,NDIF,JULD,NYRCHK,NDAY,MON(12), month

      DATA MON  /31,28,31,30,31,30,31,31,30,31,30,31/
      DATA RNAME /'JAN','FEB','MAR','APR','MAY','JUN',
     &          'JUL','AUG','SEP','OCT','NOV','DEC'/

      IF (MOD(NYRCHK,4) .EQ. 0) THEN
        MON(2) = 29
       ELSE
```

```
      MON(2) = 28
    ENDIF
    NSUM = 0

    DO JCOUNT = 1, 12
      NDIF = JULD - NSUM
      IF (NDIF .LE. MON(JCOUNT)) THEN
        NDAY = NDIF
        RMON = RNAME(JCOUNT)
        month = jcount
        RETURN
      ENDIF
      NSUM = NSUM + MON(JCOUNT)
    END DO

    RETURN

    END

C DEFINITIONS
C EO      Potential evapotranspiration  (cm/day)
C ESO     Potential soil evaporation  (cm/day)
C ES      Actual soil evaporation  (cm/day)
C EPO     Potential plant evaporation  (cm/day)
C EP      Actual plant evaporation  (cm/day)
C VPD     Estimated vapor pressure deficit for a day (kPa)
C VPDAY   Estimated vapor pressure for a day (kPa)
C VP      Estimated saturation vapor pressure for a day (kPa)
C VPDMIN  A crop specific threshold vapor pressure deficit below which the aero-
C         dynamic component in the potential evaporation equation is zero (kPa)
C CROPEC  A crop specific constant--slope of the aerodynamic component relation-
C         ship in the potential evaporation equation  (MJ/kPa)
C RADCOM  The radiation component in the potential evaporation equation (mm/day)
C AEROCOMS The aerodynamic component in the potential evaporation equation for
C         bare soil surfaces (mm/day)
C AEROCOMC The aerodynamic component in the potential evaporation equation for
C         crops surfaces (mm/day)
C GODPG   Gamma divided by delta plus gamma in the potential evap. equation
C PRES    The estimated atmospheric pressure based on elevation (kPa)
C RTLMR   The root length to mass ratio for the empirical root growth routines (cm/g)
C RUNOFFS Daily runoff related to lack of surface infiltration  (cm/day)
C RUNOFFD Daily runoff related to lack of drainage at depth  (cm/day)
C LAI     Leaf area index  (cm2/cm2)
C LAI_TAB Table of LAI for given dates (input data)
C ROOTDEP_TAB  Table of root depth for given dates (input data)
C RLD(L)  Root length density  (cm/cm3)
```

```
C COEFD   Empirical coefficient used to calculate new water content after
C         infiltration (unitless)
C CUMDEP  Cumulative soil depth at bottom of layer (cm)
C MEANDEP Soil depth at center of layer (cm)
C SW(L)   Soil water content (cm3/cm3)
C SWT     Temporary variable for a new soil water content (cm3/cm3)
C SWTD    Temporary variable for calculating water content during drainage (cm3/cm3)
C SWTI    Temporary variable for calculating water content during infiltration
(cm3/cm3)
C SWDUL(L) Soil water content at the drained upper limit (cm3/cm3)
C SWSAT(L) Soil water content at saturation (cm3/cm3)
C RHF(L)  Root hospitality factor input from soils file  unitless
C RUCO(L) Root uptake coefficient  unitless
C SWDIFU(L) Soil water content difference resulting from upward flow (vol frac)
C SWDIFD(L) Soil water content difference resulting from downward flow (vol frac)
C SWDIFR(L) Soil water content difference resulting from root uptake (vol frac)
C SWDIF(L) Net soil water content difference from all factors (vol frac)
C FLOWU(L) Flow rate upward at the layer being evaluated  (cm/day)
C FLOW(L) Net flow rate at the layer being evaluated  (cm/day)
C FLOWEXC Excess water that cannot flow downward (cm/day)
C FLOWUCO(L) Coefficient for each soil layer used to calculate evaporation rate -
unitless
C RUCO(L) Coefficient for each soil layer used to calculate root uptake - unitless
C REDCOU  Reduction coefficient to reduce upward flow to potential soil evap.
C REDCOR  Reduction coefficient to reduce root uptake to potential plant evap.
C ROOTDEP Depth of rooting cm
C INFILT  Amount of infiltration during a given period (mm). Temp.var.
C KSMACRO(L) Saturated hydraulic conductivity with macropores (cm/day).
C KSMICRO Saturated hydraulic conductivity at surface without macropores (cm/day).
C         (Should be lower than KSMACRO)
C MAXRAIN Maximum rate of rainfall (cm/day)
C NUMSTEPS Number of steps in a rainstorm
C PINF    Daily precipitation infiltrated (cm)
C PIP     Precipitaion infiltrated from ponding (cm)
C POND    Amount/depth of water held in ponding on the surface (cm)
C PONDMAX Maximum amount of water that can be stored in ponding (cm)
C RAIN    Daily measured rain from weather input file  (mm).
C         is assumed to infiltrate and the ponding routine is bypassed (mm).
C PPRECIP Amount of precipitation for a given period (cm).
C PRECIP  Sum of RAIN and irrigation (cm) convert from mm.
C RAINDUR Length of rain storm (hrs)
C RUNOFFS Daily runoff (cm).
C TIME    Current time into the storm (days)
C TIMESTEP Amount of time per step in a storm (days)
C TPAMT   For a given period amount of water that could infltrate (cm)
C TRUNOFF Amount of water runoff during a given period (cm).
```

C LR Depth increment in depth counter (L) where root depth is located

Element Spatial Soil Water Balance

```
module elemwatbal
implicit none


 !**** CONSTANTS

 !* MAX_LAYER: Maximum number of soil layers

 INTEGER,PARAMETER      :: MaxLayer = 20
 INTEGER,PARAMETER      :: MAXELEMS=100
 INTEGER,PARAMETER      :: maxdown=20
 INTEGER,PARAMETER      :: maxsoils=100
 INTEGER,PARAMETER      :: INIT = 1
 INTEGER,PARAMETER      :: RATE = 2
 INTEGER,PARAMETER      :: INTEG = 3
 REAL,PARAMETER       :: RockBD = 2.65 !Bulk density of rock material in soil


Type soil_type
  integer :: NLAYR      ! Number of layers
  Real   :: COEFW
  Real   :: KSMicro
  Real   :: PondMax
  Real   :: DLAYR(MaxLayer),ZLayr(MaxLayer)
  Real   :: BD(MaxLayer)
  Real   :: SWDUL(MaxLayer)
  Real   :: SWLL(MaxLayer)
  Real   :: SWSAT(MaxLayer)
  Real   :: KSMACRO(MaxLayer)
  Real   :: SWAD(MaxLayer)
  Real   :: FLOWUCO(MaxLayer)
  Real   :: RHF(MaxLayer)
  Real   :: RUCO(MaxLayer)
  Real   :: InitSW(MaxLayer)
end type soil_type

type element_type
  logical :: Used
  Integer :: NDownSlope
  Integer :: DownSlope(MaxDown)
  Integer :: Soil
```

```
  Integer :: EMDAY
  Integer :: LR
  Integer :: OutFlowLayer
  Integer :: SatLayer          !Highest (non-perched) saturated layer
  Real    :: DownFrac(MaxDown)
  Real    :: Pond
  Real    :: PondMax
  Real    :: Pondy             !Used for Error checking
  Real    :: CentreX, CentreY, CentreZ
  Real    :: Area
  Real    :: Slope
  Real    :: SatDepth          !Depth in meters above a base elevation
  Real    :: surfinflow
  Real    :: subsurfinflow,SumSubInFlow,SumSubInFlowYest
  Real    :: inflowdepth
  Real    :: Runoff,RunoffS,Runoffd
  Real    :: SWYest, PondEvap      !Used for Error checking
  Real    :: ROOTDEP
  Real    :: RootDepIncr
  Real    :: SW(MaxLayer)
  Real    :: VirtKSMac(MaxLayer)    !Effective Sat. Flow for virtical flow
  Real    :: Flow(MaxLayer),FlowD(0:MaxLayer+1),FlowU(0:MaxLayer+1),FlowR
  Real    ::
SWDif(MaxLayer),SWDifD(MaxLayer),SWDifU(MaxLayer),SWDifR(MaxLayer)
  Real    :: RedCOU, RedCOR
  Real    :: ES
  Real    :: EP
end type element_type

contains

!=================================================================
========
!Modified Water balance routine from Joe Ritchie.
!  Soil -- all the permenant physical properties associated with a soil
!        (LL, DUL, etc.)
!  Element -- all the dynamic properties of a soil in a given
!          geographical element (SW, ES, EP, etc.)
!=================================================================
========
!               PROGRAM SOIL WATER BALANCE
SUBROUTINE ElemCSWB(DYNAMIC, DOY, YR, SOLAR, TMAX, TMIN, RAIN,  &
          LAT, LONG, ALT, Press, dTT, LAI, RLD, SWSTR, Elem, &
          Soil,CurrSoil,CurrElem,CROPEC,RTLMR,RGRATE, &
          Elements, Soils)
```

```
!=================================================================
========

! DEFINITIONS OF VARIABLES ARE LISTED AT THE END OF THE PROGARM

INTEGER, intent(in) :: Dynamic, DOY, Yr, Elem, Soil
REAL, intent(in)   :: Solar, TMax, TMin, Rain, Lat, Long, Alt, Press, dTT, LAI
Real, intent(in)   :: RLD(MaxLayer)
REAL, intent(out)  :: SWStr
type(soil_type), intent(inout) :: CurrSoil,Soils(MaxSoils)
type(element_type), intent(inout)  :: CurrElem,Elements(MaxElems)
Real, intent(in)   :: CROPEC,RTLMR,RGRATE

Integer  :: I,L,LNU
Integer  :: Month
Integer  :: DownNum,DownElem,DownSoil
Real     :: Error       !Used for Error checking
Real     :: Precip,WInf
Real     :: a(12), b
Real     :: PESWabove,PESWaboveFAC(MaxLayer)
Real     :: MEANDEP, CUMDEP, acoef, ncoef
Real     :: runoff_slope
Real     :: Porosity, WatFilPor, halfpesw, swdryfac, swwetfac, coldfac
Real     :: TMEAN, LATHEAT, GODPG, RadCom, VPD, VPDAY, VP, AEROCOMS,
AEROCOMC
Real     :: EO, EPO, ESO, ESD, PotentialSurfaceEvap
Real     :: SWN(MaxLayer), SWTI, SWTD, SWT
Real     :: FLOWEXC
Real     :: RootPres,Coef_Wat_Ext
Real     :: RootAct(MaxLayer)
Real     :: CumDif
Real     :: Depth,SatDP,DownAmt,KSSat,KSSatDown, KSEff, LateralFlow
Real     :: DeltaX,DeltaZ
Real     :: DepthFact, RadSlope, ZLayr, TotSubSurfOutFlow

!************************INITIALIZATION*****************************
*
!     File reading will be handled outside of this routine for
!     spatial application
!
   IF (DYNAMIC.EQ.INIT) THEN
!*********************************************************************
!
!     OPEN(UNIT=2,FILE='SOIL.DAT',STATUS='UNKNOWN')
!     OPEN(UNIT=4,FILE='CROP.DAT',STATUS='UNKNOWN')
!     OPEN(UNIT=3,FILE=trim(FNAME)//'.PRN', STATUS='UNKNOWN')
```

```
!     OPEN(UNIT=5,FILE=trim(FNAME)//'.PRF', STATUS='UNKNOWN')
!        OPEN(UNIT=15,FIle=trim(FNAME)//'.Err', STATUS='UNKNOWN')
!
!     READ(4,*)
!     READ(4,*)
!     READ(4,*)CROPEC,RGRATE
!C ******************INITIALIZING AND READING SOILS
FILE***************
!     READ(2,*)
!     READ(2,*)
!     READ(2,*)NLAYR,Slope
!     READ(2,*)
!        Compute PondMax from Slope

      CurrElem.PondMax = Max(1./(0.2 + 0.35*CurrElem.Slope),CurrElem.PondMax)

! Compute the efective virtical saturated flow conductivity
!      First convert Slope from % slope to radians

      RadSlope = CurrElem.Slope * 100.0/90.0 * 0.00175
      ZLayr = 0
      Do L = 1,CurrSoil.NLayr

!        At zero depth there is no difference bewteen KSMacro and KSMacVirt
!        at two meters the correction factor will be sin(slope)

        ZLayr = ZLayr + CurrSoil.DLayr(L)
        DepthFact = 1.0 - 0.5 * (ZLayr/100.0)
        CurrElem.VirtKSMac(L) = CurrSoil.KSMacro(L) * (DepthFact + &
                                (1 - DepthFact) * sin(RadSlope))
      EndDo
!
!        Set coefficients for Runoff, currently N. Central USA eqn. from Gerakis
      b=-0.30
      Do I=1,12
        a(I)=MIN(-0.015,-0.15*sin(2.*3.1417*(I+2.)/12.)-0.05)
      ENDDO
      PESWabove = 0.
      CUMDEP=0.
      DO L=1,CurrSoil.NLayr
        CUMDEP=CUMDEP+CurrSoil.DLayr(L)
        CurrSoil.SWAD(L)=0.44*CurrSoil.SWDUL(L)**2                    !Air dry soil
water contents

WRITE(*,10)CUMDEP,CurrSoil.DLayr(L),CurrSoil.SWLL(L),CurrSoil.SWDUL(L),Cu
rrSoil.SWSAT(L), &
```

```
CurrSoil.KSMacro(L),CurrSoil.RHF(L),CurrSoil.InitSW(L),CurrSoil.BD(L),CurrSoil.S
WAD(L)

!          Set factors for root water extraction based on upper soil water

        PESWabove=PESWabove + max(0.,CurrSoil.InitSW(L)-
CurrSoil.SWLL(L))*CurrSoil.DLayr(L)
        PESWaboveFAC(L)=MIN(1.,MAX(0.,exp(2.2-0.62*PESWabove)-0.07))
        RootAct(L) = 0 !Indicates that roots have not yet been active,layer L

!               Set root water uptake coefficients for each layer

        IF(L.LT.5)THEN
          CurrSoil.RUCO(L)=CurrSoil.RHF(L)*0.30
        ELSE
          CurrSoil.RUCO(L)=CurrSoil.RHF(L)*0.10
        ENDIF

!       Compute coefficients for soil-limited evaporation from depths

        MEANDEP = (CUMDEP + (CUMDEP - CurrSoil.DLayr(L)))/2
        ncoef=-2.2-1.04*CurrSoil.SWDUL(L)
        acoef=3.20*CurrSoil.SWDUL(L)-0.15
        CurrSoil.FlowUCo(L)=acoef*MEANDEP**ncoef
      ENDDO
      CurrSoil.FlowUCo(1)=CurrSoil.FlowUCo(1)*(0.82-4.7*(0.45-
CurrSoil.SWDUL(1))**2)     !adjust top layer
      CurrElem.ROOTDEP = 0.0
      CurrElem.RootDepIncr = 0.0
      CurrElem.PondY=0.0
      CurrElem.EMDAY=0
      CurrElem.Pond = 0.0                                    !AG
      CurrElem.SumSubInFlow = 0.0
      CurrElem.SumSubInFlowYest = 0.0
      CurrElem.SatDepth = 9999
      CurrElem.SatLayer = CurrSoil.nlayr + 1
      do L=CurrSoil.nlayr,1,-1
        if (CurrElem.sw(L) .lt. CurrSoil.swdul(L)) then
          exit
        else
          CurrElem.SatDepth = CurrSoil.Zlayr(L) -  &
                          CurrSoil.Dlayr(L)
          CurrElem.SatLayer = L
        endif
      enddo
```

```
!     WRITE(3,'(A32)')HEAD
!     WRITE(5,'(A32)')HEAD
!     WRITE(3,18)LAT,LONG,ALT,CROPEC,CurrElem.PondMax
!     WRITE(3,30)
!     WRITE(5,31)
!     WRITE(3,15)(SW(I),I=1,12)
!
!
!****************************RATE
CALCULATIONS****************************
   ELSEIF (DYNAMIC.EQ.RATE) THEN
!**********************************************************************
***
!
      CurrElem.PondEvap = 0.0                                !BDB
      CurrElem.SWYest =
sum(CurrElem.sw(1:CurrSoil.nlayr)*CurrSoil.DLayr(1:CurrSoil.nlayr)) !BDB

!*********** Runoff Rate Calculations*************************************

      PRECIP=RAIN*0.1     !CONVERTS RAIN FROM mm/day to cm/day

!     Added for Spatial

      Precip = Precip + CurrElem.surfinflow                  !BDB
      CurrElem.runoffs = 0.0                          !AG
      winf = 0.0                                  !AG
      if (precip .gt. 0.0) then                       !AG
        ! Slope of curve of rain vs. runoff:                !AG
        call nailuj (doy,yr,month)                    !AG
        runoff_slope = MIN(1.0, exp (MAX (-1e1, a(month)*  &   !AG
                CurrElem.VirtKSMac(1) + b)))                !AG
        CurrElem.Runoffs = max(runoff_slope * (precip + CurrElem.Pond -
CurrElem.PondMax),0.0) !AG
        winf = min(precip - CurrElem.Runoffs, CurrElem.VirtKSMac(1))  !AG
        CurrElem.Pond = CurrElem.Pond + precip - CurrElem.Runoffs - winf !AG
        if (CurrElem.Pond .gt. CurrElem.PondMax) then          !AG
          CurrElem.Runoffs = CurrElem.Runoffs + CurrElem.Pond - CurrElem.PondMax
!AG
          CurrElem.Pond = CurrElem.PondMax                  !AG
        endif                                     !AG
      elseif (CurrElem.Pond .gt. 0.0) then                !AG
        winf = min(CurrElem.Pond, CurrElem.VirtKSMac(1))          !AG
        CurrElem.Pond = CurrElem.Pond - winf                !AG
      endif                                       !AG
```

```
      if (CurrElem.Pond .lt. -1e-5) then                          !AG
        write (*,*) '**** Negative ponding = ', CurrElem.Pond  !AG
      endif                                                !AG

      CurrElem.FLOWD(0)= winf                                     !AG
      CurrElem.Runoffd=0.

!******************RATE OF ROOT GROWTH, DOWNWARD
(cm/day)*************
      IF(LAI.GT.0.)THEN
!******************Initializing Root Depth on Day of Emergence*******
        CurrElem.EMDay=CurrElem.EMDay+1
        IF(CurrElem.EMDay.EQ.1)THEN
          CurrElem.RootDep=7.
          CurrElem.LR=2
        ENDIF
      Porosity = 1. - CurrSoil.BD(CurrElem.LR)/RockBD
                        !jwj
      WatFilPor = CurrElem.SW(CurrElem.LR)/Porosity
                        !jwj
      halfpesw = CurrSoil.SWLL(CurrElem.LR) +
0.5*(CurrSoil.SWDUL(CurrElem.LR)-CurrSoil.SWLL(CurrElem.LR))
        !jwj
      SWDRYFAC=max(0.,min(1.,(CurrElem.SW(CurrElem.LR)-
CurrSoil.SWLL(CurrElem.LR)) &
       /(halfpesw-CurrSoil.SWLL(CurrElem.LR))))
      SWWETFAC=MIN(1.,5.*(1.-WatFilPor))
        !jwj
      coldfac = 1.
      CurrElem.RootDepIncr = RGRATE * dTT *
min(CurrSoil.RHF(CurrElem.LR),swdryfac, &
          swwetfac,coldfac)
      ENDIF

!**************** POTENTIAL EVAPOTRANSPIRATION
CALCULATIONS**********
      TMEAN=TMAX*0.5+TMIN*0.5
      LATHEAT=(25.01-TMEAN/42.3)  !THIS IS FOR CM/DAY UNITS
      GODPG=(0.598-3.0E-05*PRESS)-0.017*TMEAN+1.49E-04*TMEAN**2
      IF(GODPG.GT.1.0)GODPG=1.0

!                       THE ABOVE EXPRESSION IS NOT GOOD AT VERY LOW
TEMPERATURES

      RADCOM=(1-GODPG)*SOLAR*0.63
```

```
      VPDAY=0.611*EXP(17.27*TMEAN/(TMEAN+237.3))
      VP=0.611*EXP(17.27*TMIN/(TMIN+237.3))
      VPD=VPDAY-VP
      IF(LAI.GT.0)THEN
        AEROCOMS=GODPG*15.0*VPD**1.5*EXP(-0.75*LAI)
        ESO=(RADCOM*EXP(-0.40*LAI)+AEROCOMS)/LATHEAT
        AEROCOMC=GODPG*CROPEC*VPD**1.5
        EO = (RADCOM+AEROCOMC)/LATHEAT
        EPO=EO*(1.-EXP(-0.92*LAI))
        if (lai .lt. 0.5) then
          EO = ESO
        endif
      ELSE
        AEROCOMS=GODPG*15.0*VPD**1.5
        ESO=(RADCOM+AEROCOMS)/LATHEAT
        EPO=0.0
        EO = ESO
      ENDIF   ! End of LAI if statement for PET calculations

      CurrElem.FlowR=0.
      CUMDEP=0.
      ESD=0.
      PESWabove=0.
      SWN = CurrElem.SW

! SPATIAL:
! Move water laterally in or out of the saturated zone

      CurrElem.SumSubInFlowYest = CurrElem.SumSubInFlow
      CurrElem.SumSubInFlow = CurrElem.SumSubInFlow + &
                        CurrElem.subsurfinflow

!     If water is flowing in start from the top of the water table and
!     move up

      If (CurrElem.subsurfinflow > 0) then
        L = CurrElem.SatLayer
        do while ((L > 0) .and. (CurrElem.subsurfinflow > 0))
          SWN(L) = SWN(L) + min(CurrElem.subsurfinflow, &
                    (CurrSoil.SWSAT(L) - SWN(L)))
          CurrElem.subsurfinflow = CurrElem.subsurfinflow -  &
              min(CurrElem.subsurfinflow,(CurrSoil.SWSAT(L) - SWN(L)))
          L = L -1
        enddo

!       If there is no room in the soil to store the water put it into
```

```
!       the ponded water

        If (CurrElem.subsurfinflow > 0) then
          CurrElem.pond = CurrElem.Pond + CurrElem.subsurfinflow
          CurrElem.subsurfinflow = 0
        EndIf

!       If water is to be removed start from the bottom layer and work up

      ElseIf (CurrElem.subsurfinflow < 0) then
        L = CurrSoil.NLayr
        do while ((L > 0) .and. (CurrElem.subsurfinflow < 0))
          SWN(L) = SWN(L) - min(-CurrElem.subsurfinflow, &
                    Max((SWN(L) - CurrSoil.SWDUL(L)),0.0))
          CurrElem.subsurfinflow = CurrElem.subsurfinflow + &
                    min(-CurrElem.subsurfinflow, &
                    Max((SWN(L) - CurrSoil.SWDUL(L)),0.0))
          L = L - 1
        enddo
        If (CurrElem.subsurfinflow < 0) then
          Write(*,*) 'Outward lateral flow exceeded available water!'
          CurrElem.subsurfinflow = 0
        EndIf
      Endif


      DO L=1,CurrSoil.NLayr
!*******COMPUTE DOWNWARD FLOW (INFILTRATION AND
REDISTRIBUTION)******


        SWN(L)=SWN(L)+CurrElem.FlowD(L-1)/CurrSoil.DLayr(L)
        IF(SWN(L).LE.CurrSoil.SWDUL(L))THEN
          CurrElem.FlowD(L)=0.
        ELSE
          SWTI=CurrSoil.SWDUL(L)+0.25*(1-EXP(-0.05*CurrElem.FlowD(L-1)))
          SWN(L)=MIN(SWTI,CurrSoil.SWSAT(L),SWN(L))
          SWTD=CurrElem.SW(L)-0.55*(CurrElem.SW(L)-CurrSoil.SWDUL(L))
          SWN(L)=MAX(SWN(L),SWTD)
          CurrElem.FlowD(L)=CurrElem.FlowD(L-1)-(SWN(L)-
CurrElem.SW(L))*CurrSoil.DLayr(L)

!  ALTER FLOW DOWN AND WATER CONTENTS ABOVE LAYER FOR
RESTRICTED DOWNWARD FLOW

          IF(CurrElem.FlowD(L).GE.CurrElem.VirtKSMac(L))THEN
```

```
          FLOWEXC=CurrElem.FlowD(L)-CurrElem.VirtKSMac(L)- &
              (CurrSoil.SWSAT(L)-SWN(L))*CurrSoil.DLayr(L)
          CurrElem.FlowD(L)=CurrElem.VirtKSMac(L)
          IF(FLOWEXC.GE.0.)THEN
            SWN(L)=CurrSoil.SWSAT(L)
            DO LNU=L-1,1,-1
              SWT=SWN(LNU)+FLOWEXC/CurrSoil.DLayr(LNU)
              IF(SWT.GT.CurrSoil.SWSAT(LNU))THEN
                FLOWEXC=(SWT-CurrSoil.SWSAT(LNU))*CurrSoil.DLayr(LNU)
                CurrElem.FlowD(LNU)=CurrElem.FlowD(LNU)-FLOWEXC- &
                      (CurrSoil.SWSAT(LNU)-SWN(LNU))*CurrSoil.DLayr(LNU)
                SWN(LNU)=CurrSoil.SWSAT(LNU)
              ELSE
                CurrElem.FlowD(LNU)=CurrElem.FlowD(LNU)-FLOWEXC
                FLOWEXC=0.
                SWN(LNU)=SWT
              ENDIF
              CurrElem.SWDifD(LNU)=SWN(LNU)-CurrElem.SW(LNU)
            ENDDO
          ELSE
            SWN(L)=CurrSoil.SWSAT(L)+FLOWEXC/CurrSoil.DLayr(L)
            FLOWEXC=0.
          ENDIF
          CurrElem.Pond=CurrElem.Pond+FLOWEXC
          IF(CurrElem.Pond.GT.CurrElem.PondMax)THEN
            CurrElem.Runoffd=CurrElem.Pond-CurrElem.PondMax
            CurrElem.Pond=CurrElem.PondMax
          ELSE
            CurrElem.Runoffd=0.0
          ENDIF
        ENDIF
      ENDIF
      CurrElem.SWDifD(L)=SWN(L)-CurrElem.SW(L)
      CurrElem.RUNOFF=CurrElem.Runoffs+CurrElem.Runoffd
!
!       THIS IS TOTAL RUNOFF FROM SURFACE AND SUBSURFACE FLOW
CAUSES

!*************COMPUTE SOIL LIMITED ROOT WATER
UPTAKE********************
      IF(LAI.GT.0.0)THEN
!*******************Determine bottom layer with roots**********************
        CUMDEP=CUMDEP+CurrSoil.DLayr(L)
        IF(CUMDEP-CurrSoil.DLayr(L).LT.CurrElem.RootDep)CurrElem.LR=L
!Layer where roots are growing
```

```
!C*******************************UPTAKE****************************
******
              RootPres = 1.0
          IF(L .EQ. CurrElem.LR) then
            RootPres=MIN(1.0,(CurrElem.RootDep-(CUMDEP-
CurrSoil.DLayr(CurrElem.LR))) &
                    /CurrSoil.DLayr(CurrElem.LR))
          Endif
          IF(L .GT. CurrElem.LR) RootPres = 0.0

          PESWabove=PESWabove+MAX(0.,CurrElem.SW(L)-
CurrSoil.SWLL(L))*CurrSoil.DLayr(L)
          IF(RootAct(L) .EQ. 1) THEN

!           Roots Already have been active in uptake in this layer

            PESWaboveFAC(L)=MIN(1.,MAX(0., &
             -exp(-4.8+0.3*PESWabove)+1.03))
          Else

!           Roots still have not become active in uptake from this layer yet

            PESWaboveFAC(L)=MIN(1.,MAX(0., &
                                exp(2.2-0.62*PESWabove)-0.07))
            IF(PESWaboveFAC(L)*RootPres .GE. 0.90) RootAct(L) = 1
          Endif

          Coef_Wat_Ext=CurrSoil.RUCO(L)*RootPres*PESWaboveFAC(L)
          IF(CurrElem.SW(L).LT.CurrSoil.SWLL(L))THEN
            CurrElem.SWDifR(L)=0.
          ELSE
            CurrElem.SWDifR(L)=Coef_Wat_Ext*MAX(0.,CurrElem.SW(L)-
CurrSoil.SWLL(L))
          ENDIF
        ELSEIF(CurrElem.EMDay.GT.1)THEN   !RESET ROOT GROWTH
PARAMETERS WHEN LAI = 0
          CurrElem.EMDay=0.
          CurrElem.RootDep=4.0
        ENDIF
        CurrElem.FlowR=CurrElem.FlowR+CurrElem.SWDifR(L)*CurrSoil.DLayr(L)

!*********CALCULATE SOIL LIMITED SOIL EVAPORATION
RATE**************
        CurrElem.SWDifU(L)=CurrSoil.FlowUCo(L)*(CurrElem.SW(L)-
CurrSoil.SWAD(L))
        IF(CurrElem.SW(L).GT.CurrSoil.SWDUL(L))THEN
```

```
        CurrElem.SWDifU(L)=CurrElem.SWDifU(L)*(3.-2.*(CurrSoil.SWSAT(L)-
CurrElem.SW(L))/&
            (CurrSoil.SWSAT(L)-CurrSoil.SWDUL(L)))
      ENDIF
      ESD=ESD+CurrElem.SWDifU(L)*CurrSoil.DLayr(L)

    ENDDO                    ! end of layer do loop

    IF(CurrElem.RootDep.GT.CUMDEP)THEN
      CurrElem.RootDep=CUMDEP
    ENDIF

!*****Calculate actual soil evaporation (cm/day) and water stress factor*

    if (CurrElem.Pond > 0) then
      if (CurrElem.Pond > ESO) then
        PotentialSurfaceEvap = ESO
        CurrElem.Pond = CurrElem.Pond - ESO
        CurrElem.PondEvap = ESO
      else
        PotentialSurfaceEvap = ESO - CurrElem.Pond
        CurrElem.PondEvap = CurrElem.Pond
        CurrElem.Pond = 0
      endif
    else
      PotentialSurfaceEvap = ESO
    endif
    IF(ESD.GT.PotentialSurfaceEvap)THEN
      CurrElem.RedCOU=PotentialSurfaceEvap/ESD
      CurrElem.ES=PotentialSurfaceEvap
    ELSE
      CurrElem.RedCOU=1.
      CurrElem.ES=ESD
    ENDIF
    SWSTR = 1.0
    IF(CurrElem.FlowR.GT.0.)THEN
      IF(EPO+CurrElem.ES .GT. EO)THEN
        EPO=EO-CurrElem.ES
        if (EPO < 0) then
          EPO = 0
        endif
      ENDIF
      IF(CurrElem.FlowR.GE.EPO)THEN
        CurrElem.RedCOR=EPO/CurrElem.FlowR
        CurrElem.EP=EPO
      ELSE
```

```
          CurrElem.RedCOR=1.0
          CurrElem.EP=CurrElem.FlowR
          SWSTR = CurrElem.FlowR/EPO
        ENDIF
      ELSE
        CurrElem.RedCOR=0.
        CurrElem.EP=0.
      ENDIF

!*********************INTEGRATION
CALCULATIONS*******************************
    ELSEIF (DYNAMIC.EQ.INTEG) THEN
!*********************************************************************
!
!*****************Update Root Depth*******************************
            CurrElem.RootDep = CurrElem.RootDep+CurrElem.RootDepIncr
!*********************************************************************
!
!
!******CALCULATE FINAL SOIL WATER DIFFERENCE******************

      CUMDIF=0.
      CurrElem.FlowU(CurrSoil.NLayr)=0.
      DO L=CurrSoil.NLayr,1,-1
        CurrElem.SWDif(L)=CurrElem.SWDifD(L)- &
                  CurrElem.SWDifU(L)*CurrElem.RedCOU- &
                  CurrElem.SWDifR(L)*CurrElem.RedCOR
        CurrElem.FlowU(L-1)=CurrElem.FlowU(L) + &
           CurrElem.SWDifU(L)*CurrElem.RedCOU*CurrSoil.DLayr(L)
        CurrElem.FLOW(L)=CurrElem.FlowD(L)-CurrElem.FlowU(L)
        CurrElem.SW(L)=CurrElem.SW(L)+CurrElem.SWDif(L)
        IF(CurrElem.SW(L).LT.CurrSoil.SWAD(L))THEN
          WRITE(*,19)L,CurrElem.SW(L),CurrElem.SWDifU(L), &
                CurrElem.SWDifD(L),CurrElem.SWDifR(L),L
        ENDIF
        CUMDIF=CUMDIF+CurrElem.SWDif(L)*CurrSoil.DLayr(L)
      END DO

!************ Lateral subsurface flow Added for Spatial *******************

!     calculate depth of saturated layer if any

      CurrElem.SatDepth = 9999
      CurrElem.SatLayer = CurrSoil.nlayr + 1
      do L=CurrSoil.nlayr,1,-1
        if (CurrElem.sw(L) .lt. CurrSoil.swdul(L)) then
```

```
          exit
        else
          CurrElem.SatDepth = CurrSoil.Zlayr(L) -  &
                          CurrSoil.Dlayr(L)
          CurrElem.SatLayer = L
        endif
      enddo

!     convert depth from cm from the top of the soil to meters above some
!     base level

      CurrElem.SatDepth = CurrElem.CentreZ -  &
                  (CurrElem.SatDepth/100.0)
      TotSubSurfOutFlow = 0.0
!      write(3,*) 'Sat depth = ', satdp
!
      if (CurrElem.SatLayer .LE. CurrSoil.nlayr) then

! For all saturated layers above the water table of down hill elements

        Do L = CurrElem.SatLayer, CurrSoil.nlayr
          do DownNum = 1, CurrElem.ndownslope
            DownElem = CurrElem.downslope(downnum)
            if (CurrElem.SatDepth .gt. Elements(DownElem).SatDepth) then
              deltaZ = CurrElem.SatDepth - Elements(DownElem).satdepth
              deltaX = sqrt((CurrElem.centrex-Elements(DownElem).centrex)**2+ &
                (CurrElem.centrey-Elements(DownElem).centrey)**2)
              Kssat = CurrSoil.KSMacro(L)
              kssatdown =
Soils(Elements(DownElem).soil).KSMacro(Elements(DownElem).SatLayer)
              kseff = 2/(1/Kssat + 1/kssatdown)
              LateralFlow = kseff * CurrElem.downfrac(DownNum) * (DeltaZ/DeltaX) *
&
                      (CurrElem.Area/Elements(DownElem).Area)

!             If the flow is out of the current element but there is
!             not enough water above DUL to drain

              If ((LateralFlow .gt. 0) .and.                &
                (LateralFlow .gt. (CurrElem.sw(L)-CurrSoil.SWDUL(L))))then
                Elements(DownElem).subsurfinflow = &
                  Elements(DownElem).subsurfinflow + &
                  CurrElem.sw(L)-CurrSoil.SWDUL(L)
                TotSubSurfOutFlow = TotSubSurfOutFlow + &
                  CurrElem.sw(L)-CurrSoil.SWDUL(L)
                CurrElem.SW(L) = CurrSoil.SWDUL(L)
```

```
!               If flow is out of the current element and there is
!               enough water to drain

                ElseIf (LateralFlow .gt. 0) then
                  CurrElem.SW(L) = CurrElem.SW(L) - LateralFlow
                  Elements(DownElem).subsurfinflow = &
                    Elements(DownElem).subsurfinflow + LateralFlow
                  TotSubSurfOutFlow = TotSubSurfOutFlow + &
                    LateralFlow

!               If flow is into the current element but there is not enough
!               space to hold the water

                ElseIf ((LateralFlow .lt. 0) .and.                &
                  (-LateralFlow .gt. (CurrSoil.SWSat(L) - CurrElem.sw(L))))then
                  Elements(DownElem).subsurfinflow = &
                    Elements(DownElem).subsurfinflow - &
                    (CurrSoil.SWSat(L) - CurrElem.sw(L))
                  TotSubSurfOutFlow = TotSubSurfOutFlow- &
                    (CurrSoil.SWSat(L) - CurrElem.sw(L))
                  CurrElem.SW(L) = CurrSoil.SWSat(L)

!               If flow is into the current element and there is enough
!               space to hold it

                ElseIf (LateralFlow .lt. 0) then
                  CurrElem.SW(L) = CurrElem.SW(L) - LateralFlow
                  Elements(DownElem).subsurfinflow = &
                    Elements(DownElem).subsurfinflow + LateralFlow
                  TotSubSurfOutFlow = TotSubSurfOutFlow + &
                    LateralFlow
                EndIf

              endif
            enddo
          EndDo

! Old code

!! look up ksmacro of uppermost saturated layer
!         depth = 0
!         do i=1,CurrSoil.nlayr
!           depth = depth + CurrSoil.dlayr(i)
!           if (depth > satdp) then
!             CurrElem.outflowlayer = i
```

```
!             kssat = CurrSoil.ksmacro(i)
!             exit
!           endif
!         enddo
!         write(*,*) 'Ksat = ', kssat,' for layer ', CurrElem.outflowlayer
!
!         depthlost = 0.0
!         do downnum = 1, CurrElem.ndownslope
!           downelem = CurrElem.downslope(downnum)
!           DownSoil = Elements(DownElem).Soil
!           write(*,*) 'Downslope connection to ', downelem
!
!! subsurface flow happens when elevation of saturated layer (z - satdp)
!! is higher than the elevation of the downslope element's saturated layer
!
!           deltaZ = (CurrElem.centrez - satdp) - &
!               (Elements(DownElem).centrez - Elements(DownElem).satdepth)
!           write(*,*) 'deltaZ = ',deltaZ
!           if (deltaZ .gt. 0) then
!
!! set depth of inflow equal from elevation of highest contributing inflow
!! adjusting depth for elevation difference of the two elements
!
!             if (CurrElem.centrez - satdp .gt. &
!               Elements(DownElem).centrez - &
!                Elements(DownElem).inflowdepth) then
!               Elements(DownElem).inflowdepth = satdp - &
!                (Elements(DownElem).centrez - CurrElem.centrez)
!             endif
!
!             depth = 0
!             do i=1,CurrSoil.nlayr
!               depth = depth + CurrSoil.dlayr(i)
!               if (depth > Elements(DownElem).inflowdepth) then
!                 kssatdown = Soils(DownSoil).KSMacro(i)
!                 exit
!               endif
!             enddo
!             kseff = 2/(1/kssat + 1/kssatdown)
!             write(*,*) 'kssatdown = ',kssatdown,' kseff = ',kseff
!
!! calculate amount of water moving laterally subsurface
!
!             deltaX = sqrt((CurrElem.centrex-Elements(DownElem).centrex)**2+ &
!               (CurrElem.centrey-Elements(DownElem).centrey)**2)
!             SurfSlope = deltaZ / deltaX
```

```
!            slopeangle = atan(SurfSlope)
!            flowdistance = kseff * sin(slopeangle) * &
!                      CurrElem.downfrac(downnum)
!            depthlost = depthlost + flowdistance
!              Elements(DownElem).subsurfinflow = &
!              Elements(DownElem).subsurfinflow + &
!              flowdistance * Currelem.area / elements(downelem).area
!              write(*,*) 'flowdist =',flowdistance
!          endif
!        enddo
!
!        CurrElem.sw(CurrElem.outflowlayer) = &
!           CurrElem.sw(CurrElem.outflowlayer) - depthlost
!
      endif

      ERROR=PRECIP+CurrElem.PondY-CurrElem.Runoffs-CurrElem.Runoffd- &
          CurrElem.Pond-CurrElem.FlowD(CurrSoil.NLayr)+ &
          CurrElem.SWYest- &
          sum(CurrElem.SW(1:CurrSoil.NLayr)*CurrSoil.DLayr(1:CurrSoil.NLayr))- &
          CurrElem.EP-CurrElem.ES-CurrElem.PondEvap-TotSubSurfOutFlow  !BDB
      IF(ERROR**2.GT.0.0000000001)THEN
        WRITE(15,22)YR,DOY,Elem,ERROR
        WRITE(*,22)YR,DOY,Elem,ERROR
      ENDIF
      CurrElem.PondY=CurrElem.Pond
      WRITE(13,25)YR,DOY,PRECIP,CurrElem.RUNOFF,CurrElem.Pond, &
             CurrElem.FlowD(CurrSoil.NLayr),CurrElem.ES, &
             CurrElem.EP,LAI,CurrElem.RootDep, SWSTR, &
             (CurrElem.SW(I),I=1,12)
!
WRITE(5,26)YR,DOY,PRECIP,CurrElem.Runoffs,CurrElem.Runoffd,CurrElem.Pond,(
FLOW(I),I=1,12)
!
!
    ENDIF

    RETURN

10  FORMAT(2F6.0,3F6.3,F6.1,F6.3,3F6.3)
15  FORMAT(8X,'----------cm/day----------        cm',8X,12(1x,F7.3))
18  FORMAT('LAT',F5.1,' LONG',F6.1,' ALT',F5.0,' CROPEC',F5.1,' VPD' &
   'MIN',F4.2,' PONDMAX',F5.1)
19  FORMAT(' UNACCEPTABLE RESULT, SW BELOW AIR DRY,
SW(L),UPWARD FLOW,DOWN FLOW,ROOT UPTAKE,DEPTH L',I3,4F7.3,I3)
```

```
22   FORMAT(' YR',I4, 'DAY',I4,' ELEMENT',I4,' WATER BALANCE ERROR (cm)
=',F9.6)
25   FORMAT(2I4,F6.2,6F5.2,F6.0,F6.3,2X,12(1x,F8.7))
30   FORMAT(' YR DOY  RAIN ROFF POND DRAN   ES   EP  LAI RTDEP
SWSTR' &
       ,'  SW1    SW2    SW3    SW4    SW5    SW6    SW7' &
       ,'  SW8    SW9   SW10   SW11   SW12')
26   FORMAT(2I4,4F6.2,12F7.4)
31   FORMAT(' YR DOY  RAIN RNOFS RNOFD  POND  FLOW1  FLOW2  FLOW3
F', &
   'LOW4  FLOW5  FLOW6  FLOW7  FLOW8  FLOW9 FLOW10 FLOW11
FLOW12')

END SUBROUTINE ElemCSWB

! DEFINITIONS
! EO      Potential evapotranspiration  (cm/day)
! ESD     Amount of water available for soil evaporation? (cm/day)
! ESO     Potential soil evaporation  (cm/day)
! ES      Actual soil evaporation  (cm/day)
! EPO     Potential plant evaporation  (cm/day)
! EP      Actual plant evaporation  (cm/day)
! VPD     Estimated vapor pressure deficit for a day (kPa)
! VPDAY   Estimated vapor pressure for a day (kPa)
! VP      Estimated saturation vapor pressure for a day (kPa)
! CROPEC  A crop specific constant--slope of the aerodynamic component relation-
!         ship in the potential evaporation equation  (MJ/kPa)
! RADCOM  The radiation component in the potential evaporation equation (mm/day)
! AEROCOMS The aerodynamic component in the potential evaporation equation for
!         bare soil surfaces (mm/day)
! AEROCOMC The aerodynamic component in the potential evaporation equation for
!         crops surfaces (mm/day)
! GODPG   Gamma divided by delta plus gamma in the potential evap. equation
! PRES    The estimated atmospheric pressure based on elevation (kPa)
! RUNOFFS Daily runoff related to lack of surface infiltration  (cm/day)
! RUNOFFD Daily runoff related to lack of drainage at depth  (cm/day)
! LAI     Leaf area index  (cm2/cm2)
! LAI_TAB Table of LAI for given dates (input data)
! ROOTDEP_TAB  Table of root depth for given dates (input data)
! COEFD   Empirical coefficient used to calculate new water content after
!         infiltration  (unitless)
! CUMDEP  Cumulative soil depth at bottom of layer  (cm)
! MEANDEP Soil depth at center of layer  (cm)
! SW(L)   Soil water content  (cm3/cm3)
! SWT     Temporary variable for a new soil water content (cm3/cm3)
! SWTD    Temporary variable for calculating water content during drainage (cm3/cm3)
```

! SWTI Temporary variable for calculating water content during infiltration (cm3/cm3)
! SWDUL(L) Soil water content at the drained upper limit (cm3/cm3)
! SWSAT(L) Soil water content at saturation (cm3/cm3)
! RHF(L) Root hospitality factor input from soils file unitless
! RUCO(L) Root uptake coefficient unitless
! SWDIFU(L) Soil water content difference resulting from upward flow (vol frac)
! SWDIFD(L) Soil water content difference resulting from downward flow (vol frac)
! SWDIFR(L) Soil water content difference resulting from root uptake (vol frac)
! SWDIF(L) Net soil water content difference from all factors (vol frac)
! FLOWU(L) Flow rate upward at the layer being evaluated (cm/day)
! FLOW(L) Net flow rate at the layer being evaluated (cm/day)
! FLOWEXC Excess water that cannot flow downward (cm/day)
! FLOWUCO(L) Coefficient for each soil layer used to calculate evaporation rate - unitless
! RUCO(L) Coefficient for each soil layer used to calculate root uptake - unitless
! REDCOU Reduction coefficient to reduce upward flow to potential soil evap.
! REDCOR Reduction coefficient to reduce root uptake to potential plant evap.
! ROOTDEP Depth of rooting cm
! INFILT Amount of infiltration during a given period (mm). Temp.var.
! KSMACRO(L) Saturated hydraulic conductivity with macropores (cm/day).
! MAXRAIN Maximum rate of rainfall (cm/day)
! NUMSTEPS Number of steps in a rainstorm
! PINF Daily precipitation infiltrated (cm)
! PIP Precipitaion infiltrated from ponding (cm)
! POND Amount/depth of water held in ponding on the surface (cm)
! PONDMAX Maximum amount of water that can be stored in ponding (cm)
! RAIN Daily measured rain from weather input file (mm).
! is assumed to infiltrate and the ponding routine is bypassed (mm).
! PPRECIP Amount of precipitation for a given period (cm).
! PRECIP Sum of RAIN and irrigation (cm) convert from mm.
! RAINDUR Length of rain storm (hrs)
! RUNOFFS Daily runoff (cm).
! TIME Current time into the storm (days)
! TIMESTEP Amount of time per step in a storm (days)
! TPAMT For a given period amount of water that could infltrate (cm)
! TRUNOFF Amount of water runoff during a given period (cm).
! LR Depth increment in depth counter (L) where root depth is located
! acoef
! ncoef
! dTT Thermal time on current day, oC-d (base of 10 oC)
! BD Bulk density of soil(g/cm3)
! RockBD Bulk density of the solid material in soil (g/cm3)
! Porosity Fraction of soil volume that is pore space
! WatFilPor Fraction of soil pore space filled with water
! HalfPESW Soil water content when half of available water remains
! RootDepIncr Daily growth rate of roots, vertical direction (cm/d)

```
! coldfac            Factor reducing root growth in a layer due to cold temperature (0-1)
! Slope        Average slope of the soil surface (%)
! RootPres     Indicator of root presence in a layer, fraction (0 to 1)
! PESWabove     volume of plant avaialble water above a layer (for computing root
activity)
! PESWaboveFAC  Factor (0-1) to indicate root activity in water uptake
! Coef_Wat_Ext  Relative rate at which water is extracted from a layer (1/d)
! RootAct                    Indicator that roots have been taking up water, each layer
!


end module elemwatbal
```

REFERENCES

Abbott, M.B., J.C. Bathrust, J.A. Cunge, P.E. O'Connell, and J. Rasmussen. 1986. An introduction to the European System-System Hydrologique Europeen, "SHE", 2, Structure of a physically-based, distributed modeling system. J. Hydrol. 87: 61-77.

Adams, R.M., Rosenzweig, R.M. Peart, J.T. Ritchie, B.A. McCarl, J.D. Glycer, R.B. Curry, J.W. Jones, K.J. Boote, and L.H. Allen, Jr. 1990. Global Climate change and U.S. Agriculture. Nature 345: 219-224.

Addiscott, T.M., and R. J. Wagenet. 1985. Concepts of solute leaching in soils: A review of modeling approaches. J. Soil Sci. 36: 411-424.

Barnes, E.M., P.J. Pinter Jr., B.A. Kimball, G.W. Wall, R.L. LaMorte, D.J. Hunsaker, F. Adamsen, S. Leavitt, T. Thompson, and J. Mathius. 1997. Modification of CERES-Wheat to accept leaf area index as an input variable. Written for Presentation at the 1997 ASAE Annual International Meeting, Sponsored by ASAE, Minneapolis, MN, August 10-14, 1997. Paper No. 973016.

Batchelor, W.D., and J.O. Paz. 1998. Process-Oriented Crop Growth Models as a Tool to Evaluate Spatial Yield Variability. In: Proceedings of the First International Conference on Geospatial Information in Agriculture and Forestry, Vol. 1. pp. I198-205. 1-3 June 1998, Lake Buena Vista, Florida, USA. ERIM International.

Bell, J.C., R.L. Cunningham, and M.W. Havens. 1992. Calibration and validation of a soil-landscape model for predicting soil drainage class. Soil Sci. Soc. Am. J. 56: 1860-1866.

Bell, J.C., R.L. Cunningham, and M.W. Havens. 1994. Soil drainage class probability mapping using a soil-landscape model. Soil Sci. Soc. Am. J. 58: 464-470.

Beven, K.J., and M.J. Kirky. 1979. A physically-based variable contributing area model of basin hydrology. Hydrol. Sci. Bull., 24, 43-69.

Blackmer, A.M., and S.E. White. 1996. Remote sensing to identify spatial patterns in optimal rates of nitrogen fertilization. In: P.C. Robert, R.H. Rust, and W.E. Larson (eds.), Proceedings of the Third International Conference on Precision Agriculture, Minneapolis, MN, 23-26 June 1996. ASA Miscellaneous Publication, pp. 33-41. ASA, CSSA, and SSSA, Madison, WI.

Booltink, H.W.G., and J. Verhagen. 1997. Using decision support systems to optimize barley management on spatial variable soil. In: M.J. Kropff, P.S. Teng, P.K. Aggarwal, J. Bouma, B.A.M. Bouma, J.W. Jones, and H.H. van Laar (ed.), Application of systems approaches at the field level, pp. 219-233. Kluwer Academic Publishers, Dordrecht, The Netherlands.

Boote, K.J., J.W. Jones, G. Hoogenboom, and N.B. Pickering. 1998. CROPGRO model for grain legumes. In: G.Y. Tsuji, G. Hoogenboom, and P.K. Thornton (eds.), Understanding Options for Agricultural Production, pp. 99-128. Kluwer Academic Publishers, Dordrecht, Netherlands.

Braga, R.P., J.W. Jones, and B. Basso. 1999. Weather Variability in Site-Specific Management Profitability: A Case Study. In: P.C. Robert, R.H. Rust, and W.E. Larson (ed.), Precision Agriculture, pp. 1853-1863. ASA-CSSA-SSSA, Madison, Wisconsin, USA.

Brown, D.G. 1994. Predicting vegetation types at treeline using topography and biophysical disturbance variables. Journal of Vegetation Science, 5: 641-656.

Cambardella, C.A., T.S. Colvin, D.L. Karlen, S.D. Logsdon, E.C. Berry, Radke, T.C. Kaspar, T.B. Parkin and D.B. Jaynes. 1996. Soil property contributions to yield variation pattern. In P.C. Robert, R.H. Rust, and W.E. Larson (eds.). Proceedings of the Third International Conference on Precision Agriculture. ASA, CSSA, SSSA, Inc., Madison, WI. pp 417-424.

Carlson, T.N., and D.A. Ripley. 1997. On the Relation between NDVI, Fractional Vegetation Cover, and Leaf Area Index. Remote Sens. Environ. 62: 241-252.

Carter, J.R. 1988. Digital representations of topographic surfaces. Photogrammetric Engineering and remote sensing, 54: 1577-1580.

Cassel, D.K., L.F. Ratliff, and J.T. Ritchie. 1983. Models for estimating in-situ potential extractable water using soil physical and chemical properties. Soil. Sci. Soc. Am. J. 47:764-769.

Chong, S.-K. 1983. Calculation of sorptivity from constant rate rainfall infiltration measurement. Soil Sci. Soc. Am. J. 47: 627-630.

Cochrane, T.A., and D.C. Flanagan. 1999. Assessing water erosion in small watershed using WEPP with GIS and digital elevation models. Journal of Soil and Water Conservation, 54: 678-686.

Cora, J.E., F.J. Pierce, B. Basso, and J.T. Ritchie. 1999. Simulation of within-field variability of corn yield with Ceres-Maize model. In: P.C. Robert, R.H. Rust, and W.E. Larson (ed.), Precision Agriculture, pp. 1309-1319. ASA-CSSA-SSSA, Madison, Wisconsin, USA.

Dunne, T., and R.D. Black. 1970. Partial-area contributions to storm runoff in a small New England watershed, Water Resour. Res. 6: 1296-1311.

Dunne, T. 1983. Relation of field studies and modeling in the prediction of storm runoff. J. Hydrol. 65: 25-48.

ESRI. 1993. Surface modeling with TIN, in "FrameViewer (TM) 3.1X", the on-line help manual of ARC/INFO System that was developed and is supported by Environmental Systems Research Institute, Inc. (ESRI).

Feddes, R.A., P.J. Kowalik, and H. Zaradny. 1978. Simulation of field water use and crop yield. Pudoc, Wageningen.

Freeze, R.A. 1972. Role of subsurface flow in generating surface runoff, 2, Upstream source areas, Water Resour. Res. 8: 1272-1283.

Gabrielle, B., S. Menasseri, and S. Houot. 1995. Analysis and field-evaluation of the CERES models water balance component. Soil Sci. Am. J. 59: 1403-1412.

Gallant, J.C., and J.P. Wilson. 1996. TAPES-G: a grid-based terrain analysis program for the environmental sciences. Computers and Geosciences, 22: 713-722.

Gallant, J.C., and M.F. Hutchinson. 1997. Scale dependence in terrain analysis. Mathematics and Computers in Simulation 43: 313-321.

Gallant, J.C. 1999. TERRAE: A new element network tool for hydrological modelling. 2nd Inter-Regional Conference on Environment-Water: Emerging Technologies for Sustainable Water Management, Lausanne, Switzerland, 1-3 September 1999.

Gamma Design Software, Gs+: geostatistics for the environmental scienc. Version 3.01. Gamma Design Software, Plainwell, MI, p.44, 1994.

Gardner, W. 1960. Dynamic aspects of water availability to plants. Soil Sci.: 89-93.

Gerakis, A., and J.T. Ritchie. 1998. Simulation of atrizine leaching in relation to watertable management using the CERES model. Journal of Environmental Management 52: 241-258.

Gessler, P.E., I.D. Moore, N.J. McKenzie, and P.J. Ryan. 1995. Soil landscape modeling and spatial prediction of soil attributes. International Journal of Geographical Information Systems, 9: 421-432.

Gessler, P.E., N.J. McKenize and M.F. Hutchinson. 1996. Progress in soil-landscape modelling and spatial prediction of soil attributes for environmental models. Proceedings of the Third International Conference/Workshop on Integrating GIS and Environmental Modelling. National Centre for Geographic Information and Analysis, Santa Barbara, CA, USA.

Hall, G.F., and C.G. Olson. 1991. Predicting variability of soils from landscape models. In: M.J. Mausbach and L.P. Wilding (eds.), Spatial Variabilities of Soils and Landforms, pp. 9-24. SSSA Special Publication No. 28.

Hoogenboom, G.J., J.W. Jones, P.W. Wilkens, W.D.Batchelor, W.T. Bowen, L.A. Hunt, N. Pickering, U. Singh, D.C. Godwin, B. Baer, K.J. Boote, J.T. Ritchie, and J.W. White. 1994. Crop models. In: G.Y. Tsuji, G. Uehara, and S. Balas (eds.). 1994. DSSAT v3. Vol. 2-2. University of Hawaii, Honolulu, Hawaii.

Horton, R. E. 1933. The role of infiltration in the hydrologic cycle, Eos Trans. AGU, 14: 446-460.

Hutchinson, M.F. 1996. A locally adaptive approach to the interpolation of digital elevation models. Proceedings of the Third International Conference/Workshop on Integrating GIS and Environmental Modelling. National Centre for Geographic Information and Analysis, Santa Barbara, CA, USA.

Hutchinson, M.F. 1997. ANUDEM Version 4.6. http://cres.anu.edu.au/software/anudem46.html.

IBSNAT. 1984. International Benchmark Sites Network for Agrotechnology Transfer. Department of Agronomy and Soil Science, University of Hawaii, Honolulu, HI, U.S.A.

ISBRAM. 1991. International Board for Soil Research and Management. Evaluation for sustainable land management in the developing world; Volume I Towards the development of an International framework. IBSRAM Proceedings no.12.

Jackson, R.D. and A.R. Huete. 1991. Interpreting vegetation indeces. Preventive Veterinary Medicine 11: 185-200.

Jasinski, M.F. 1996. Estimation of subpixel vegetation density of natural regions using satellite multispectral imagery. IEEE Trans. Geosci. Remote Sens. 34: 804-813.

Johannsen, C.J., M.F. Baumgardner, P.R. Willis, and P.G. Carter. 1998. Advances in Remote Sensing Technologies and Their Potential Impact on Agriculture. In: Proceedings of the First International Conference on Geospatial Information in Agriculture and Forestry, Vol. 1. pp. I6-11. 1-3 June 1998, Lake Buena Vista, Florida, USA. ERIM International.

Jones, A.J., L.M. Mielke, C.A. Bartles, and C.A. Miller. 1989. Relationship of landscape position and properties to crop production. J. Soil Water Conserv. 44: 328-332.

Jones, J.W., K.J. Boote, G. Hoogenboom, S.S. Jagtap, and G.G. Wilkerson. 1989. SOYGRO V5.42, Soybean crop growth simulation model user's guide. Florida Agricultural Experiment Station Journal N° 8304. University of Florida, Gainesville, Florida, USA.

Jones, J.W., and J.T. Ritchie. 1991. Crop growth models. In: G.J. Hoffman, T.A. Howell, and K.H. Soloman (eds.), Management of farm irrigation systems. ASAE, St. Joseph, MI.

Kirkby, M.J., A.C. Imeson, G. Bergkamp, and L.H. Cammeraat. 1996. Scaling up processes and models. Journal of Soil and Water Conservation, 51: 391-396.

Kovács, G.J., T. Németh, and J.T. Ritchie. 1995. Testing Simulation Models for the Assessment of Crop Production and Nitrate Leaching in Hungary. Agricultural Systems 49: 385-397.

Kumler, M.P. 1994. An intensive comparison of triangulated irregular networks (TINs) and digital elevation models (DEMs). Cartographica, 31: 1-99.

Laflen, J.M., W.J Elliot,. D.C., Flanagan, C.R., and M.A. Nearing. 1997. WEPP-Predicting water erosion using a process-based model. Journal of Soil and Water Conservation, 52: 96-103.

Lafolie, F.L., Bruckler, A.M. deCockborne, and C. Laboucarie. 1997. Modeling the water transport and nitrogen dynamics in irrigated salad crops. Irrigation Science. 17: 95-104.

Liu, Q., and A. Huete, 1995. A feedback based modification of the NDVI to minimize canopy background and atmosphere noise. IEEE Trans. Geosci. Remote Sens. 33: 457-465.

Maune, D. 1996. DEM extraction editing matching and quality control techniques. In: C.W. Greve (ed.), Digital Photogrammetry: An Addendum to the Manual of Photogrammetry. Bethesda, MD: American Society for Photogrammetry and Remote Sensing.

Miller, C.L., and R.A. Laflamme. 1958. The digital terrain model – theory and application. Photogrammetric Engineering 24: 433-42.

Moore, I.D., E.M. O'Laughlin, and G.J. Burch. 1988. A contour-based topographic model for hydrological and ecological application. Earth Surf.Processes Landforms, 13: 305-320.

Moore, I.D., and R.B. Grayson. 1989. Hydrologic and Digital Terrain Modelling using vector elevation data, EOS Trans. AGU 70: 1091.

Moore, I.D., and R.B. Grayson. 1991. Terrain-Based catchment Partitioning and Runoff Prediction Using Vector Elevation Data. Water Resour. Res. 27: 1177-1191.

Moore, I.D., and M.F. Hutchinson. 1991. Spatial Extension of Hydrologic process Modelling. Proc. Int. Hydrology and Water Resources Symposium. Institution of Engineers-Australia 91/22, pp. 803-808.

Moore, I.D., R.B. Grayson, and A.R. Ladson. 1991. Digital Terrain Modelling: A review of hydrological, geomorphological and biological applications. In: K.J. Beven and I.D. Moore (eds.), 1991. Terrain Analysis and distributed Modelling in hydrology. J.Wiley & Sons.

Moore, I.D., and P.E. Gessler, G.A. Nielsen and G.A. Peterson. 1993. Terrain Analysis for Soil Specific Crop Management. In: Soil Specific Crop Management. ASA-CSSA-SSSA.

Moore, I.D., J.C. Gallant, and L. Guerra. 1993. Modelling the spatial variability of hydrological processes using GIS in HydroGIS 93: Application of Geographic Information Systems in Hydrology and Water Resources Management. Proceedings of Vienna Conference, April 1993. IAHS publ. No. 211. p. 161-169.

Moore, I.D., A. Lewis, and J.C. Gallant. 1993. Terrain attributes: estimation methods and scale effects. In: A.J. Jakeman, M.B. Beck, and M.J. McAleer (eds.), Modeling Change in Environmental Systems, pp. 191-214. New York: John Wiley and Sons.

Moore, I.D., P.E. Gessler, G.A. Nielsen, and G.A. Peterson. 1993. Soil attribute prediction using terrain analysis. Soil Sci.Soc. Amer.J. 57: 443-452.

Moran, M.S., Y. Inoue, E.M. Barnes. 1997. Opportunities and Limitations for Image-Based Remote Sensing in Precision Crop Management. Remote Sensing of the Environment Vol. 61: 319-346.

Mueller, T.G. 1998. Ph.D. Dissertation, Department of Crop and Soil Science, Michigan State University, East Lansing, MI, USA.

Nix, H.A. 1983. Minimum Data Sets for Agrotechnology Transfer. Proceedings of the International Symposium on Minimum Data Sets for Agrotechnology Transfer. 21-23 March, ICRISAT AP 502324. India.

O'Laughlin, E.M. 1986. Prediction of surface saturation zones in natural catchments by topographic analysis, Water Resour. Res. 22: 229-246.

Onstad, C.A., and D.L. Brakensiek. 1968. Watershed simulation by stream path analogy. Water Resour. Res. 4: 965-971.

Onstad, C. A. 1973. Watershed flood routing using distributed parameters, In: E.S. Shultz, V.A. Koelzer, and K. Mahmood (eds.), Floods and Droughts, pp. 418-428. Water Resources Publications, Fort Collins, CO.

Passioura, J.B. 1996. Simulation Models: Science, Snake Oil, Education or Engineering? Agronomy Journ. 88: 690-695.

Paz, J.O., W.D. Batchelor, T.S. Colvin, S.D. Logsdon, T.C. Kaspar, and D.L. Karlen. 1997. Analysis of Water Stress Effects Causing Spatial Yield Variability in Soybeans. Trans. ASAE 41: 1527-1534.

Paz, J.O., W.D. Batchelor, B.A. Babcock, T.S. Colvin, S.D. Logsdon, T.C. Kaspar, and D.L. Karlen. 1999. Model-based technique to determine variable rate nitrogen for corn. Agric. Syst. 61: 69-75.

Pierce, F.J., D.D. Warncke, and M.W. Everett. 1995. Yield and nutrient availability in glacial soils of Michigan. p. 133-151. In P.C. Robert et al. (ed.) Proc. Of the Int. Conf. on Site Specific Management for Agricultural Systems, 2nd. Bloomington/Minneapolis, WI.

Pierce, F.J., N.W. Anderson, T.S. Colvin, J.K. Schueller, D.S. Humberg and N.B. McLaughlin. 1997. Yield Mapping. In: F.J. Pierce and E.J. Sadler (ed.), The State of Site Specific Management for Agriculture, p. 211-243. ASA Misc. Publ., ASA, CSSA, and SSSA, Madison, WI.

Pierce, F.J., and P. Nowak. 1999. Aspects of Precision Agriculture. Advances in Agronomy, 67: 1-86.

Pierce, F.J., and D.D. Warncke. 2000. Soil and Crop Response to Variable-Rate Limiting for Two Michigan Fields. Soil Sci. Soc. Am J. 64:

Price, J.C. 1992. Estimating Vegetation Amount from Visible and Near Infrared Reflectances. Remote Sens. Environ. 41: 29-34.

Priestley, C.H.B., and R.J. Taylor. 1972. On the assessment of the surface heat flux and evaporation using large-scale parameters. Monthly Weather Review 100: 81-92.

Refsgaard, J.C., S.M. Seth, J.C. Bathurst, M. Erlich, B. Storm, G.H. Jørgensen, and S. Chandra. 1992. Application of the SHE to catchments in India, Part 1. General results. J. Hydrol. 140: 1-23.

Richardson, C.W., and J.T. Ritchie. 1973. Soil Water Balance for Small Watershed. Transactions of the ASAE. 16: 72-77.

Ritchie, J.T. 1972. Model for predicting evaporation from a row crop with incomplete cover. Water Resour. Res. 8: 1204-1213.

Ritchie J.T., D.C. Godwin, and S. Otter-Nacke. 1985. CERES-Wheat: A simulation model of wheat growth and development. Texas A&M University Press, College Station, TX.

Ritchie, J.T. 1985. A user-oriented model of the soil water balance in wheat. In: W. Day and R.K. Atkin (ed.), Wheat growth and modeling, pp. 293-305. Series A: Life Sciences Vol. 86. Plenum Press, NY.

Ritchie J.T. 1986. Using Simulation Models for Predicting Crop Performance. Symposium on the Role of Soils in Systems Analysis for Agrotechnology Transfer. August 1986. ISSS Congress. Hamburg, Germany.

Ritchie, J.T. 1987. Using crop models as a decision support system to reduce nitrate leaching. In: F.M. D'Itri and L.G. Wolfson (ed.), Rural groundwater contamination, pp. 179-192. Lewis Publishers, Chelsea, Michigan.

Ritchie J.T. and J.Crum. 1989. Converting soil survey characterization data into IBSNAT crop model input. In: J. Bouma and A.K. Berget (eds.), Land Qualities in Space and Time, 155-167.Wageningen, The Netherlands.

Ritchie, J.T., and U. Singh, D.C. Godwin and L. Hunt. 1989. A user's guide to CERES Maize-V.2.10- Muscle Shoals, AL. International Fertilizer Development Center.

Ritchie J.T. and B.S Johnson. 1990. Soil and Plant factors affecting evaporation. In: B.A. Stewart and D.R. Nielsen (eds.), Irrigation of Agricultural Crops. Madison, WI. Amer. Soc. of Agronomy.

Ritchie J.T., and D.S. Nesmith. 1991. Temperature and Crop Development. In: Hanks and Ritchie (eds.), Modelling plant and soil systems. Agronomy 31: 5-29.

Ritchie, J.T. 1991. Specifications of the ideal model for predicting crop yield. In: R.C. Muchow and J.A. Bellamy (ed.), Climatic Risk in Crop Production: Model and Management for the semi-arid tropic and subtropic, p. 97-122. Proc. Intl. Symp. S. Lucia, Brisbane, Queensland, Australia. July 2-6, 1990. CAB International Wallingford, U.K.

Ritchie, J.T. 1998. Soil water balance and plant water stress. In: G.Y. Tsuji, G. Hoogenboom, and P.K. Thornton (eds.), Understanding Options for Agricultural Production, pp. 41-54. Kluwer in cooperation with ICASA, Dordrecht/Boston/London.

Ritchie, J.T., A. Gerakis,. and A. Suleiman . 1999. Simple Model To Estimate Field-Measured Soil Water Limits. Tran. ASAE 42: 1609-1614.

Rosensweigh, C., and D. Hillel. 1998. Climate Change and the Global Harvest: Potential Impacts of the Greenhouse Effect on Agriculture. (Cary, N.C.: Oxford University Press).

Sadler, E.J., and Russell G. 1997. Modeling Crop Yield for Site Specific Management. p. 69-80. In: F.J. Pierce and E.J. Sadler. (ed.), The State of Site Specific Management for Agriculture. ASA Misc. Publ., ASA, CSSA, and SSSA, Madison, WI.

Shanholtz, V.O. and T.M. Younos. 1994. A soil water balance model for no-tillage and conventional till systems. Agricultural Water management 26: 155-168.

Singh, P., G. Alagarswamy, G. Hoogenboom, P. Pathak, S.P. Wani, and S.M. Virmani. 1999. Soybean-Chickpea rotation on Vertic Inceptisol, 2, Long-term simulation of waterbalance and crop yields. Field Crops Research 63: 225-236.

Speight, J.G. 1974. A parametric approach to landform regions. In: E.H. Brown and D.L. Linton (eds.), The Progress of Geomorphology, 7: 213-230. The British Geographers.

Sudduth, K.A., S.T. Drummond, S.J. Birrell, and N.R. Kitchen. 1996. Analysis of spatial factors influencing crop yield. In: P.C. Robert, R.H. Rust, and W.E. Larson (ed.), Proceedings of the Third International Conference on Precision Agriculture, pp. 129-140. ASA, CSSA, SSSA. Madison, WI.

Swaney, D.P., J.W. Jones, W.G. Bogess, G.G. Wilkerson, and J.W. Mishoe. 1983. Real-time Irrigation Decision Analysis using Simulation. Transactions of the ASAE 26: 562-568.

Tsuji, G.Y., G. Uehara, S. Balas. 1994. DSSAT: A Decision Support System for Agrotechnology Transfer. Vol. 3. University of Hawaii, Honolulu, HI, USA.

USDA. 1996. Soil survey Laboratory Methods Manual. Soil Survey Investigation Report No. 42. Vers. 3.0. Washington, D.C.: USDA.

Verhagen, A., H.W.G. Booltink, and J. Bouma. 1995. Site-specific management: Balancing production and environmental requirements at farm scale. Agric. Syst. 49: 369-384.

Verhagen, J., and Bouma J. 1997. Modeling Soil Variability. p. 55-68. In: F.J. Pierce and E.J. Sadler. (ed.), The State of Site Specific Management for Agriculture. ASA Misc. Publ., ASA, CSSA, and SSSA, Madison, WI.

Vertessy, R.A., J.T. Hatton, P.J. O'Shaughnessy, and M.D.A. Jayasuriya. 1993. Predicting water yield froma amountain ash forest catchment using a terrain analysis based catchment model. J. Hydrol. 150: 665-700.

Wang, M. and A.T. Hjelmfelt. 1998. DEM Based Overland Flow Routing Model. Journal of Hydrologic Engineering, Vol. 3, No. 1: 1-8.

Weibel, R., and M. Heller. 1991. Chapter 19: Digital Terrain Modeling. In Goodchild, M.F. and D. Rhind (eds.), Geographic Information Systems, Principles and Applications. New York: Taylor and Francis.

White, I., and P. Broadbridge. 1988. Constant rate rainfall infiltration: A versatile nonlinear model, 2, Applications of solutions, Water Resour. Res. 24: 155-162.

White, I., M.J. Sully, and M.D. Melville. 1989. Use and hydrological robustness of Time-to-incipient-ponding. Soil Sci. Soc. Am. J. 29: 1343-1346.

Wiegand, C.L., A. J. Richardson, D.E. Escobar, and A.H. Gerbermann. 1991. Vegetation Indeces in Crop Assessments. Remote Sens. Environ. 35: 105-119.

World Resources Institute. 1992. World Resources, 1992-1993. Oxford University Press.

Xu, T. 1999. Mapping Soil Properties with Landscape Analysis. Ph.D. Dissertation, Centre for Resource and Environmental Studies, Australian National University, Canberra, A.C.T., Australia.

Yates, D.N. 1996. WatBal: An Integrated Water Balance Model for Climate Impact Assessment of River Basin Runoff. Water Resources Development, 12: No.2. 121-139.

Young, R. A., C.A. Onstad, D.D. Bosch, and W.P. Anderson. 1996. AGNPS: A nonpoint source pollution model for evaluating agricultural watersheds, Journal of Soil and Water Conservation, 44, 168-193.